THE ROLE OF CALCIUM CHANNEL DRUGS IN LIPOPOLYSACCHARIDE-INDUCED ORAL CANCER CELL PROLIFERATION

Rajdeep Chakraborty

Bachelor of Dental Surgery, The West Bengal University of Health Sciences, Kolkata, India

Master of Science (Biomedical Sciences), Lancaster University, Lancaster, U.K

A thesis submitted in fulfilment of the requirements for the degree of

Master of Research

June 2020

Department of Biomedical Sciences

Macquarie University, Sydney, Australia

Declaration

I hereby declare that all the components of this thesis are original. The thesis has been written abiding by the rules of plagiarism. I have strictly followed the rules of the MRes Year 2 of the Faculty of Medicine and Health Sciences, Macquarie University for submission of theses. The structure of the thesis similar to by previously submitted theses written by MRes Year 2 students in the Faculty of Medicine and Health Sciences of Macquarie University.

All the oral cancer cells were gifted by Dr Charbel Darido. Authentication of all the cells was undertaken by Dr Darido using short tandem repeat profiling. The concept of bacterial antigen on oral cancer cells is a novel idea introduced by Assoc Prof Karen Vickery, Dr Honghua Hu, Dr Charbel Darido and Rajdeep Chakraborty. The concept of calcium channels in oral cancer was developed by Dr Marina Santiago (Connor group). The selection and structural analysis of the calcium channel drugs was done by Prof Shoba Ranganathan and Amara Jabeen. The combined drugs strategy was designed by Rajdeep Chakraborty. The design and characterisation of the primers was done under the supervision of Dr Honghua Hu.

The experimental work was carried out in the laboratory setup of the Surgical Infection Research group led by Assoc Prof Karen Vickery. All the raw data and laboratory notebooks have been electronically submitted to the Surgical Infection Research group. The laboratory work involving mammalian cell culture was done following ethics clearance from the Biosafety Committee in Macquarie University's Office of the Deputy Vice Chancellor (Research). The details of all reagents and equipment used during the project are provided in the thesis.

An annual research report has been submitted to Sydney Vital (as a part of the funding contract). Overall, I take full responsibility for all the results generated from the project and declare that they are genuine and free from any manipulation or copying from any other source.

Statement of Originality

This work has not previously been submitted for a degree or diploma in any university. To the best of my knowledge and belief, the thesis contains no material previously published or written by another person except where due reference is made in the thesis itself.

(Signed)_____ Date: 15thJune 2020
Candidate's name

Acknowledgements

cancer cells, reagents and technical support required for the project. This project would never have been possible without the support of Assoc Prof Vickery, Dr Hu, and Dr Darido. They not only assisted in the writing of the research proposal, but also provided the technical, financial, and moral support required for the project. I have no hesitation in saying that they turned an average student like me into a research student. Whenever I required any help or had problems, I always found them standing beside me.

After the cells arrived, I was extensively assisted by Dr Maria Mempin. Despite her busy laboratory schedule, she found time to help me learn the basic techniques involved in the project. Her advice was invaluable. She not only helped me with the project, but also helped me to successfully apply for the Lorne Cancer Travel Award. Many times, she helped me with providing feedback on my other assignments, which was not part of her job. Thank you so much Maria.

I also had to devote much extra time to learn fundamental cell biology and biochemistry laboratory techniques, because of my different academic background. Dr Marina Santiago took responsibility for explaining the basics of cell culture and helping me understand the various calculations required for drug combination assays. Marina spent many hours of her valuable time sitting beside me and untiringly demonstrating and helping me learn cell culture techniques without any benefit to herself. The demonstrations were so thorough that within a couple of weeks, I had gained confidence and begun culturing oral cancer cells independently. It was her observation of one of the assays that identified calcium spikes in the oral cancer cells. She proposed examining gene expression of calcium channel and cannabinoid receptors in the oral cancer cells. Thus, the idea of calcium channel drugs came into the project. She also suggested to the group that we employ the MT Glo and clonogenic assays, and proteome profiling, which proved to be the most successful research component of the project. Marina obtained all the positive control cell lines for the project from Dr Charlie Ahn, Dr Benjamin Heng, and Prof Helen Rizos from the precision cancer therapy group. During that time Prof Mark Connor supported my project and shared various useful tips that later proved to be highly beneficial. I do not have enough words to thank you Marina.

However, the most crucial aspect of the project was the selection and understanding of calcium channel drugs that ought to work in the presence of bacterial antigens or after the stimulation of oral cancer cells with bacterial antigens. I thus contacted Prof Shoba Ranganathan, chair of bioinformatics in the Department of Chemistry. Prof Ranganathan

I would also like to acknowledge the support of the technical teams of R&D Technologies, Tocris Biosciences, Sigma Aldrich and Thermo Fisher Scientific for providing important advice during the project.

Finally, I would like to acknowledge Macquarie University for providing me with the International Macquarie University Research Excellence Scholarship for MRes Year 2, Sydney Vital for providing me with funding for the project, and above all the beautiful country of Australia for giving me the opportunity to carry out my dream project on oral cancer. I love you Australia.

Abstract

Introduction: Oral biofilms harbour Gram-negative and Gram-positive bacterial antigens—lipopolysaccharide (LPS) and lipoteichoic acid (LTA) respectively. LPS and alterations in calcium channels are known to influence oral cancer progression. Drugs that respectively activate or block these channels include the TRPV1 agonist capsaicin and ML218 HCl, a T-type voltage-gated calcium channel blocker.

Hypothesis: Calcium channel drugs can reduce LPS-induced oral cancer cell proliferation.

Method: Oral cancer cell lines SCC4, SCC9, SCC25 and CAL27, and the normal oral cell line OKF6 were used in this project. The level of calcium channel receptors expression was determined using qPCR. The effect on oral cancer cell proliferation of stimulation with LPS, LTA, ML218 HCl and capsaicin, either singly or in combination, was determined using MT Glo, trypan blue and clonogenic assays. RT-qPCR, phosphokinase array, western blot, TNF α ELISA and caspase-3/7 assays were employed to study proliferative and apoptotic pathways in bacterial antigen-stimulated oral cancer cells exposed to calcium channel drugs.

Result: CAL27 showed higher Cav 3.3 ($p \leq 0.05$), TRPV1 (by 20%) and lower Cav 3.1 (by 20%) expression than normal oral cells. Bacterial antigens stimulated CAL27 ($p \leq 0.001$). CAL27 proliferation was lowest with treatment conditions involving ML218 HCl ($p \leq 0.001$). Bacterial antigens and calcium channel drugs affected the expression of proliferation and tumour suppression factors ($p \leq 0.001$).

Conclusions: Bacterial antigens stimulate oral cancer cell proliferation, while calcium channel drugs reduce this effect. ML218 HCl may be a suitable drug for future treatment of oral cancer.

Statement of Conflict of Interest

I declare that there are no conflicts of interest and this project was conducted without any commercial interest. I have undertaken the project abiding by the intellectual property policies of Macquarie University.

Rajdeep Chakraborty

Assoc Prof Karen Vickery

Dr Honghua Hu

Prof Shoba Ranganathan

Dr Charbel Darido

Contents

List of figures

List of tables

1

Introduction

1.1 Normal oral histology

The mucosal lining of the oral cavity functions to protect the underlying tissue from mechanical, chemical and microorganism-induced insults (Squier & Kremer, 2001). The mucosa of the mouth and oesophagus differ from the lining of the gastrointestinal tract, with which it is continuous (Squier & Kremer, 2001). Oral mucosa has more in common with skin, in that it forms a junction at the lips (Squier & Kremer, 2001).

The soft tissue of the human oral cavity is covered by a stratified squamous cell epithelium (Jones & Klein, 2013; Squier & Kremer, 2001). Regions subject to mechanical forces (gingiva and hard palate) are covered by a keratinised epithelium that is tightly attached to the underlying tissues by collagenous connective tissue or lamina propria, while regions that require flexibility to accommodate the processes of mastication and speech (floor and buccal aspects of the mouth) are covered with a non-keratinised epithelium (Jones & Klein, 2013; Squier & Kremer, 2001). The tongue is covered by a specialised epithelium, which can be represented as a mosaic of keratinised and non-keratinised epithelia (Squier & Kremer, 2001).

The main ultrastructural features that characterise both keratinised and non-keratinised oral epithelia include a basal layer, spinous layer, granular layer and superficial layer

(Jones & Klein, 2013; Squier & Kremer, 2001). The basal layer attaches to the underlying connective tissue through the lamina propria via rete ridges (crypts formed by invagination of the epithelium into the lamina propria) (Squier & Kremer, 2001).

1.2 Normal bacterial flora of the oral environment

The oral cavity comprises many surfaces, each covered with a plethora of microorganisms (Aas et al., 2005). Among these the predominant species are bacteria, creating what is known as a bacterial biofilm (Aas et al., 2005).

A total of 141 bacterial taxa representing six phyla have been detected in the human mouth (Aas et al., 2005). These phyla are the *Firmicutes* (Gram-positive species such as *Streptococcus*, *Gemella*, *Eubacterium*, *Selenomonas* and *Veillonella*); *Actinobacteria* (Gram-positive species such as *Actinomyces*, *Atopobium* and *Rothia*); *Proteobacteria* (e.g. *Neisseria*, *Eikenella* and *Campylobacter*); *Bacteroidetes* (e.g. *Porphyromonas*, *Prevotella* and *Capnocytophaga*); *Fusobacteria* (e.g. *Fusobacterium* and *Leptotrichia*); and *Saccharibacteria* (Aas et al., 2005).

There is a distinctive bacterial flora in the healthy oral cavity, which differs from that in oral disease (Aas et al., 2005; Huang, Li & Gregory, 2011). For example, species associated with periodontal disease, such as *Porphyromonas gingivalis*, *Tannerella forsythensis* and *Treponema denticola*, are not detected in the healthy oral cavity (Huang, Li & Gregory, 2011).

1.3 Bacteria involved in oral biofilm formation

The reason for the increased number of virulent species such as *Streptococcus mutans* and *Porphyromonas gingivalis (P. gingivalis)*in oral disease can be attributed to the formation of the biofilm (Huang, Li & Gregory, 2011). The oral biofilm is unique among various types of biofilm as it typically requires the host salivary glycoproteins for attachment (Huang, Li & Gregory, 2011). Bacterial biofilm formation occurs by three steps: (1) initial adhesion, (2) maturation and (3) dispersion of biofilm cells (Huang, Li & Gregory, 2011).

The initial adhesion of *Actinomyces* spp., *Streptococcus* spp., *Haemophilus* spp. and *Capnocytophaga* spp. helps later-colonising species occupy space and gain an advantage in later competition with other species (Huang, Li & Gregory, 2011). During the maturation step, later-colonising bacteria such as *Fusobacterium nucleatum*, *Treponema* spp., *Tannerella forsythensis*, *P. gingivalis* and *Aggregatibacter actinomycetemcomitans* recognise the polysaccharide or protein receptors on the pioneer bacterial cell surfaces and attach to them, forming the typical corn-cob and bristle-brush forms, among others, in mature oral biofilm (Huang, Li & Gregory, 2011).

Anaerobic bacteria such as *P. gingivalis* and *Fusobacterium nucleatum* have been observed to be associated with periodontal disease (Karpinski, 2019; Utispan et al., 2018). Further, they have been found to promote oral cancer progression by causing proliferation of cancer cells through activation of the JAK/STAT and Wnt pathways (Karpinski, 2019; Utispan et al., 2018).

1.4 Oral cancer incidence and pathophysiology

Oral cancer is the third most common cancer in India and the sixth most common cancer in the world (Coelho, 2012). Oral cancer is one of the top 10 most diagnosed cancers in Oceania (Elwood et al., 2014). It is predicted that by 2030 there will be an increase of 45% of oral cancer cases in Oceania (Elwood et al., 2014). The use of alcohol and tobacco is the major causative agent in oral cancer (Das & Nagpal, 2002). More than 90% of oral cancers are squamous cell carcinomas (Das & Nagpal, 2002). Oral squamous cell carcinomas occur after the squamous cell epithelium encounters dysplastic changes that lead to precancerous lesions like erythroplakia and leucoplakia (Reibel, 2003). According to the Pindborg classification (1997), epithelial dysplasia can be diagnosed by the loss of polarity of the basal cells, increased nuclear–cytoplasmic ratio, drop-shaped rete ridges, irregular epithelial stratification, increased number of mitotic cells, cellular and nuclear pleomorphism, loss of intercellular adherence and increased keratinisation (Reibel, 2003). Based on the Pindborg classification and Ljubljana system, epithelial dysplasia can be categorised as Grade 1 (simple hyperplasia), Grade 2 (basal hyperplasia), Grade 3 (atypical hyperplasia) or Grade 4 (carcinoma in situ) (Reibel, 2003).

1.5 Molecular biological aspects of cancer

Cancer proliferates via various mechanisms, including the (a) Wnt (Zhan, Rindtorff & Boutros, 2017), (b) PI3K/Akt (Martini et al., 2014), (c) Ras/MAPK (Molina & Adjei, 2006), (d) JAK/STAT (Thomas et al., 2015), (e) TGFβ/Smad3/4 (Millet & Zhang, 2007) and (f) mTOR pathways (Populo, Lopes & Soares, 2012) (Figure 1.1). All these pathways have been seen to be inhibited by tumour suppressor proteins such as p53 (cell cycle regulator and apoptosis), Chk2 (checkpoint kinase 2) and SOCS3 (suppressor of cytokine signalling 3) (Yang & Karin, 2014).

The interaction of TGFβ (transforming growth factor beta) with Smad3/4 (part of the bone morphogenetic protein family) results in TGFβ target genes being activated by STAT3 (signal transducer and activator of transcription 3), followed by proliferation (Thaker et al., 2013). GSK3β (glycogen synthase kinase 3 beta) is activated by DSH (dishevelled cytoplasmic phosphoprotein). LRP (low-density lipoprotein-related protein) inhibits β-catenin, which is activated by α-catenin and β-catenin interaction following activation of E-cadherin (responsible for cell–cell interaction). Then, β-catenin translocates to the nucleus and activates TCF (T-cell factor) and LEF (lymphoid-enhancer factor), which activates cyclin D1, c-myc and other matrix metalloproteinase (MMP) genes to produce proteins responsible for cancer proliferation and metastasis (Thaker et al., 2013). Ras (serine/threonine protein kinase) activates RAF, MEK (serine/tyrosine/threonine kinase) and ERK (extracellular receptor kinase), which leads to proliferation that is inhibited by SOCS3 (Yu & Jove, 2004); PI3K (phosphoinositide 3-kinase) activation transforms PIP2 (phosphatidylinositol (3,4)) bisphosphates to PIP3 (phosphatidylinositol (3,4,5)) trisphosphates, which leads to the activation of Akt (protein kinase B) to proliferation (Liu et al., 2009), inhibited by SOCS3 (Francipane et al., 2009). Akt activation leads to TSC1 and TSC2 (tuberous sclerosis 1 and 2) complex interactions, which activates Rheb (Ras homolog enriched in brain), which leads to mTOR (mechanistic target of rapamycin) activation, which leads to S6K (ribosomal 40S subunit substrate 6 kinase protein) activation and ultimately to proliferation (Laplante & Sabatini, 2009). IL-6 (interleukin 6) phosphorylates gp130 (glycoprotein 130), which leads to autophosphorylation of serine 757 in the STAT3 domain, activating the JAK/STAT pathway to proliferation (Johnson, O'Keefe & Grandis 2018), which is also inhibited by SOCS3 (Croker, Kiu & Nicholson 2008).
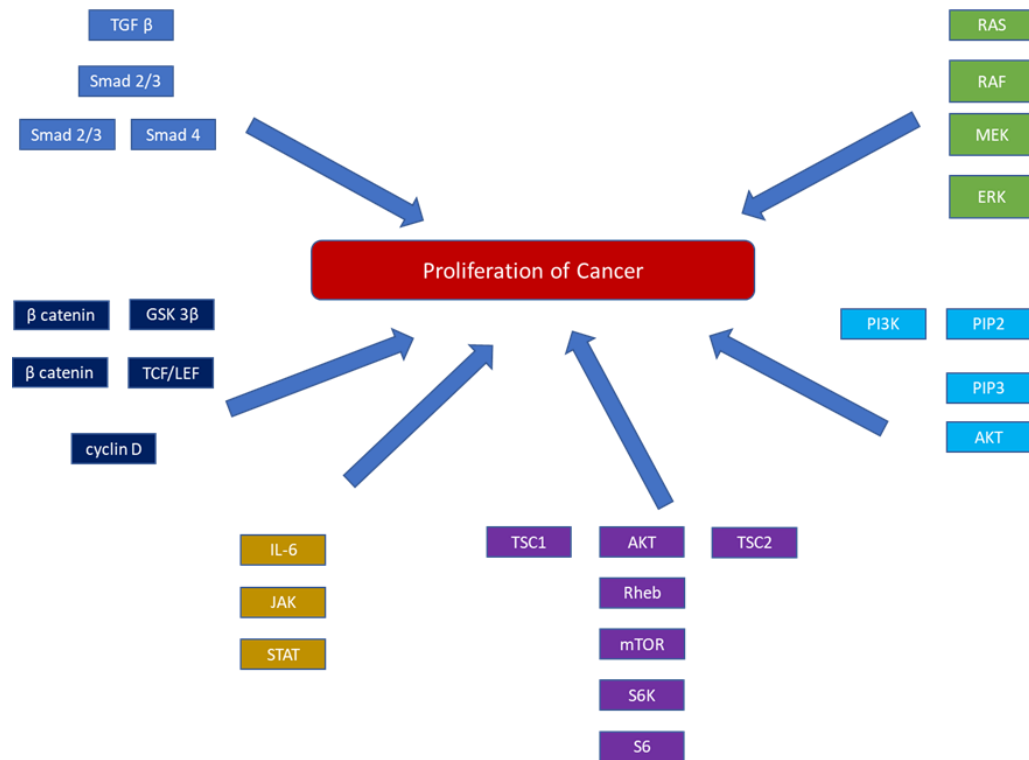
FIGURE 1.1: Various pathways of cancer cell proliferation. Six different pathways of cancer cell proliferation are shown in the figure.

1.6 Molecular biological aspects of oral cancer

Genetic alterations have been linked to oral cancer progression (Das & Nagpal, 2002). These genetic perturbations provide a yardstick by which to estimate the degree of genetic damage (Das & Nagpal, 2002). Genetic alterations, particularly related to oncogenes (whose overexpression leads to uncontrolled proliferation of cells and tumorigenesis) such as epidermal growth factor receptor (*EGFR*), mitogen-activated kinases (*c-Myc/K-ras*), the Wingless pathway (*cyclin D*), *STAT3* and phosphoinositide 3-kinase (*PIK3CA*) have been previously seen to be upregulated in the oral squamous cell carcinoma (Das & Nagpal, 2002).

Tumour suppressors have profound effects on cell cycle progression (Cotran et al., 1999). Loss of tumour suppressor proteins has shown progression of precancerous conditions to cancer (Cotran et al., 1999). A number of tumour suppressor genes and proteins have been discovered, including Rb (cell cycle regulator) (Du & Searle, 2009), p53 (Ozaki & Nakagawara, 2011), WT1 (transcriptional regulation) (Qi et al., 2015), NF1 (Ras inactivation) (Kiuru & Busam, 2017), APC (signalling through adhesion molecules to

nucleus) (Aoki & Taketo, 2007), MEN1 (DNA repair) (Marini et al., 2009), MSH2/MLH1 (DNA mismatch repair) (Dowty et al., 2013), VHL (activation of ubiquitin complex) (Kim & Kaelin, 2004), TSC1/TSC2 (inhibitor of mTOR) (Rosset, Netto & Ashton-Prolla, 2017), DPC4/SMAD4 (TGFβ/BMP signal regulator) (Zhao, Mishra & Deng, 2018), BRCA1/BRCA2 (DNA repair/chromosomal stability) (Sopik et al., 2015), SOCS3 (inhibits JAK/STAT pathway [Croker et al., 2008] and upregulates cytotoxic T-cells [Yu et al., 2003]), which helps in the regression of cancer and p16, which encodes a protein kinase that phosphorylates/inactivates cyclin-dependent kinase 4, which inactivates pRb (retinoblastoma protein) (Das & Nagpal, 2002). Previous studies have shown that loss of function of SOCS3, p53, p16 and Rb is associated with the initiation and growth of oral cancer cells (Das & Nagpal, 2002).

Loss of telomeres during cell division leads to the fusion of chromosomes and karyotypic abnormality, resulting in cell death (Das & Nagpal, 2002). Telomerase (ribonucleoprotein enzyme) inhibits the loss of telomeres (Das & Nagpal, 2002). It is inactive in normal epithelial cells but almost 100% active in all oral cancer cell lines and dysplastic lesions (Das & Nagpal, 2002).

1.7 Lipopolysaccharide and lipoteichoic acid

Lipopolysaccharides (LPS) are found in the cell wall of Gram-negative bacteria such as *P. gingivalis* and *Fusobacterium nucleatum*, which take part in biofilm formation (Utispan et al., 2018). LPS have been reported to be associated with the progression of oral cancer (Utispan et al., 2018).

LPS occur in the outer layer of the cell membrane of non-capsulated strains of the cell surface of Gram-negative anaerobic bacteria (Raetz & Whitfield, 2002). They contribute to the integrity of the cell membrane and protect the bacteria against the action of lipophilic antibiotics and bile salts (Raetz & Whitfield, 2002).

LPS are composed of a hydrophobic lipid (that exhibits toxic properties), a hydrophilic core polysaccharide chain and a hydrophilic O-antigenic polysaccharide side chain (Raetz & Whitfield, 2002). Strain-specific structural diversity is exhibited by a change in the structure of the O-antigenic oligosaccharide side chain (sugar constituent, sequence of the oligosaccharide and the linkage mode) (Raetz & Whitfield, 2002).

Since LPS confer antigenic properties on the cell, they have been termed O-antigens (Raetz & Whitfield, 2002). These O-antigens protect Gram-negative bacteria from phagocytosis and lysis (Raetz & Whitfield, 2002). There are different serotypes of bacteria depending on the oligosaccharide side chain (Raetz & Whitfield, 2002). The common serotypes are O, H and LPS (Raetz & Whitfield, 2002). Bacteria with common serotypes share antigenic properties (Raetz & Whitfield, 2002); for example, O55:B5 and O26:B6 for the *Escherichia coli (E. coli)* bacterium exhibit similar antigenic properties (Raetz & Whitfield, 2002).

Lipoteichoic acid (LTA) is a teichoic acid (highly immunogenic polymer made from ribitol-phosphate and/or glycerol phosphate) that is found in the cell wall of Gram-positive bacteria like *Streptococcus* spp. (Neuhaus & Baddiley, 2003). LTA is an amphipathic (i.e. it has both polar and non-polar ends) linear polymer of phosphodiester-linked glycerol phosphates bound to a lipid by covalent bonding (Neuhaus & Baddiley, 2003). LTA is thought to act as an adhesin (Neuhaus & Baddiley, 2003). It helps Gram-positive bacteria to bind to the host tissue and helps other bacteria to colonise and form a biofilm (Neuhaus & Baddiley, 2003).

LTA from *Staphylococcus aureus* has been shown to stimulate proliferation of human non-small cell lung cancer cells (Hattar et al., 2017). However, the possible molecular biological aspects of the proliferation of cancer cells by LTA remain elusive (Hattar et al., 2017).

1.8 The role of LPS and LTA in oral cancer

Previous studies have shown that *P. gingivalis* LPS at high concentrations tend to increase the viability of oral cancer cells (Goncalves et al., 2016). Studies of the tumour microenvironment have shown that macrophages demonstrate increased IL-6 and CD14 expression after the stimulation of LPS (Karpinski, 2019) (Figure 1.2). *P. gingivalis* LPS-induced macrophages increase their nitric oxide secretion (Karpinski, 2019). Bacterial infection has been shown to be associated with chronic inflammation, anti-apoptotic activity and pro-proliferative activities (Karpinski, 2019). *Fusobacterium nucleutum* LPS has been shown to upregulate β-catenin, which activates the c-myc, NF-kB and cyclin D kinases, resulting in the activation of cyclin D and consequent cell survival and proliferation (Karpinski, 2019) (Figure 1.2). On the other hand, *F. nucleutum* LPS

activates p38, which activates MMP-9 and MMP-13, which results in oral cancer invasion (Karpinski, 2019). Conversely, *P. gingivalis* LPS downregulates p53 and upregulates NF-kB, MMP-9 and the JAK/STAT pathway, particularly STAT3 (which controls the intrinsic mitochondrial apoptotic pathway) (Karpinski, 2019) (Figure 1.2). This results in inflammation, anti-apoptosis, increased viability of oral cancer cells and increased oral cancer invasion (Karpinski, 2019). It has been reported that in macrophages, LPS upregulate tumour necrosis factor alpha (TNFα), which induces SOCS3 and inhibits IL-6-induced activation of STAT3 (Bode et al., 1999); whereas the LPS–squamous cell carcinoma–monocyte interaction leads to rapid STAT3 activation (Kurago et al., 2008) (Figure 1.2).

LPS are also known to trigger inflammatory reactions that result in cancer invasion and angiogenesis (new blood circulation for tumour cells) (Hsu et al., 2011). Toll-like receptors are expressed in many cancer cells (Hsu et al., 2011). TLR4 (one of the toll-like receptor variants) has been found in many cancer cells, including those in breast, colon, pancreatic and liver cancer (Hsu et al., 2011). TLR4 is a specific receptor of LPS (Hsu et al., 2011). In breast cancer cells, the LPS/TLR4 axis was found to be strongly associated with the metastasis of the tumour cells (Seol et al., 2017). It has also been found that the LPS/TLR4 axis activates TOPK (T-LAK cell-originated protein kinase), MAPK (serine/threonine mitogen-activated protein kinase) and iNOS (inducible nitric oxide synthase), which are highly expressed in various cancer cases and are related to tumorigenesis (Seol et al., 2017). Also, LPS-activated TOPK has been seen to upregulate MMP-9 via NF-kB (nuclear factor kappa light chain enhancer of activated B cells) (Seol et al., 2017). MMP-9 (a 92-kDa type IV collagenase) mediates extracellular matrix remodelling and metastasis by degrading type IV and type V collagens (Seol et al., 2017). It has shown that LPS stimulation of MCF-7 (breast cancer cell line) results in upregulation of IL-6, VEGF (vascular endothelial growth factor), which helps in angiogenesis, and MMP-9 (Seol et al., 2017). LPS-induced TLR4 signalling has also been seen to upregulate β1 integrin-mediated cell adhesion and metastasis via activation of PI3K/Akt signal, by activating oncogenes such as *PI3KCA* (Hsu et al., 2011).

Other oncogenes, such as *EGFR* are trans-activated by LPS-induced COX-2 (cyclooxygenase-2), which increases inflammatory mediators in the tumour microenvironment and helps in the progression of various cancers (McElroy et al., 2012).

Inflammatory changes in bronchial epithelium by LPS induce expression of PI3K/Akt, ERK, NF-kB, and FKN (fractalkaline, encoded by *CX3CL1*) ([Jiang et al., 2016](#)).

Human hepatocyte growth factor (HuHGF)—which has been shown to be associated with the progression of oral cancer by stimulating stromal fibroblast-induced invasion (epithelial mesenchymal cells) ([Matsumoto et al., 2017](#))—has been seen to be upregulated by LTA from *Streptococcus mutans*, *Streptococcus pyogenes*, *Streptococcus faecalis*, *Streptococcus sanguis* and *Streptococcus aureus* ([Sugiyama et al., 1996](#)) (Figure 1.2). Other than its induction of HuHGF, the role of LTA in the proliferation of oral cancer cells remains elusive ([Sugiyama et al., 1996](#)).
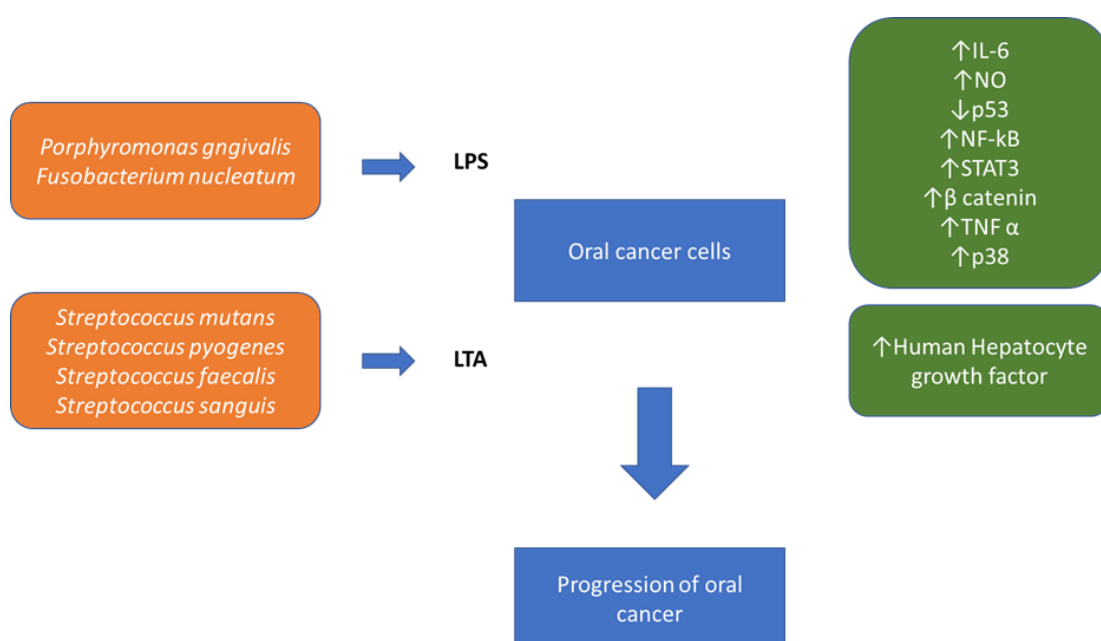
FIGURE 1.2: Bacterial antigen in oral cancer cell proliferation. LPS previously found to be downregulating tumour suppressor proteins (p53 and related proteins) and upregulating anti-apoptotic mechanisms (JAK/STAT and Wnt pathways). LTA previously found to upregulate proliferation related protein (Human Hepatocyte growth factor).

1.9 Calcium and cancer

Calcium channels are linked directly or indirectly to all the 'hallmarks of cancer' (Monteith et al., 2012) (Table 1.1). Changes in the same calcium channel, pumps, and exchangers that occur in their normal counterpart also occur in cancer cells (Monteith et al., 2012). Pronounced changes in expression levels, altered cellular localisation, altered post-translational modifications, genetic mutations and changes in the activity of calcium channels lead to alterations in the calcium flux across plasma membrane and intracellular organelles in cancer cells, relative to their normal counterparts (Monteith et al., 2012). The influx of calcium across the plasma membrane triggers tumour proliferation, migration, differentiation and apoptosis (Varghese et al., 2019). Calcium oscillations thus can result in both proliferation and apoptosis of cancer cells via the calcium endoplasmic reticulum–mitochondrial calcium transfer axis (Pinton et al., 2008).

TABLE 1.1: Role of calcium in hallmarks of cancer.

Aspect of cancer	Mechanisms	Role of calcium	References
Sustaining proliferating signals	RAS, MYC; B-Raf; MAPK; PI3K/Akt/PKB; loss of function of PTEN (phosphatase & tensin homologue)	Calcium & p38 play important roles in apoptotic signalling pathways	(Hanahan & Weinberg, 2011; Mu et al., 2008)
Evading growth suppressors	Loss of function of TP53 & RB; defect in NF2 (neurofibromatosis 2) gene product; defect in LKB1, mechanism of contact inhibition; aberrant behaviour of TGFβ	Calcium regulates p53-dependent apoptosis	(Hanahan & Weinberg, 2011; Scotto et al., 1998)
Resisting cell death	Autophagy; necrosis	Calcium signalling regulates autophagy	(Hanahan & Weinberg, 2011; Medina et al., 2015)
Enabling replicative immortality	Telomere, TERT (telomerase reverse transcriptase); BFB (break–fusion–bridge) cycles	Upregulation of intracellular calcium downregulates telomerase activity	(Bickenbach et al., 1998; Hanahan & Weinberg, 2011)
Inducing angiogenesis	VEGF, TSP-1 (thrombospondin 1), FGF (fibroblast growth factor)	Calcium affects VEGF and angiogenesis	(Faehling et al., 2002; Hanahan & Weinberg, 2011)

Aspect of cancer	Mechanisms	Role of calcium	References
Invasion and metastasis	EMT (epithelial–mesenchymal transition) & MET (mesenchymal epithelial transition); reduction of E-cadherin, Snail, Slug, Twist & Zeb 1/2; RANTES CCL5 (chemotactic cytokine 5)	EMT is calcium signal dependent	(Davis et al., 2014; Hanahan & Weinberg, 2011)
Tumour-promoting inflammation	Chemokines, cytokines & prostaglandins	Prostaglandin synthesis depends on cellular levels of calcium	(Hanahan & Weinberg, 2011; Hassid & Oudinet, 1986)
Genome instability and mutation	Comparative genomic hybridization revealed loss and gain of gene copy numbers across the genome	Copy number variation is highly correlated with differential gene expression related to calcium signalling	(Hanahan & Weinberg, 2011; Shao et al., 2019)
Dysregulating cellular energetics	Glycolysis & anaerobic glycolysis by upregulating GLUT1 (glucose transporter 1); altered calcium homeostasis	Mitochondrial calcium uptake drives aerobic glycolysis in various cancers	(Chakraborty et al., 2017; Hanahan & Weinberg, 2011)
Avoiding immune destruction	CD8+ CTLs (cytotoxic T lymphocytes), CD4+ Th1 helper T cells or natural killer cells decrease; upregulation of Treg; binding of Treg to APC leading to T-cell anergy & death	Malignant T-cells show increased response to calcium signalling	(Hanahan & Weinberg, 2011; Stewart, Yapa & Monteith, 2015)

Molecular biological aspects of the calcium channel and cancer progression are shown in Figure 1.3. Various types of calcium channels and their roles in different cancers are shown in Table 1.2. T-type voltage-gated calcium channel Cav 3.1, Cav 3.2 and Cav 3.3, and other voltage-gated channels like Cav 1.1 and L-type voltage-gated calcium channels affect the proliferation of cells (Varghese et al., 2019). RDC (receptor-dependent calcium channel) and SMDC (second messenger-dependent calcium channel) affect the apoptosis of cells (Varghese et al., 2019). They cause mitochondrial calcium overload, resulting in activation of cytochrome-c, which activates caspase-9 and caspase-3, resulting in apoptosis (Varghese et al., 2019). VDCC (voltage-dependent calcium channel), ORai (store-dependent calcium channel), RDC and SMDC also lead to the entry of calcium

channels into the cytosol, which activates the MAPK pathway and upregulates transcription factors like c-JUN, NF-kB and c-myc, resulting in the proliferation of cancer cells (Capiod, 2016). Calcium channels are mainly activated during the G1/S phase transition of the cell cycle. The calcium influx/efflux via T-type calcium channels affects the intracellular calcium concentration, which affects the G1/S phase transition of the cell cycle, which determines whether the cancer cells will undergo differentiation or proliferation (Lory, Bidaud & Chemin, 2006).
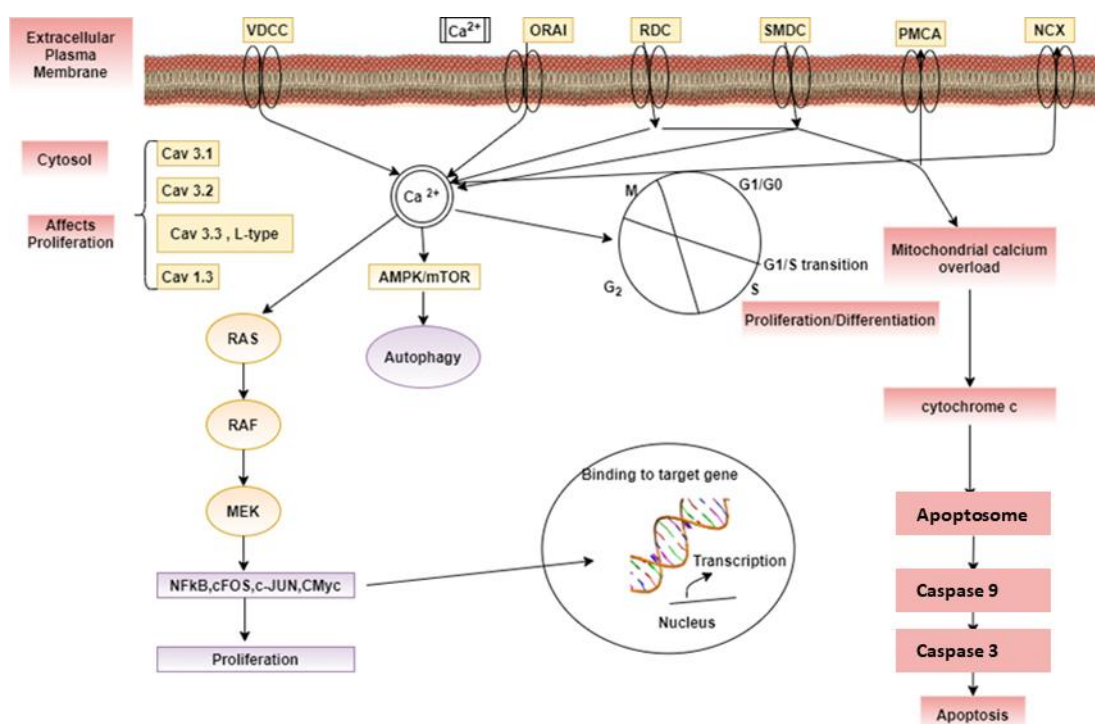
FIGURE 1.3: Calcium signal in proliferation, differentiation and apoptosis. Calcium balance is regulated by different calcium channels and pumps on various biological membranes. VDCC is voltage-dependent calcium channels; ORai is a store-dependent calcium channel or calcium release-activated calcium channel protein 1; RDC is receptor-dependent calcium channel; SMDC is second messenger-dependent calcium channel; PMCA is plasma membrane calcium-ATPase channel.

TABLE 1.2: Calcium channels and cancer.

Receptor	Receptor name	Gene	Genomic location and site	Role in cancer	Reference
TRPC1	Transient receptor potential cation channel (TRPC) subfamily C member 1	*TRPC1*	Chromosome 3	Upregulated in breast cancer tissue samples	(Monteith et al., 2012)
TRPC6	TRPC subfamily C member 6	*TRPC6*	Chromosome 11	Increased expression in oesophageal, liver & breast cancer	(Monteith et al., 2012)
TRPV1	TRPC subfamily V member 1	*TRPV1*	Chromosome 17, mainly found in the liver	Blocking of TRPV1 shown to decrease bone cancer-related pain	(Ghilardi et al., 2005)
TRPA1	TRPC subfamily A member 1	*TRPA1*	Chromosome 8, mainly found in the gastrointestinal tract & renal tissue	Blocking of TRPA1 shown to decrease chemotherapy-induced persistent sensory neuropathy	(Trevisan et al., 2013)
TRPC3	TRPC subfamily C member 3	*TRPC3*	Chromosome 4	Increased expression in ovarian & breast cancer	(Monteith et al., 2012)
TRPM7	TRPC subfamily M member 7	*TRPM7*	Chromosome 15	Increased expression in pancreatic & breast cancer	(Monteith et al., 2012)
TRPM8	TRPC subfamily M member 8	*TRPM8*	Chromosome 2	Increased expression in pancreatic, prostate, colorectal & breast cancer, & melanoma	(Monteith et al., 2012)

Receptor	Receptor name	Gene	Genomic location and site	Role in cancer	Reference
TRPV6	TRPC subfamily V member 6	*TRPV6*	Chromosome 7	Increased expression in pancreatic, prostate, colorectal, thyroid, ovary & breast cancer	(Monteith et al., 2012)
Cav 3.1	Calcium voltage-gated channel subunit alpha1 G	*CACNA1G*	Chromosome 17, mainly found in the brain	Inactivated in various cancers; may play a role in proliferation & apoptosis; associated with apoptotic resistance & proliferation of neuroblastomas, lung cancer & pancreatic cancer	(Toyota et al., 1999)
Cav 3.2	Calcium voltage-gated channel subunit alpha1 H	*CACNA1H*	Chromosome 16, mainly found in the brain	Lower expression levels seen in various cancers & are associated with proliferation, differentiation & apoptotic resistance of breast & prostate cancers	(Buchanan & McCloskey, 2016; Phan et al., 2017)
Cav 3.3	Calcium voltage-gated channel subunit alpha1 I	*CACNA1I*	Chromosome 22, mainly found in the breast	Lower expression levels seen in various cancers & are associated with proliferation of oesophageal cancer	(Buchanan & McCloskey, 2016; Phan et al., 2017)
Cav 1.2	Calcium voltage-gated channel subunit	*CACNA1C*	Chromosome 12	Increased expression in colorectal cancer	(Monteith et al., 2012)
ORai1	Store-dependent calcium channels 1	*ORai1*	Chromosome 12	Increased expression in breast cancer	(Monteith et al., 2012)

Receptor	Receptor name	Gene	Genomic location and site	Role in cancer	Reference
PMCA2	Plasma membrane calcium ATPase 2	*ATP2B1*	Chromosome 12	Increased expression in breast cancer	(Monteith et al., 2012)
PMCA4	Plasma membrane calcium ATPase 4	*ATP2B4*	Chromosome 1	Decreased expression in colon cancer	(Monteith et al., 2012)
SERCA2	Sarcoplasmic /endoplasmic reticulum calcium ATPase 2	*ATP2A2*	Chromosome 12	Decreased expression in oral cancer	(Endo et al., 2004)
SERCA3	Sarcoplasmic /endoplasmic reticulum calcium ATPase 3	*ATP2A3*	Chromosome 17	Decreased expression in colon and breast cancer	(Gelebart et al., 2002)

1.10 The role of calcium channels in oral cancer

Changes in calcium channels result in the progression of oral cancer (Endo et al., 2004). PMCA1 (plasma membrane calcium ATPase 1) silencing, SERCA2 (sarcoplasmic/endoplasmic reticulum calcium ATPase) downregulation and abrogation of the function of SERCA2 have been found to be responsible for oral squamous cell tumour growth (Saito et al., 2006). TRPV1 (TRPC subfamily V member 1) and TRPA1 mediate oral cancer-related pain (Gonzales et al., 2014; Ruparel et al., 2015). TRPM8 has been shown to play a role in the migration and invasion of oral cancer cell lines (HSC3 and HSC4) via enhanced MMP-9 activity (Okamoto et al., 2012). Finally, Orai1 has been found to promote oral cancer stem cell proliferation (Lee et al., 2016).

1.11 Hypothesis

Calcium channel drugs can reduce LPS-induced oral cancer cell proliferation.

1.12 Aim of the project

The aims of this study were to identify:

- the presence of calcium channel receptors in oral cancer and normal oral cells
- the effect of calcium channel drugs on oral cancer cell proliferation in the presence and absence of oral bacterial antigens
- the effect of calcium channel drugs on oral cancer cell proliferation pathways and apoptotic pathways in the presence and absence of oral bacterial antigens.

1.13 The experimental model

To accomplish the aims of the project an experimental model was designed (Figure 1.4). Biofilms are formed by initial-coloniser Gram-positive bacteria containing LTA antigen, and Gram-negative bacteria containing LPS antigen. This study hypothesised that both play a potent role in the growth of oral cancer cells. Oral cancer cells were therefore stimulated with both of these bacterial antigens. They were then treated with calcium channel drugs to examine their effects on proliferation (via MT Glo, trypan blue live/dead cell count and clonogenic assay), apoptosis (via caspase-3/7 live cell green detection assay), expression of SOCS3/STAT3/EGFR/PI3K (via quantitative reverse transcription polymerase chain reaction [RT-qPCR] and western blot) and proliferating factors (via phosphokinase array proteome profiling).
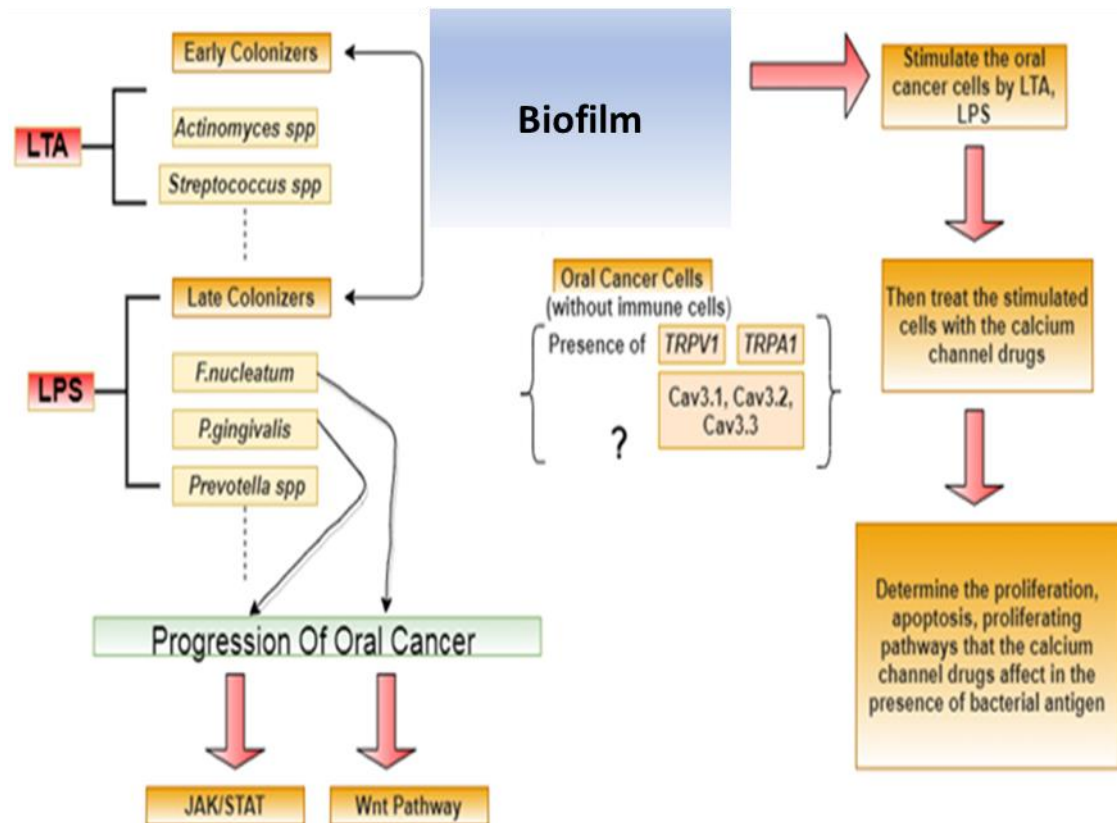
FIGURE 1.4: The experimental model. The presence of calcium channels was first identified in oral cancer and normal cells. Oral cancer cells were then stimulated using LTA and LPS. Cells were then treated with calcium channel drugs to identify proliferation, apoptosis and proliferating pathways affected by the calcium channel drugs in the presence of bacterial antigens.

2

Cell Lines and Materials

Two types of cell line were used for the project: (a) adherent and (b) non-adherent. The adherent cell lines used were SCC4, SCC9, SCC25, CAL27, OKF6, SHSY5Y, HT-29 and MCF-7. PBMC was the non-adherent cell line. Four oral cancer cell lines—SCC4 (ATCC CRL-1623), SCC9 (ATCC CRL-1629), SCC25 (ATCC CRL-1628), CAL27 (ATCC CRL-2095)—and one normal oral cell line OKF6 (CVCL_L222) were used in this study in collaboration with Dr Charbel Darido from the Peter MacCallum Cancer Research Centre at the University of Melbourne (Tables 2.1 and A2). These cells are epithelial-like adherent cell types. Molecular profiling of head and neck cancer cell lines has shown that SCC4, SCC9, SCC25, CAL27 and OKF6 can be used as preclinical models for oral cancer translational research. (Li et al., 2014) SCC4, SCC9, SCC25 and CAL27 are derived from the primary sites of tongue squamous cell carcinoma. Other head and neck cancer cell lines such as HSC2, HSC3 and HSC4, which are derived from metastatic lymph nodes, were excluded.

As the project aimed to identify the presence of calcium channels and cannabinoid receptors CB1 and CB2 in the oral cancer cell and normal oral cell lines by quantitative (real-time) polymerase chain reaction (qPCR). A list of cell lines containing cannabinoid and calcium channel receptors acted as positive control for qPCR (Tables 2.2 and A3).

2.1 Maintenance of cell lines

2.1.1 Thawing of cells

After the adherent cell line frozen vials were thawed in a 37°C water bath, the thawed cell suspension was added drop by drop to growing medium containing appropriate growth factors (10% FBS or bovine pituitary extract + EGF) and antibiotics (1% P/S) in a 75-cm^2 flask to avoid heat or osmotic shock, which might reduce the viability of the cells. The flask was kept in an incubator (humidified) overnight at 37°C in 5% CO_2.

For PBMC, the thawed cell suspension was added to RPMI and then centrifuged at 1400 g for 8 minutes. To the cell pellet, 1 ml warm 1X PBS was added and the tube was re-centrifuged at 1400 g for 8 minutes. To the final pellet 1 ml of cold 1X PBS was added. Note that PBMC cells were not cultured further and experiments based on PBMC were performed immediately.

TABLE 2.1: Cell lines and their respective medium.

Cell line	Medium	Manufacturer of medium	Additives and concentration	Manufacturer of additives
SCC4	DMEM	Gibco	10% FBS + 100 units/ml penicillin and 100 µg/ml streptomycin	Life Technologies
SCC9	DMEM	Gibco	10% FBS + 100 units/ml penicillin and 100 µg/ml streptomycin	Life Technologies
SCC25	K-SFM	Life Technologies	human recombinant epithelial growth factor (EGF) (0.035 µg/µl), bovine pituitary extract (15.1 mg/ml) + 100 units/ml penicillin and 100 µg/ml streptomycin	Life Technologies
CAL27	DMEM	Gibco	10% FBS + 100 units/ml	Life Technologies

			penicillin and 100 µg/ml streptomycin	
OKF6	K-SFM	Life Technologies	human recombinant epithelial growth factor (EGF) (0.035 µg/µl), bovine pituitary extract (15.1 mg/ml) + 100 units/ml penicillin and 100 µg/ml streptomycin	Life Technologies

TABLE 2.2: Cell lines and their respective medium.

Cell line	Medium	Manufacturer of medium	Additives and concentration	Manufacturer of additives
MCF-7	DMEM	Gibco	10% FBS + 100 units/ml penicillin and 100 µg/ml streptomycin	Life Technologies
PBMC	RPMI	Gibco	-	-
HT-29	DMEM	Gibco	10% FBS + 100 units/ml penicillin and 100 µg/ml streptomycin	Life Technologies
SH-SY5Y	DMEM	Gibco	10% FBS + 100 units/ml penicillin and 100 µg/ml streptomycin	Life Technologies

2.1.2 Culture of cells

On the day following thawing, the adherent cell culture 75-cm^2 flask was visually assessed under the microscope for adherence. If satisfactory the medium (that contained DMSO) was removed using a sterile suction apparatus and 8 ml of fresh pre-warmed medium was then added. On the following days, the confluency of the cells was checked

by visual observation under microscope on a regular basis. At 90% confluence, cells were split/passaged.

2.1.3 Cell counting and viability

Ten µl of final cell suspension was added to 10 µl 0.4% trypan blue, mixed gently and kept for 30 seconds. Then 10 µl of the mixture was placed in the groove of a haemocytometer and the number of live cells was counted in each outline grid. The average cell count from each grid was multiplied by 10^4 to give a measure of cells/ml. The following formula was used to calculate the cell viability percentage: Cell viability % = (Number of live cells ÷ [Number of live cells + Number of dead cells]) x 100

2.1.4 Passaging of cells

After the appropriate time of trypsin incubation for each cell line, the cell suspension was collected and centrifuged at 1000 g for 5 minutes at 37°C. After centrifugation, the medium was removed and 2–3 ml medium added to the pellet, resulting in the final cell suspension. Each $75cm^2$ flask of cells acted as a biological replicate. Generally, the biological replicate was split into three technical replicates. Biological replicates i.e. flasks were usually (or always) from two or more different cell passages and conducted on different days (or at different time points). Throughout this thesis "n" refers to the number of biological replicates.

2.2 Flow of the project

After culturing the cell lines, the project determined the presence of calcium channel and cannabinoid receptors via qPCR. Then stimulated the oral cancer cells with various bacterial antigens and calcium channel drugs. Then various other assays were done to determine the effect of bacterial antigen and calcium channel drugs on the proliferation apoptosis of the oral cancer cells. List of materials used during the project are given in Table 2.3 and Table A1.

TABLE 2.3: List of materials used during the project.

Material	Manufacturer
Determination of gene expression of calcium channel receptor	
TaqMan Fast Advanced Cells-to-CT Kit	Thermo Fisher Scientific
Drugs and bacterial antigens	
LPS	Sigma-Aldrich
PHA	Sigma-Aldrich
LTA	Sigma-Aldrich
Capsazepine	Sigma-Aldrich
ML218 HCl (hydrochloride)	Tocris
Capsaicin	Sigma-Aldrich
CID16020046	Sigma-Aldrich
Calcium chloride	Univar
Proliferation assay	
RealTime-Glo MT Cell Viability Assay	Promega
Trypan blue stain 0.4%	Invitrogen
Crystal violet acetate	Sigma Aldrich
Methanol	Chem-Supply
Cell Countess cell-counting chamber slides	Invitrogen
Protein estimation	
Pierce BCA Protein Assay kit	Thermo Fisher Scientific
Kinase profiling	
Human Phospho-Kinase Array kit	R&D Systems
Determination of proliferation related gene expression	
Pure Link RNA mini kit	Invitrogen
Trizol reagent	Invitrogen
Ethyl alcohol	Sigma Aldrich
SSIV VILO Master mix W/ EzDNASE	Invitrogen
POWRUP SYBR Master Mix, 5 ml	Invitrogen
Chloroform	BDH AnalaR
MicroAmp Fast plate	Applied Biosciences, Life Biosystems
Optical adhesive cover	Applied Biosystems, Life Technologies
Western blot	
Human/Mouse SOCS-3 MAb	R&D Systems
Human/Mouse/Rat STAT3 MAb	R&D Systems
Human PI 3-Kinase p110 beta MAb	R&D Systems
Anti-G3PDH/GAPDH	R&D Systems
Human EGF R/ErbB1 Polyclonal Ab	R&D Systems
Novex Sharp pre-stained protein standard	Life Technologies
Clarity Western ECL Substrate	Bio-Rad
Ponceau S solution	Sigma-Aldrich
Anti-goat IgG HRP conjugate	R&D Systems
Anti-rabbit IgG HRP conjugate	R&D Systems
Anti-mouse IgG HRP conjugate	R&D Systems
NuPAGE LDS sample buffer (4X)	Invitrogen
NuPAGE 10% bis-tris gel	Invitrogen
NuPAGE 10% bis-tris gel	Invitrogen
20X NuPAGE MOPS SDS Running Buffer	Invitrogen
Apoptotic assay	
CellEvent Caspase-3/7 Green Detection Reagent	Invitrogen
TNF α assay	
Human TNF α ELISA kit	Invitrogen

3

Methods

3.1 Determination of calcium channel receptors

To determine the presence and differential expression of calcium channel receptors in the oral cancer and normal oral cells, quantitative PCR (qPCR) was performed. qPCR has previously been used to identify receptors or targets present in oral cancer cells (Arya et al., 2005). The thermostable Thermus aquaticus (Taq) DNA polymerase enzyme has 5' to 3' exonuclease activity, which was used to detect amplification of the target-specific probe (Lawyer et al., 1993). Probes were used to determine the presence of calcium channel and cannabinoid receptors (Table 3.1).

3.1.1 Selection of probes

TRPV1, TRPA1, Cav 3.1, Cav 3.2 and Cav 3.3 are calcium channel receptors. Since cannabinoids have also been shown to function via the selected calcium channels, the project also determined the presence of endogenous cannabinoid receptors related to various cancers, including CB1, CB2 and GPR55. Selection of probes was based on human genome maps available from Thermo Fisher Scientific https://www.thermofisher.com/order/genome-database/ .

Only probes with suffix_m were selected because they span exon–exon junctions, which helps to reduce the chances of genomic DNA (gDNA) amplification. Exons are protein coding components of the genome, while introns are non-functional coding regions.

3.1.2 Reference genes

qPCR can produce errors resulting from minor differences in the starting amounts of ribonucleic acid (RNA), the quality of RNA, differences in the synthesis efficiency of complementary deoxyribonucleic acid (cDNA) and PCR amplification. (Arya et al., 2005) To minimise errors and correct for sample–sample variation, an internal reference or housekeeping gene (RNA) was simultaneously amplified along with the target. (Arya et al., 2005) The target RNA gene expression values were normalised against the housekeeping gene values (Yuan et al., 2006). Reference gene commonly used in research employing oral cancer cells are GAPDH (glyceraldehyde 3-phosphate dehydrogenase) (Lallemant et al., 2009).

TABLE 3.1: Probes used in the project.

Name of the gene	Name of the receptor	Gene	Probe
TRPC subfamily V member 1	TRPV1	*TRPV1*	TaqMan Gene Expression Assay (FAM) Assay ID: Hs00218912_m1
TRPC subfamily A, member 1	TRPA1	*TRPA1*	TaqManGene Expression Assay (FAM) Assay ID: Hs00175798_m1
Calcium voltage-gated channel subunit alpha1 G	Cav 3.1	*CACNA1G*	TaqMan Gene Expression Assay (FAM) Assay ID: Hs00367969_m1
Calcium voltage-gated channel subunit alpha1 H	Cav 3.2	*CACNA1H*	TaqMan Gene Expression Assay (FAM) Assay ID: Hs01103527_m1
Calcium voltage-gated channel subunit alpha1 I	Cav 3.3	*CACNA1I*	TaqMan Gene Expression Assay (FAM) Assay ID: Hs01096207_m1
Glyceraldehyde 3-phosphate dehydrogenase	GAPDH	*GAPDH*	TaqMan Gene Expression Assay (FAM) Assay ID: Hs99999905_m1

Name of the gene	Name of the receptor	Gene	Probe
G protein-coupled receptor 55	GPR55	*GPR55*	TaqMan Gene Expression Assay (FAM) Assay ID: Hs00995276_m1
Cannabinoid receptor 1	CB1	*CNR1*	TaqMan Gene Expression Assay (FAM) Assay ID: Hs00275634_m1
Cannabinoid receptor 2	CB2	*CNR2*	TaqMan Gene Expression Assay (FAM) Assay ID: Hs00361490_m1

3.1.3 qPCR method

Following the manufacturer's instructions, the TaqMan Fast Advanced Cell-to-CT kit was used to conduct qPCR. To conduct qPCR, four positive control cell lines previously reported to express specific receptors and targets were used (Table 3.2).

TABLE 3.2: Positive control cell lines for specific receptors.

Cell line	Previously found cannabinoid receptor and target	References
MCF-7	TRPV1, Cav 3.2, Cav 3.3	(Buchanan & McCloskey, 2016; Vercelli et al., 2015)
HT-29	TRPA1	(Baram et al., 2019)
PBMC	CB2	(Nong et al., 2001)
SH-SY5Y	CB1 and Cav 3.1	(Marini et al., 2009)

First, lysis of adherent cells was performed to obtain total RNA. The lysis solution contained DNase I, which helps to minimise gDNA contamination in the sample. After lysis of the cells, 5 µl of stop solution was added per reaction to stop the activity of the lysis solution and avoid further degradation of the RNA/DNA (Table 3.3). The lysed sample was added to reverse transcription buffer and placed in a thermal cycler (Thermo Fisher Scientific) (set at 37°C for 30 min, followed by 95°C for 5 min and held at 4°C

until required) to convert total RNA to cDNA. cDNA (which acts as the template for the qPCR reaction) was combined with the qPCR cocktail (containing a TaqMan probe with a reporter fluorophore and quencher) prepared in a nuclease-free microcentrifuge tube at room temperature (Tables 3.4 and 3.6). Each qPCR plate contained internal control (reference gene), positive control, no-template controls and minus reverse transcription (RT) controls. Minus RT controls were used to determine whether the templates contained genomic contamination (Table 3.5). No-template controls were used to confirm that none of the qPCR reagents were contaminated with gDNA; or qPCR products from previous reactions. ViiA 7 System (384-well block) with TaqMan reagents was used to run the qPCR experiments. qPCR reactions were set up following the manufacturer's instructions (Tables 3.6 and 3.7). When the TaqMan probe is intact, the reporter and quencher remain close to each other, preventing emission of fluorescence. The primer and the TaqMan probe anneal to the cDNA strand (template) following denaturation via activation of endonuclease enzyme activity. After hybridisation and during extension of the forward primer, the 5' endonuclease activity of the TaqMan DNA polymerase results in cleavage of the probe, which separates the reporter and quencher, resulting in the emission of fluorescence (Arya et al., 2005). During the qPCR, Ct (threshold cycle) and ΔRn (fluorescence emission of the product at each time point minus fluorescence emission of the baseline, where baseline is defined as the qPCR cycle at which a reporter fluorescence signal accumulates below the limits of detection of the instrument) were noted (Arya et al., 2005). The threshold is 10 times the standard deviation of the average signal of the baseline fluorescent signal between cycles 3 and 15 (Arya et al., 2005). Ct is defined as the fractional qPCR cycle number at which the reporter fluorescence is greater than the threshold level (Arya et al., 2005).

TABLE 3.3: Lysis reaction.

Component	Volume		
	Per reaction	**96 reactions**	**384 reactions**
Lysis solution	49.5 µl	5.23 ml	20.91 ml
DNase I	0.5 µl	52.8 µl	211 µl
Total	50 µl	5.28 ml	21.12 ml

Note: Volume includes 10% excess

TABLE 3.4: Reverse transcription reaction.

Component	Volume		
	Per reaction	**96 reactions**	**384 reactions**
20X Fast advanced RT buffer	25 µl	2.64 ml	10.56 ml
20X Fast advanced RT enzyme mix	2.5 µl	264 µl	1.056 ml
Nuclease-free water	12.5 µl	1.32 ml	5.28 ml
Total	40 µl	4.22 ml	16.9 ml

Note: Volume includes 10% excess

TABLE 3.5: Negative reverse transcription reaction.

Component	Volume		
	Per reaction	**96 reactions**	**384 reactions**
20X Fast advanced RT buffer	25 µl	2.64 ml	10.56 ml
20X Fast advanced RT enzyme mix	-	-	-
Nuclease-free water	15 µl	1.58 ml	6.33 ml
Total	40 µl	4.22 ml	16.9 ml

Note: Volume includes 10% excess

TABLE 3.6: qPCR reaction setup.

Component	Volume	
	10 µl PCR reaction	**20 µl PCR reaction**
TaqMan Fast Advanced Master mix	5 µl	10 µl
TaqMan Assays	0.5 µl	1 µl
Nuclease free water	2.5 µl	5 µl
Total	8 µl	16 µl

TABLE 3.7: qPCR machine setup.

Step	Stage	Cycles	Temperature	Time
UDG activation	1	1	50°C	2 minutes
Enzyme activation (hold)	2	1	95°C	20 seconds
PCR	3	50	95°C	1 seconds
			60°C	20 seconds

Note: UDG, uracil-DNA glycosylase

3.1.4 Optimisation of the PCR reaction

cDNA was synthesised from 25,000, 50,000 and 100,000 cells per well of a 96-well plate for SCC4, SCC9, SCC25, CAL27, and OKF6 cell lines. Based on the optimisation results (archived on the Surgical Infection group V drive), further PCR reactions were performed on the cDNA synthesised from 50,000 cells per well of a 96-well plate for all the oral cancer, normal and positive control cell lines.

3.1.5 qPCR results

QuantSudio RealTime PCR Software v1.3 was used to collect the results from the PCR reactions. Amplification (ΔRn v. cycle; Rn v. cycle; Ct v. well number), multicomponent (FAM, ROX), raw data and gene expression plots were obtained. Rn was calculated as the fluorescence of the reporter dye divided by the fluorescence of a passive reference dye; that was, Rn is the reporter signal normalised to the fluorescence signal of ROX dye. ΔRn is Rn minus the baseline; ΔRn is plotted against PCR cycle number.

3.1.6 Analysis of results

In the experiment, it was assumed that the efficiency of the probes or TaqMan™ Gene Expression Assay (FAM) was 100%. Therefore, the delta−delta C_t formula ($2^{-\Delta\Delta Ct}$) was used to calculate the relative fold gene expression of calcium channel receptors and cannabinoid receptors. C_t is the threshold cycle.

The formula used was as follows:

$$\Delta C_t = C_t \text{ (gene of interest)} - C_t \text{ (housekeeping/reference gene)}$$
$$\Delta\Delta Ct = \Delta C_t \text{ (Sample)} - \Delta C_t \text{ (Control average)}$$
$$\text{Fold gene expression} = 2^{-(\Delta\Delta Ct)}$$

3.2 Selection of the drugs

Calcium channel drugs were selected, based on the results of the qPCR, LPS (Gram-negative bacterial antigen) (Raetz & Whitfield, 2002), LTA (Gram-positive bacterial antigen) (Neuhaus & Baddiley, 2003), phytohemagglutinin (PHA; plant-based Gram-negative bacterial antigen) (Banwell et al.,1983), capsaicin (TRPV1 agonist) (Yang & Zheng, 2017), capsazepine (TRPV1 antagonist) (Nguyen et al., 2010), ML218 HCl (T-type voltage-gated calcium channel [Cav 3.2 and Cav 3.3] inhibitor) (Li et al., 2017), and CID16020046 (GPR55 antagonist) (Stancic et al., 2015) were assayed to stimulate the oral cancer cells and determine the effect of calcium channel drugs on the oral cancer cells (Table 3.8).

The calcium channel drugs were DMSO soluble. Molar concentrations were used for working stock solutions of all the drugs. The number of moles of the supplied drug was first calculated using the formula:

$$n = m \div M$$

where m is the mass of the supplied drug and M is the molecular weight. Molarity was then calculated as follows:

$$M_{\text{working stock}} = n \div V$$

where $M_{working\ stock}$ is the molar concentration of the prepared working stock solutions of the drug supplied, n is the number of mole, and V is the final volume. All the bacterial antigens were water soluble. They were prepared in their respective growth medium without growth factors and antibiotics. The working stocks of bacterial antigens prepared were 110 µg/ml.
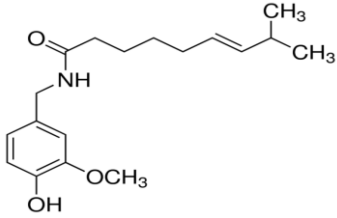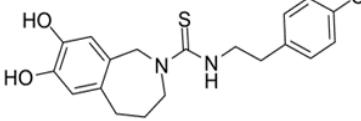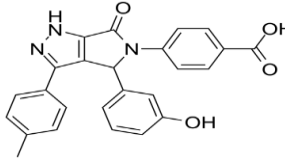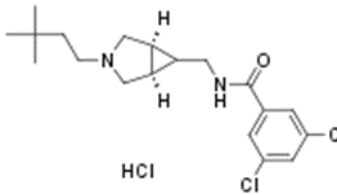
The preparation of the bacterial antigens and calculation for DMSO used the formula:

$$C_1 \times V_1 = C_2 \times V_2$$

where C_1 is the initial concentration of the drugs, C_2 is the final concentration, V_1 is the initial volume of the working stock and V_2 is the final volume required for each experiment. Based on the DMSO assay, the maximum vehicle concentration used to make the drugs was 0.1% (Section A4, Figure A1).

TABLE 3.8: Calcium channel drug preparation.

Name of the drug	MW (Daltons)	Supplied mass	Vol. of DMSO	Conc. of stock solution	Structure of the drug
Capsaicin	305.41	250 mg	9 ml	91.00 mM	
Capsazepine	376.90	5 mg	1 ml	13.50 mM	
CID16020046	425.44	5 mg	2 ml	5.90 mM	
ML218 HCl	405.79	10 mg	1 ml	24.64 mM	

Please note that the structures of the drugs are used after the permission from the manufacturer

To determine the effect of calcium channel drugs on the bacterial antigen-stimulated oral cancer cells, it was imperative to first optimise the number of oral cancer cells per well required for bacterial antigen stimulation. This required optimising the concentration of the calcium channel drugs to be applied to the oral cancer cells. The optimisation and initial metabolic effects were determined using the Real Time-Glo MT Cell Viability Assay.

3.3 MT Glo cell viability assay

The Real Time-Glo MT Cell Viability Assay is a non-lytic, homogenous, bioluminescent (luminometric) method (Riss et al., 2004) that helps to determine the metabolic changes that occur because of different drug/bacterial antigen concentrations and combinations, in real time. The non-lytic nature of this assay allows the cells to be used for further

downstream applications, including multiplexing with a variety of assay chemistries (Riss et al., 2004). It helps determine the number of metabolically active or otherwise viable cells in a culture by measuring the reducing potential of cells (Riss et al., 2004). The assay involves adding NanoLuc luciferase enzyme and a cell permeant pro-substrate, the MT Cell Viability substrate, to cells in culture (Riss et al., 2004). Viable/metabolically active cells reduce the pro-substrate to generate a substrate that diffuses from cells into the surrounding culture medium, where it is used by the NanoLuc luciferase enzyme to produce a luminescent signal (Riss et al., 2004). Both MT Cell Viability substrate and NanoLuc luciferase enzyme are stable in complete cell culture medium at 37°C for at least 72 hours (Riss et al., 2004). The assay can be performed in two formats: continuous read measurement or endpoint measurement (Riss et al., 2004).

3.3.1 Cell viability assay set up

The oral cancer cells were plated in a transparent flat-bottomed, Costar 96-well plate with a white opaque border. This was kept in a humidified incubator at 37°C/5% CO_2 for 24 hours. On the following day, before the start of the MT Glo assay, cell culture medium, MT Cell Viability Substrate and NanoLuc luciferase enzyme were equilibrated to 37°C. The total volume of the reagents and the desired bacterial antigen/calcium channel drugs was 100 µl per well of the 96-well plate. The ratio of the volume of MT Glo reagents and the desired bacterial antigen/calcium channel drugs applied to the oral cancer cells was 1:1. In the experiment, addition of MT Glo reagents was done at 2X concentration. Therefore, 1 ml of 2X RealTime-MT Glo reagent preparation was made by adding 2 µl of MT Cell Viability substrate and 2 µl NanoLuc luciferase enzyme to 996 µl of cell culture medium (respective to the cell line used for the assay). Plates were incubated in a humidified incubator at 37°C/5% CO_2 for the desired period for each assay. During the assay no cell washing, removal of medium or further reagent addition was required to determine the number of metabolically active cells. The luminescence of the cells was recorded using a microplate reader.

3.3.2 Plate reading

A plate-reading luminometer was used to measure the luminescence of the treated cells. BMG Labtech microplate reader PHERAstar was set up with optical module LUM plus, gain 3600, focal height 14.3 mm, top optic (for comparing different kinetic windows; all measurement values normalised to 1 second), settling time (0.1 second), bidirectional, horizontal left to right, top to bottom reading at a constant target temperature of 37°C.

3.4 Optimisation of the bacterial antigen and calcium channel drugs

The optimum number of cells per well of a 96-well plate to be used further in the project was first determined for the oral cancer and normal oral cells. This involved plating 500, 1000, 5000, 7500, 10,000 and 100,000 cells per well for each cell line in triplicate, with 0 µg/ml, 5 µg/ml, and 10 µg/ml LPS, PHA and LTA. After determining the optimum cell number per well of a 96-well plate and the optimum concentration of the bacterial antigen required to stimulate the oral cancer cells, optimisation of the calcium channel drugs was performed. For this, (based on the previous researcher's work) CID16020046 (0.5, 1, 3, 5, 7 and 10 µM); capsaicin (10, 25, 50, 75, 100, 125 and 150 µM); capsazepine (1, 5, 10, 15, 20, 2, and 30 µM); and ML218 HCl (1, 10, 20, 30, 40, 50, 60, 70, 80, 90 and 100 µM) were tested with the previously determined optimum cell number per well of a 96-well plate (Stancic et al., 2015, Yang & Zheng, 2017, Nguyen et al., 2010, Li et al., 2017) (Section A6 and Figure A3).

3.4.1 Stimulation index

The stimulation index for each bacterial antigen was calculated to determine the most appropriate cell line among the oral cancer cells; that is, the one that showed the maximum stimulation index at different time points (24, 48 and 72 hours). Based on the optimisation results, 5000 cells were plated for CAL27, SCC4, SCC9, SCC25 and OKF6.

The stimulation index was calculated as follows: (Luminescence of stimulated cells - Luminescence of blank well) ÷ (Luminescence of unstimulated cells - Luminescence of blank well)

3.5 Drug combination strategy

After determining the concentration of the calcium channel drugs and the bacterial antigens that resulted in the maximum inhibition of the oral cancer cell line CAL27 (it was selected based on the results of the previous steps) (Section A5 and Figure A3), a drug combination strategy was designed (Figure 3.1; Table 3.9). Since the study hypothesis was that not only LPS but biofilms affect the proliferation of oral cancer cells, the drug combination strategy was designed in such a way that both the Gram-positive and Gram-negative bacterial antigens were combined to determine the effect of calcium channel drugs on LPS/LTA/PHA/LPS+LTA-stimulated oral cancer cells. The drug combination strategy was designed in six phases of treatment. In the first phase, plated cells were treated with different combinations of bacterial antigens in combination with calcium channel drugs. In the second and third phases, inhibitory drugs were introduced in the presence of bacterial antigens after 24 hours and 72 hours of bacterial antigen stimulation. In the fourth and fifth phases, inhibitory drugs were added after 24 hours and 72 hours of bacterial antigen stimulation. In the final phase, inhibitory drugs were applied in the absence of, and without stimulation with, bacterial antigens.
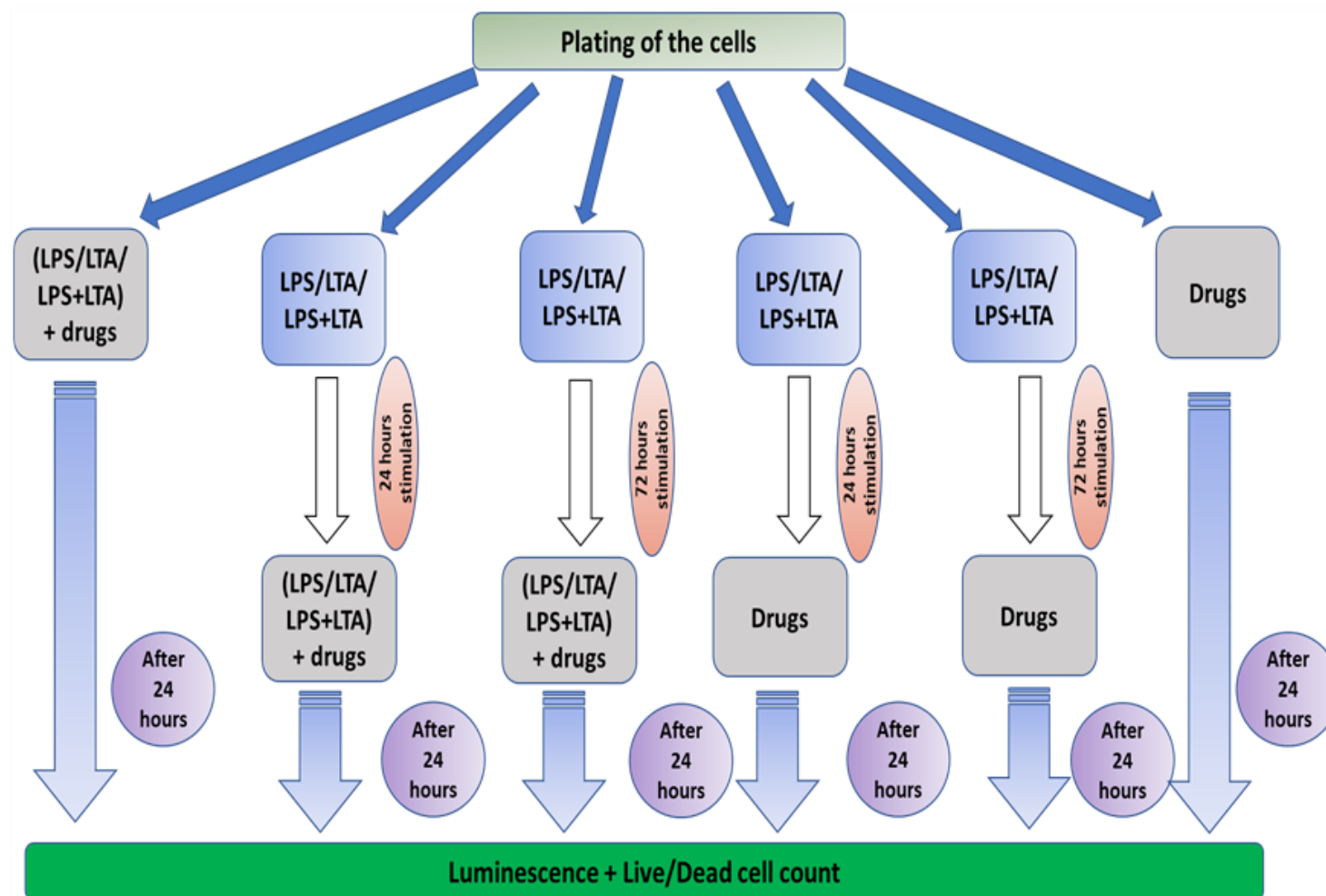
FIGURE 3.1: Drug combination strategy.

TABLE 3.9: Drug combination strategy of MT Glo assay.

Combination	Concentration and Volume of bacterial antigens/drugs	MT Glo
After 0-hour, 24 hours, and 72 hours LPS stimulation		
LPS	10 µg/ml, 50 µl	50 µl
LPS+Capsaicin 10 µM	(LPS) 20 µg/ml, 25 µl; (Capsaicin) 40 µM, 25 µl	50 µl
LPS+Capsaicin 150 µM	(LPS) 20 µg/ml, 25 µl; (Capsaicin) 600 µM, 25 µl	50 µl
LPS+ML218 HCl 1 µM	(LPS) 20 µg/ml, 25 µl; (ML218 HCl) 4 µM, 25 µl	50 µl
LPS+ML218 HCl 100 µM	(LPS) 20 µg/ml, 25 µl; (ML218 HCl) 400 µM, 25 µl	50 µl
LPS+Capsazepine 30 µM	(LPS) 20 µg/ml, 25 µl; (Capsazepine) 120 µM, 25 µl	50 µl
Capsaicin 10 µM	20 µM, 50 µl	50 µl
Capsaicin 150 µM	300 µM, 50 µl	50 µl
ML218 HCl 1 µM	2 µM, 50 µl	50 µl
ML218 HCl 100 µM	200 µM, 50 µl	50 µl
Capsazepine 30 µM	60 µM, 50 µl	50 µl
After 0-hour, 24 hours, and 72 hours PHA stimulation		
PHA	10 µg/ml, 50 µl	50 µl
PHA+Capsaicin 10 µM	(PHA) 20 µg/ml, 25 µl; (Capsaicin) 40 µM, 25 µl	50 µl
PHA+Capsaicin 150 µM	(PHA) 20 µg/ml, 25 µl; (Capsaicin) 600 µM, 25 µl	50 µl
PHA+ML218 HCl 1 µM	(PHA) 20 µg/ml, 25 µl; (ML218 HCl) 4 µM, 25 µl	50 µl
PHA+ML218 HCl 100 µM	(PHA) 20 µg/ml, 25 µl; (ML218 HCl) 400 µM, 25 µl	50 µl
PHA+Capsazepine 30 µM	(PHA) 20 µg/ml, 25 µl; (Capsazepine) 120 µM, 25 µl	50 µl
After 0-hour, 24 hours, and 72 hours LTA stimulation		
LTA	10 µg/ml, 50 µl	50 µl
LTA+Capsaicin 10 µM	(LTA) 20 µg/ml, 25 µl; (Capsaicin) 40 µM, 25 µl	50 µl
LTA+Capsaicin 150 µM	(LTA) 20 µg/ml, 25 µl; (Capsaicin) 600 µM, 25 µl	50 µl
LTA+ML218 HCl 1 µM	(LTA) 20 µg/ml, 25 µl; (ML218 HCl) 4 µM, 25 µl	50 µl
LTA+ML218 HCl 100 µM	(LTA) 20 µg/ml, 25 µl; (ML218 HCl) 400 µM, 25 µl	50 µl
LTA+Capsazepine 30 µM	(LTA) 20 µg/ml, 25 µl; (Capsazepine) 120 µM, 25 µl	50 µl
After 0-hour, 24 hours, and 72 hours LPS + LTA stimulation		
LPS+LTA	(LPS) 20 µg/ml, 25 µl; (LTA) 20 µg/ml, 25 µl	50 µl
LPS+LTA+Capsaicin 10 µM	(LPS) 30 µg/ml, 17 µl; (LTA) 30 µg/ml, 17 µl; (Capsaicin) 60 µM, 17 µl	50 µl

LPS +LTA+ML218 HCl 100 µM	(LPS) 30 µg/ml, 17 µl; (LTA) 30 µg/ml, 17 µl; (ML218 HCl) 600 µM, 17 µl	50 µl
LPS+LTA+Capsazepine 30 µM	(LPS) 30 µg/ml, 17 µl; (LTA) 30 µg/ml, 17 µl; (Capsazepine) 180 µM, 17 µl	50 µl
Capsaicin 10 µM	20 µM, 50 µl	50 µl
Capsaicin 150 µM	300 µM, 50 µl	50 µl
ML218 HCl 1 µM	2 µM, 50 µl	50 µl
ML218 HCl 100 µM	200 µM, 50 µl	50 µl
Capsazepine 30 µM	60 µM, 50 µl	50 µl
Drugs without any stimulation or presence of bacterial antigens		
Capsaicin 10 µM	20 µM, 50 µl	50 µl
Capsaicin 150 µM	300 µM, 50 µl	50 µl
ML218 HCl 1 µM	2 µM, 50 µl	50 µl
ML218 HCl 100 µM	200 µM, 50 µl	50 µl
Capsazepine 30 µM	60 µM, 50 µl	50 µl

3.5.1 Analysis of the results

The results were expressed as relative luminescence units. The percentage inhibition of metabolism was calculated to compare the effect on bacterial antigen-stimulated or unstimulated-oral cancer cells (CAL27) of calcium channel drugs in the presence and absence of different combinations of bacterial antigens. The formula used to calculate percentage inhibition was: Inhibition % = [(Luminescence of the control cells – Luminescence of the treated cells) ÷ Luminescence of the control cells] x 100

3.6 Trypan blue assay

Following the luminometric assay, MT Glo helped to determine the metabolic activity of CAL27 cells under different treatment conditions. Therefore, a trypan blue assay was performed to determine the total live/dead cell count. This is a dye exclusion assay (Riss et al., 2004). Trypan blue is a negatively charged molecule that is excluded by live cells and retained by dead cells. (Riss et al., 2004)

3.6.1 Method

After treatment of CAL27 cells in a Costar 96-well transparent flat-bottomed well plate under different conditions for different times (Table 3.10), they were detached from the wells by treatment with 40 µl of trypsin EDTA (Sigma Life Sciences) for 4–5 minutes. The cell suspension was transferred to 1.5-ml Eppendorf tubes. Ten µl of cell suspension was added to 10 µl of trypan blue (0.4%) (Invitrogen). The trypan blue–cell suspension was then loaded onto Cell Countess cell-counting chamber slides (Invitrogen). The total live/dead cell count was achieved using a Cell Countess automatic cell-counting chamber (Invitrogen) with the machine set to its default cell size program for calorimetric analysis of the total live/dead cell count.

3.6.2 Results

The total number of cells, live cells and dead cells were calculated from the trypan blue live/dead cell assay for each treatment condition.

The effect of calcium channel drugs on the bacterial antigen was determined by the MT Glo and the trypan blue live/dead cell assays, which are metabolic and cell viability assays respectively. The clonogenic assay was performed to determine the effect of calcium channel drugs and bacterial antigens on the growth or proliferation of CAL27 under eight different conditions (Table 3.11).

TABLE 3.10: Drug combination strategy of Trypan Blue assay.

Combination	Concentration and Volume of bacterial antigens/drugs
After 0-hour, 24 hours, and 72 hours LPS stimulation	
LPS	5 µg/ml, 100 µl
LPS+Capsaicin 10 µM	(LPS) 10 µg/ml, 50 µl; (Capsaicin) 20 µM, 50 µl
LPS+Capsaicin 150 µM	(LPS) 10 µg/ml, 50 µl; (Capsaicin) 300 µM, 50 µl
LPS+ML218 HCl 1 µM	(LPS) 10 µg/ml, 50 µl; (ML218 HCl) 2 µM, 50 µl
LPS+ML218 HCl 100 µM	(LPS) 10 µg/ml, 50 µl; (ML218 HCl) 200 µM, 50 µl
LPS+Capsazepine 30 µM	(LPS) 10 µg/ml, 50 µl; (Capsazepine) 60 µM, 50 µl
Capsaicin 10 µM	10 µM, 100 µl
Capsaicin 150 µM	150 µM, 100 µl
ML218 HCl 1 µM	1 µM, 100 µl
ML218 HCl 100 µM	100 µM, 100 µl
Capsazepine 30 µM	30 µM, 100 µl
After 0-hour, 24 hours, and 72 hours PHA stimulation	
PHA	5 µg/ml, 100 µl
PHA+Capsaicin 10 µM	(PHA) 10 µg/ml, 50 µl; (Capsaicin) 20 µM, 50 µl
PHA+Capsaicin 150 µM	(PHA) 10 µg/ml, 50 µl; (Capsaicin) 300 µM, 50 µl
PHA+ML218 HCl 1 µM	(PHA) 10 µg/ml, 50 µl; (ML218 HCl) 2 µM, 50 µl
PHA+ML218 HCl 100 µM	(PHA) 10 µg/ml, 50 µl; (ML218 HCl) 200 µM, 50 µl
PHA+Capsazepine 30 µM	(PHA) 10 µg/ml, 50 µl; (Capsazepine) 60 µM, 50 µl
After 0-hour, 24 hours, and 72 hours LTA stimulation	
LTA	10 µg/ml, 50 µl
LTA+Capsaicin 10 µM	(LTA) 10 µg/ml, 50 µl; (Capsaicin) 20 µM, 50 µl
LTA+Capsaicin 150 µM	(LTA) 10 µg/ml, 50 µl; (Capsaicin) 300 µM, 50 µl
LTA+ML218 HCl 1 µM	(LTA) 10 µg/ml, 50 µl; (ML218 HCl) 2 µM, 50 µl
LTA+ML218 HCl 100 µM	(LTA) 10 µg/ml, 50 µl; (ML218 HCl) 200 µM, 50 µl
LTA+Capsazepine 30 µM	(LTA) 10 µg/ml, 50 µl; (Capsazepine) 60 µM, 50 µl
After 0-hour, 24 hours, and 72 hours LPS + LTA stimulation	
LPS+LTA	(LPS) 10 µg/ml, 50 µl; (LTA) 10 µg/ml, 50 µl
LPS+LTA+Capsaicin 10 µM	(LPS) 15 µg/ml, 34 µl; (LTA) 15 µg/ml, 34 µl; (Capsaicin) 30 µM, 34 µl
LPS+LTA+Capsaicin 150 µM	(LPS) 30 µg/ml, 34 µl; (LTA) 30 µg/ml, 34 µl; (Capsaicin) 450 µM, 34 µl
LPS+LTA+ML218 HCl 1 µM	(LPS) 30 µg/ml, 34 µl; (LTA) 30 µg/ml, 34 µl; (ML218 HCl) 3 µM, 34 µl
LPS+LTA+ML218 HCl 100 µM	(LPS) 15 µg/ml, 34 µl; (LTA) 15 µg/ml, 34 µl; (ML218 HCl) 300 µM, 34 µl
LPS+LTA+Capsazepine 30 µM	(LPS) 15 µg/ml, 34 µl; (LTA) 15 µg/ml, 34 µl; (Capsazepine) 90 µM, 34 µl
Capsaicin 10 µM	10 µM, 100 µl
Capsaicin 150 µM	150 µM, 100 µl
ML218 HCl 1 µM	1 µM, 100 µl
ML218 HCl 100 µM	100 µM, 100 µl
Capsazepine 30 µM	30 µM, 100 µl
Drugs without any stimulation or presence of bacterial antigens	
Capsaicin 10 µM	10 µM, 100 µl
Capsaicin 150 µM	150 µM, 100 µl
ML218 HCl 1 µM	1 µM, 100 µl
ML218 HCl 100 µM	100 µM, 100 µl
Capsazepine 30 µM	30 µM, 100 µl

3.7 Clonogenic assay

A clonogenic assay is a colony formation assay mainly based on the ability of a single cell to grow into a colony (Franken et al., 2006). The assay was performed in a Costar 24-well transparent flat-bottomed plate on which oral cancer cells were plated with medium without growth factors and antibiotics. The assay detected all cells that retained the inherent capacity to produce many progeny cells (Franken et al., 2006) after treatment with calcium channel drugs that might have caused cell reproductive death via the calcium metabolism machinery.

3.7.1 Plating of the cells

CAL27 were detached and plated following the protocol for cell passaging described in Section 2.1.4. Following optimisation of the clonogenic assay with CAL27, 5000 cells were plated into each well of a 24-well plate in 400 µl of DMEM (without 10% FBS and without 1% P/S), since the optimization results suggested that the effect of calcium channel drugs in the presence/absence of bacterial antigens on bacterial antigen-stimulated CAL27 with 10% FBS and 1% P/S might have had a dampening effect of bacterial antigens on the stimulation of CAL27.

The plates were then kept in a humidified incubator at 37°C/5% CO_2 for 24 hours. The following day the medium was removed, and respective treatments were performed on the cells, which were put back into the humidified incubator under the same conditions. The treatment was continued for 14 days or stopped earlier until the control or any of the treatment wells showed almost 100% confluence. The clonogenic assay was performed following the strategy: Day 1: Plating of the cells; Day 2: LPS+CAL 27 or LPS+LTA+CAL27; Day 5: stimulants added and A, B, C, D and E; Day 6 stimulants added to A, B, C, D and E; Day 8: stimulants added to stimulant control; Day 9: A, B, C, D and E added; Day 10: stimulants added to A, B, C, D and E; Day 11: stimulants added to stimulant control; Day 13: A, B, C, D and E added; Day 14: stimulants added to stimulant control; Day 15: The cells were fixed and stained for analysis of the number of colonies and colony intensity percentage for each condition (Table 3.11).

3.7.2 Fixation and staining of the cells

After achieving the desired confluency of the colonies (based on visual investigation under a microscope), the medium was removed, and cells rinsed carefully with 1X PBS. One ml of 100% ice cold methanol was then added to each well for 1 minute to fix the cells. After 1 minute the methanol was removed and the plates were air dried until completely dry. Then 500 µl of 0.1% crystal violet was added to the wells and the plate placed on a rocking platform for 20 minutes. Plates were then washed with deionised water three times (each time for 5 minutes) on a rocking platform. After the final wash, the plates were air dried until completely dry.

TABLE 3.11: Drug combination strategy for clonogenic assay.

Treatment	Concentration and volume of drug and bacterial antigens used per well
CAL27 (untreated)	Only medium without growth factor and antibiotic (400 µl)
LPS 72-hour stimulation	5 µg/ml LPS (400 µl)
LPS+LTA 72-hour stimulation	10 µg/ml LPS (200 µl) + 10 µg/ml LTA (200 µl)
A = LPS+LTA+ML218 HCl after LPS+LTA 72-hour stimulation	15 µg/ml LPS (133 µl) + 15 µg/ml LTA (133 µl) + 300 µM ML218 HCl (133 µl)
B = LPS+LTA+capsaicin after LPS+LTA 72-hour stimulation	15 µg/ml LPS (133 µl) + 15 µg/ml LTA (133 µl) + 450 µM capsaicin (133 µl)
C = ML218 HCl after LPS+LTA 72-hour stimulation	100 µM ML218 HCl (400 µl)
D = capsaicin after LPS+LTA 72-hour stimulation	150 µM capsaicin (400 µl)
E = LPS+LTA for 72 hours then $CaCl_2$ for 24 hours	2 mM $CaCl_2$ (400 µl)

Note: The labels A, B, C, D and E are used in all to denote these treatments for the remainder of the thesis.

3.7.3 Imaging and analysis

Uncompressed RGB (photometric interpretation) tiff images (1580 × 1178 pixels, [horizontal and vertical resolution], 600 dpi, 32-bit depth, 2-resolution unit, 35-mm focal length) were acquired by a Bio-Rad Chemidoc MP Imaging system and processed using Image Lab version 6.0.0 build 25, © 2017 (Bio-Rad Laboratories). The plates were also imaged using a Nikon Coolpix 4500 camera. Analysis of the images was done using ImageJ 1.52a (National Institutes of Health, USA, http://imagej.nih.gov.ij Java 1.8.0_112; 64 bit). Analysis of colony area intensity and the total number of colonies was done with the help of the colony area plugin (Figure 3.2) and by analysing the particles respectively (Section A6).
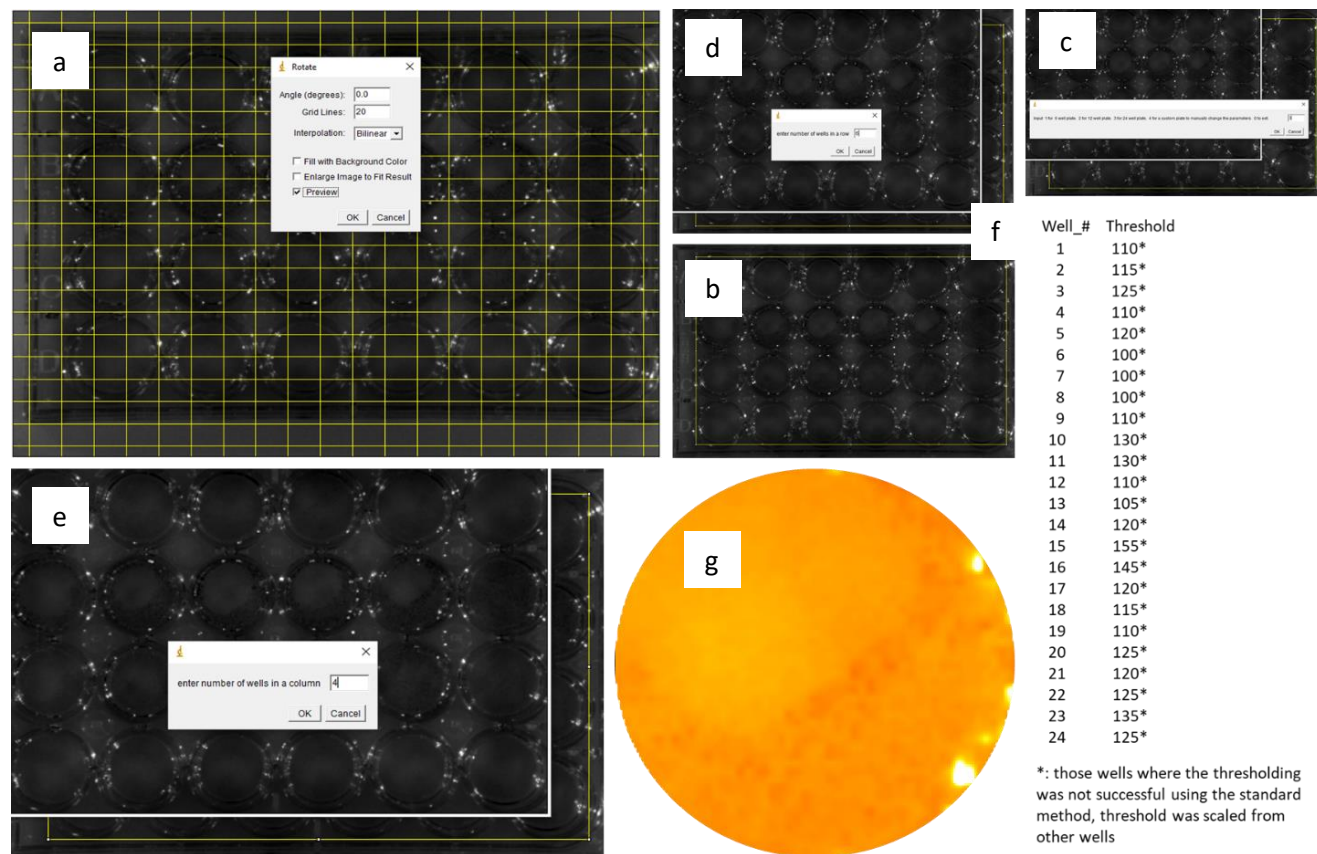
FIGURE 3.2: Image analysis of clonogenic assay. a. Grid line determination, b. Selection of the region of interest, c. Selection of the 24-well plate, d. Selection of the number of rows of the region of interest, e. Selection of the number of columns of the region of interest, f. Selection of the threshold from the stacked and cropped image files for analysis, and g. Fire look-up image for colony intensity percentage analysis.

3.8 Phosphokinase array

Determination of the phosphorylation profiles of kinases (i.e. post-translational modification) and their protein substrates is imperative to elucidate how oral cancer cells recognise and respond to bacterial antigens (Ardito et al., 2017). The Human Phospho-Kinase Array is a fast, sensitive and economical screening tool to determine the relative levels of phosphorylation of 37 kinase phosphorylation sites and two related total proteins without performing multiple immunoprecipitation and western blot assays. Knowledge of the proliferating factors affected by the bacterial antigens LPS and LTA helped us to understand the importance of biofilms in the proliferation of oral cancer cells, in addition to the already-known proliferating mechanisms affected by LPS.

3.8.1 Principle of the assay

Capture and control antibodies were spotted in duplicate onto nitrocellulose membranes (Table 3.12 and Figure 3.3). Cell lysates (protein) from the respective treatments were diluted and incubated overnight with the human phosphor-kinase array. The array was washed to eliminate unbound proteins, followed by incubation with a cocktail of biotinylated detection antibodies. Streptavidin-HRP and chemiluminescent detection reagents were added, and a signal was produced at each capture spot that corresponded to the amount of bound phosphorylated protein (Pedersen, 1989).

TABLE 3.12: Membrane coordinates of the phosphokinase array.

Membrane/coordinate	Target/control	Phosphorylation site
A-A1, A2	Reference spot	—
B-A11, A12	Akt 1/2/3	T308
B-A13, A14	Akt 1/2/3	S473
B-A17, A18	Reference spot	—
A-B3, B4	CREB	S133
A-B5, B6	EGFR	Y1086
A-B7, B8	eNOS	S1177
A-B9, B10	ERK 1/2	T202/Y204, T185/Y187
B-B11, B12	Chk2	T68
B-B13, B14	c-Jun	S63
A-C3, C4	Fgr	Y412
A-C5, C6	GSK3α/β	S21/S9
A-C7, C8	GSK3β	S9
A-C9, C10	HSP 27	S78/S82
B-C11, C12	p53	S15
B-C13, C14	p53	S46
B-C15, C16	p53	S392
A-D3, D4	JNK 1/2/3	T183/Y185, T221/Y223
A-D5, D6	Lck	Y394
A-D7, D8	Lyn	Y397
A-D9, D10	MSK 1/2	S376/S360
B-D11, D12	p70 S6 kinase	T389
B-D13, D14	p70 S6 kinase	T421/S424
B-D15, D16	PRAS40	T246
A-E3, E4	p38α	T180/Y182
A-E5, E6	PDGF Rβ	Y751
A-E7, E8	PLC-γ1	Y783
A-E9, E10	Src	Y419
B-E11, E12	PYK2	Y402
B-E13, E14	RSK 1/2	S221/S227
B-E15, E16	RSK 1/2/3	S380/S386/S377
A-F3, F4	STAT2	Y689
A-F5, F6	STAT5a/b	Y694/Y699
A-F7, F8	WNK1	T60
A-F9, F10	Yes	Y426

Membrane/coordinate	Target/control	Phosphorylation site
B-F11, F12	STAT1	Y701
B-F13, F14	STAT3	Y705
B-F15, F16	STAT3	S727
A-G1, G2	Reference spot	—
A-G3, G4	β-catenin	—
A-G9, G10	PBS (negative control)	—
B-G11, G12	STAT6	Y641
B-G13, G14	HSP 60	—
B-G17, G18	PBS (negative control)	—
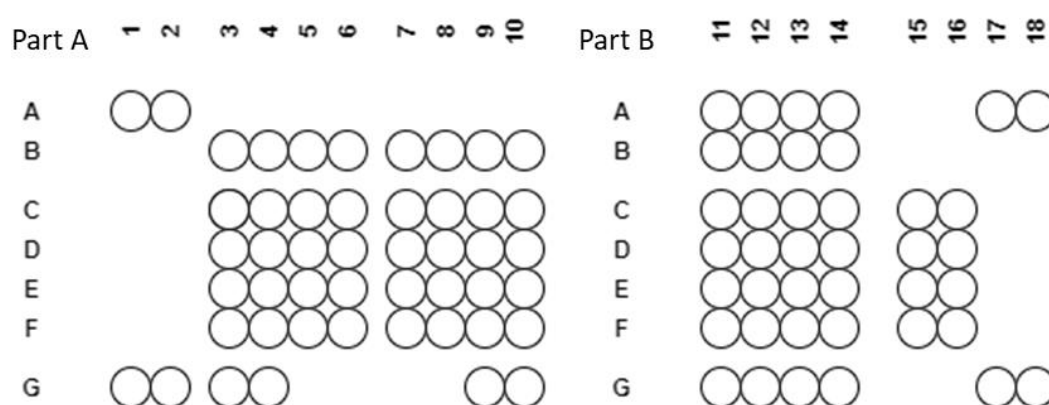
FIGURE 3.3: Membrane coordinates of the phosphokinase array.

3.8.2 Sample preparation

CAL27 cells in 75-cm^2 T flasks were kept in a humidified incubator at 37°C, 5% CO_2. After confluence of 80% was reached, the cells were treated with 5 µg/ml of bacterial antigen. Therefore, a total of 8 ml of DMEM (without 10% FBS and 1% P/S) was added to each flask, Specific assays required: 8 ml of 5µg/ml LPS for the LPS treatment; 8 ml of 5µg/ml LTA for LTA treatment; and 4 ml of each of 10 µg/ml LPS 10 µg/ml LTA, for the combined LPS+LTA treatment. The cells were incubated in a humidified incubator at 37°C, 5% CO_2 for 72 hours. After the treatment period, the cells were then detached using trypsin-EDTA for 4 minutes. After the desired detachment of the cells, they were centrifuged at 1000 g for 5 minutes at 4°C. After the final acquisition of cell pellets, the pellet from each condition was added to 100 µl of lysis solution, made up of 90 µl of RIPA (radioimmunoprecipitation assay buffer containing 20 mM Tris-HCl (pH 7.5)

150 mM NaCl, 1 mM Na$_2$EDTA, 1 mM EGTA 1% NP-40, 1% sodium deoxycholate, 2.5 mM sodium pyrophosphate, 1 mM β-glycerophosphate, 1 mM Na$_3$VO$_4$) and 10 µl of protease inhibitor (10 µg/ml leupeptin, 10 µg/ml aprotinin, 10 µg/ml pepstatin). The protease inhibitor was added to inhibit proteases from cleaving the total protein. The lysate (cell suspension + lysis buffer) was then kept on ice for 5 minutes, sonicated at a speed of 40 kHz for 5–10 seconds. The lysates were kept on the ice for a further 30 minutes and then centrifuged at 14,000 g for 15 minutes at 4°C. After centrifugation, the pellet (containing the cytoplasmic inclusions) was discarded and the supernatant (containing the protein desired for each condition) was transferred to −80°C until it was used for further protein estimation and proteome profiling.

3.8.3 Bicinchoninic acid protein assay

Pierce BCA Protein Assay kit (Thermo Fisher Scientific) was used to estimate the total amount of protein present in the samples. The kit contains a detergent-compatible formulation based on bicinchoninic acid (BCA). It relies on the phenomenon of the biuret reaction, where cupric ions (Cu^{2+}) are reduced to cuprous ions (Cu$^+$) by protein in an alkaline medium (Walker, 1994). The Cu$^+$ ions are detected by BCA (Walker, 1994). Two molecules of BCA chelate with one ion of Cu$^+$ to impart a purple colour during the reaction (Walker, 1994). The BCA–Cu$^+$ complex is water soluble and exhibits strong absorbance at 562 nm that is linear with increasing protein concentrations over a range of 20–20,000 µg/ml (Walker, 1994). The colour formation with BCA is mainly determined by the macromolecular structure of the protein, the number of peptide bonds and the presence of four amino acids (cysteine, cystine, tryptophan and tyrosine) (Walker, 1994). A series of dilutions of known concentration was prepared from bovine serum albumin (BSA; supplied) and assayed alongside the unknowns and the concentration of each unknown was determined based on a standard curve generated from the known-concentration BSA standards.

For protein estimation for the samples of CAL27 (untreated), LPS (treated), LTA (treated) and LPS+LTA (treated), BSA standards were first prepared (Table 3.13). Then, a BCA working solution was prepared by mixing Reagent A (sodium carbonate, sodium bicarbonate, Pierce Detection Reagent A, sodium tartrate in 0.1 N sodium hydroxide) and Reagent B (Pierce Detection Reagent B). For each well, 200 µl of Reagent A + Reagent B at a 1:50 ratio was added. Ten µl of standard sample and 10 µl of sample (1 µl of sample

+ 9 µl of diluent) of unknown concentration was added to the BCA working solution, in triplicate, in Greiner 96-well flat-bottomed (transparent) plates. The reaction was then kept in the incubator at 37°C for 30 minutes. Absorbance was then recorded using a spectrophotometer at 562 nm with shaking frequency 300 g, double orbital shaking mode and a settling time of 0.2 seconds: with a reading direction of bidirectional, horizontal left to right, top to bottom, at a constant temperature of 37°C. The readings from the standards were plotted and estimation of the unknown protein concentration of the samples was done based on the formula for the standard curve, $y =$ Slope $* x +$ offset. Here, y was the absorbance and x were the unknown protein concentration of the samples (Section A9, Figure A6, Tables A5 and A6).

TABLE 3.13: BSA protein estimation assay dilution strategy.

Vial	Volume of the diluent (µl)	Volume and source of BSA (µl)	Final BSA concentration
A	0	300 of stock	2000
B	125	375 of stock	1500
C	325	325 of stock	1000
D	175	175 of B	750
E	325	325 of C	500
F	325	325 of E	250
G	325	325 of F	125
H	400	100 of G	25
I	400	0	0

Note: the diluent was the lysis buffer used to lyse the samples.

After the average blank-corrected absorbance (optical density) of the samples were determined, they were multiplied by a factor of 10. Dilutions were used in the assay to ensure that the unknown sample absorbance fell within the range of the standards. Following protein concentration analysis, the samples were kept on ice while reagents were prepared for the proteome profiling assay. All reagents were brought to room temperature prior to the start of the assay.

TABLE 3.14: Reagent preparation for the phosphokinase array.

Reagent	Preparation
Human Phosphokinase Array	8 nitrocellulose membranes. Part A contained 21 antibodies printed in duplicate and Part B contained 18 antibodies printed in duplicate. Part A and Part B used together.
Detection Antibody Cocktail A	1 vial of lyophilised biotinylated antibodies used for Part A membrane. Detection A antibody cocktail reconstituted in 100 µl sterile of deionised water.
Detection Antibody Cocktail B	1 vial of lyophilised biotinylated antibodies used for Part B membrane. Detection B antibody cocktail reconstituted in 100 µl sterile of deionised water.
1X Array Buffer 2/3	2 ml of 5X Array Buffer 2 was added to 8 ml of Array Buffer 3. They were prepared fresh for each use.
1X Wash Buffer	40 ml of 25X Wash Buffer concentrate was added to 960 ml of sterile deionised water. Thus 1000 ml of 1X Wash Buffer was prepared.
Chemi Reagent Mix	Chemi Reagent 1 and 2 mixed in equal volumes.
1X Streptavidin HRP	Streptavidin HRP was supplied in 1:2000 concentration; 5 µl was diluted in 10 ml of 1X Array Buffer 2/3.

3.8.4 Array procedure

The array procedure was done following the manufacturer instruction and the list of reagents supplied (Table 3.14). Following the manufacturer instruction, protein concentration used for each treatment condition for the assay was 600 µg per array set A and B.

3.8.5 Imaging and analysis of the images

High-resolution (2417 pixels wide $\times$ 3236 high, 600 dpi horizontal and vertical resolution, 24-bit depth, LZW compression, 2-resolution unit 2, 35-mm focal length) RGB (photometric interpretation) tiff images following exposure of 1–600 seconds were acquired using the Bio-Rad Chemidoc MP Imaging system and processed using Image Lab version 6.0.0 build 25, © 2017 (Bio-Rad Laboratories). Densitometric analysis of the images was performed with the help of the Microarray plugin using ImageJ 1.52a (National Institutes of Health, USA, http://imagej.nih.gov.ij Java 1.8.0_112; 64 bit).

The following formula was used to calculate the relative expression of each target compared with the control CAL27: (1) Normalized pixel density = Pixel Density of each target ÷ Pixel Density of reference target; (2) Relative pixel density = Normalized pixel density of LPS/LTA/LPS+LTA treated CAL27$_{target}$ ÷ Normalized pixel density of CAL27$_{target}$

The proteome profiler results showed that the proliferation, higher colony intensity or total number of colonies formed as a result of bacterial antigen stimulation were because of lower expression of tumour suppressor proteins and higher expression of some of the proliferating factors (Section 5.4 and 5.5). Thus, RT-qPCR was performed to quantify gene expression of the common proliferating and tumour suppressor proteins previously shown to be related to the proliferation of oral cancer cells. Also, based on the integrative molecular characterisation of head and neck cancer cell model genomes, CAL27 showed the highest copy number among genes related to proliferating mechanisms—EGFR, PI3K and guanine monophosphate synthase (GMPS)—compared with other cell lines such as SCC4, SCC25 and SCC9 (Li et al., 2014). Therefore, in this project EGFR, PI3K, GMPS, STAT3 and SOCS3 differential gene expression under different conditions was determined using RT-qPCR.

3.9 Quantitative reverse transcription PCR (RT-qPCR)

RT-qPCR is a molecular technique that involves the reverse transcription of RNA to cDNA followed by amplification of the resulting cDNA target via qPCR (Arya et al., 2005). In this project, total RNA was extracted from the samples and mRNA reverse transcribed to cDNA, and the target cDNA was finally amplified to determine the relative gene expression (ΔRn) for the samples.

3.9.1 Primer design

The complete gene sequences of target genes were retrieved from http://www.ncbi.nlm.nih.gov/. The Primer blast tool https://www.ncbi.nlm.nih.gov/tools/primer-blast/ from the National Center for Biotechnology Information was then used to design the primers. As the primers were to be used for downstream qPCR amplification, stringent criteria were employed in their design: PCR product size 100−200 bp, 18−22 bp (length of the primer), T_m (melting temperature) > 60°C, and GC content 50−60%. It was also considered that the primers should hybridise to around half the 3'end of one exon and the 5'end of the next exon; that is, one of the primers should be in the exon–exon junction to avoid gDNA co-amplification.

Further screening and validation of the specificity of the primers was done using the multi-functional primer analysis software Oligo (version 6.67, Wojciech & Piotr Rychlik, Molecular Biology Insights, USA).

Primers that formed 3' terminal dimers, hairpin loops or cross-dimers, and those with palindromes or repeats were excluded. Other primer characteristics such as upper primer and lower primer composition, upper primer and lower primer T_m difference (which should < 4°C for optimum annealing of both primers), negative free energy (ΔG) (nucleic acid duplex stability) for all primers to maintain stability, internal stability of primers and primer efficiency were also evaluated to ensure maximum specificity of the primers to achieve the best PCR results. This is because using low-specificity primers may result in high background because of base pairing between a primer's 3' terminus and sites other than the intended target in the DNA (template). Characteristics of the primers used to determine the expression of proliferation protein are shown in Tables 3.15 and 3.16.

TABLE 3.15: Primers used for RT-qPCR.

Gene Name	Accession Number	Sequence (5'-3')	Position	Exon – Exon	PCR product length
SOCS3_F	NM_003955.4	GCGCGAAGGCTCCTTTGTG	191	330/331	135
SOCS3_R		GGGGGGCTGGTCCCGAATC	336		
STAT3_F	NM_139276.2	GGACATCAGCGGTAAGACCC	2118	2128/2129	168
STAT3_R		CTCTGGCCGACAATACTTTC	2310		
EGFR_F	NM_005228.5	AGCTACGGGGTGACTGTTTG	2956	2962/2963	106
EGFR_R		GAACTTTGGGCGACTATCTG	3114		
GMPS_F	NM_003875.3	TCAGGGAGTCTGGGTATGCT	2017	2028/2029	92
GMPS_R		AGGCTGCTTTTGAAGTGGGT	2108		
GAPDH_F	NM_002046.7	GACAGTCAGCCGCATCTTCT	21	105/106	181
GAPDH_R		ACCAAATCCGTTGACTCCGA	112		
PIK3CA_F	NM_006214.4	TGG GGATGATTTACGGCAAG	2732	2739/2740	129
PIK3CA_R		TCCCACACAGTCACCGATTGA	2861		

TABLE 3.16: Primers supplied by Sigma Aldrich.

Batch	Oligo Name	Oligo	Len	Pur	Scale	MW	T_m	µg/OD	OD
SDS00750914	SOCS3_191F	3024302577-000010	19	DST	0.05	5836	70.4	33.9	8.68
SDS00750915	SOCS3_336R	3024302577-000020	19	DST	0.05	5886	74.1	33.0	8.31
SDS00750916	STAT3_2118F	3024302577-000030	20	DST	0.05	6136	65.7	30.8	10.43
SDS00750917	STAT3_2310R	3024302577-000040	20	DST	0.05	6028	61.3	33.5	8.68
SDS00750918	EGFR_2956F	3024302577-000050	20	DST	0.05	6204	64.0	32.3	10.0
SDS00750919	EGFR_3114R	3024302577-000060	20	DST	0.05	6148	61.3	32.4	9.0
SDS00750920	GMPS_2017F	3024302577-000070	20	DST	0.05	6204	63.7	32.2	9.12
SDS00750921	GMPS_2108R	3024302577-000080	20	DST	0.05	6219	64.9	32.6	11.68
SDS00750922	GAPDH_21F	3024302577-000090	20	DST	0.05	6053	64.6	32.9	8.81
SDS00750923	GAPDH_112R	3024302577-000100	20	DST	0.05	6046	66.6	31.4	8.5
SDS00750924	PIK3CA_2732F	3024302577-000110	20	DST	0.05	6237	66.7	31.0	11.37
SDS00750925	PIK3CA_2861R	3024302577-000120	21	DST	0.05	6335	69.0	31.7	9.12

Batch	Oligo Name	µg	nmol	Epsilon 1/(mMcm)	Dimer	2ndry	GC%	Description
SDS00750914	SOCS3_191F	294.5	50.5	172.0	No	Very weak	63.1	505 µl/100 µM/TE buffer
SDS00750915	SOCS3_336R	274.9	46.7	177.9	No	Moderate	73.6	468 µl/100 µM/TE buffer
SDS00750916	STAT3_2118F	322.0	52.5	198.7	No	Weak	60	525 µl/100 µM/TE buffer
SDS00750917	STAT3_2310R	291.4	48.4	179.5	No	None	50	484 µl/100 µM/TE buffer
SDS00750918	EGFR_2956F	323.6	52.5	191.7	No	None	55	522 µl/100 µM/TE buffer
SDS00750919	EGFR_3114R	292.4	47.6	189.2	No	None	50	476 µl/100 µM/TE buffer
SDS00750920	GMPS_2017F	294.3	47.5	192.2	No	Weak	55	475 µl/100 µM/TE buffer
SDS00750921	GMPS_2108R	381.1	61.3	190.6	No	Very weak	50	613 µl/100 µM/TE buffer
SDS00750922	GAPDH_21F	290.2	48.0	183.7	No	None	55	480 µl/100 µM/TE buffer
SDS00750923	GAPDH_112R	267.5	44.2	192.1	No	None	50	443 µl/100 µM/TE buffer
SDS00750924	PIK3CA_2732F	353.3	56.7	200.7	No	None	50	567 µl/100 µM/TE buffer
SDS00750925	PIK3CA_2861R	289.1	45.6	199.8	No	Very weak	52.3	457 µl/100 µM/TE buffer

3.9.2 Sample preparation

CAL27 cells were plated at a density of 50,000 cells per well in 96-well plates in triplicate. On subsequent days, drug treatments were done. At the completion of the treatment period, total RNA was isolated from the samples.

3.9.3 RNA isolation

3.9.3.1 Lysis of samples and separation of phases

Following the manufacturer's protocol and the reagents supplied by the manufacturer for RNA extraction (Table 3.17), 900 µl of Trizol reagent was added to approximately 1.5×10^5 cells of CAL27 (untreated), LPS treated and LPS+LTA treated. Six hundred µl of Trizol reagent was added to approximately 1.5×10^5 cells of A, B, C, D and E (abbreviations shown in Table 3.11). Then, 180 µl of chloroform was added to 900 µl of cell lysate from each of CAL27 (untreated), LPS treated and LPS+LTA treated and 120 µl of chloroform was added to 600 µl of cell lysate of A, B, C, D and E and incubated for 2–3 minutes at room temperature. They were then mixed well and centrifuged at 12,000 g at 4°C for 15 minutes. The mixture separated into lower red phenol – chloroform and interphase, and a colourless upper aqueous phase containing total RNA; approximately 350 µl of this phase was transferred to a new tube. An equal volume of 70% ethyl alcohol was added, mixed and vortexed to observe any precipitate.

3.9.3.2 Binding and washing of RNA on the membrane

Approximately 700 µl of the prepared samples (mRNA + ethyl alcohol) were transferred to a spin cartridge (with collection tube). The spin cartridge was centrifuged in a collection tube at 12,000 g for 15 seconds. Then, 700 µl of Wash Buffer I was added to the spin cartridge, which was again centrifuged at 12,000 g for 15 seconds. Then 500 µl of Wash Buffer II was added to the spin cartridge, which was again centrifuged at 12,000 g for 15 seconds. After every spin cartridge centrifugation, the flow-through was again discarded.

3.9.3.3 Elution of the RNA

The membrane in the spin cartridge was first dried at 12,000 g for 1 minute. The collection tube was discarded, and the spin cartridge inserted into a recovery tube. Fifty µl of RNase-free water was added to the centre of the spin cartridge, which was incubated for 1 minute at room temperature and then centrifuged at 12,000 g for 2 minutes. This step was repeated once more. The spin cartridge was discarded, and the recovery tube containing the purified RNA was stored at −80°C until reverse transcription.

TABLE 3.17: Reagents for total RNA extraction.

Contents	Amount
Trizol Plus RNA Purification kit	
Trizol Reagent	100 ml
PureLink RNA Mini Kit	1 kit
PureLink RNA Mini kit	
Spin cartridges	50 cartridges
Collection tubes	50 tubes
Wash Buffer I	50 ml
Wash Buffer II	15 ml
RNase-free water	15.5 ml
Recovery tubes	50 tubes
Lysis Buffer	125 ml

3.9.3.4 RNA quantification

Nanodrop 2000 (Thermo Fisher Scientific) was used to quantify the RNA concentration in the samples based on 260 nm absorbance. The purity of RNA samples was also checked based on the A260/280 ratio and A260/230 ratio. 260/280 nm < 1.7 indicates protein impurities and 260/230 nm < 2 indicates chemical contamination (Table A7).

3.9.4 Reverse transcription

3.9.4.1 gDNA digestion

Eight µl of each extracted RNA sample was mixed with 1 µl of 10X ezDNase Buffer and 1 µl of ezDNase Enzyme (Table 3.18). The preparation was done on ice. No water was added, so that the amount of RNA was maximised. The reaction was mixed gently, incubated for 5 minutes at 37°C and then put back on ice.

TABLE 3.18: gDNA digestion reagents.

Component	Volume
10X ezDNase Buffer	1 µl
ezDNase Enzyme	1 µl
Template RNA 1µg total RNA	8 µl

3.9.4.2 Preparation of reverse transcription mix

The preparation of the reverse transcription mix was done according to Table 3.19. Ten µl of the reverse transcription mix was added to 10 µl of the reaction mix from the previous step. The final reverse transcription mix was placed in the thermal cycler (Thermo Fisher Scientific) to convert total RNA to cDNA and the reaction proceeded according to the protocol in Table 3.20. The resulting cDNA was stored at −20°C until the PCR reaction.

TABLE 3.19: Reverse transcription reaction setup.

Component	Volume	
	RT reaction	No RT reaction
SuperScript IV VILO Master Mix	4 µl	-
SuperScript IV VILO No RT control	-	4 µl
Nuclease-free water	6 µl	6 µl

TABLE 3.20: Thermal cycler setup.

Step	Cycle	Temperature	Duration
Anneal primers	1	25°C	10 minutes
Reverse transcribe RNA	1	50°C	10 minutes
Inactivate enzyme	1	85°C	5 minutes
qPCR amplification	1	4°C	Indefinite

3.9.5 qPCR

3.9.5.1 Primer preparation

All primers for the target genes (forward and reverse) were supplied at a concentration of 100 µM. Therefore, 10-µM working stock solutions of all the primers were first prepared. Then, final working stock concentrations of 300 nM (forward and reverse) were prepared from the 10-µM working stock solution for EGFR. GMPS, GAPDH and STAT3. For SOCS3, a 200-nM final working stock solution was prepared from the 10-µM working stock. This difference in concentration was chosen because of the lower difference between Tm (melting temperature) and Ta (annealing temperature) for these primers. Using a lower concentration of these primers in the reaction was expected to reduce the chance of false primer amplification.

3.9.5.2 Setting up plate document and sample preparation

First, the plate document was configured following guidelines for the Vii-A 7-2 PCR machine (Thermo Fisher Scientific). Each plate contained positive control (CAL27 (untreated)), negative control (no template control) and housekeeping gene (GAPDH) to normalise the relative gene expression. The cDNA samples were then thawed on ice, vortexed and centrifuged briefly.

3.9.5.3 Setting up the qPCR reaction

Reagents were prepared for the appropriate number of reactions following Tables 3.21, 3.22 and 3.23. Reactions were transferred to a MicroAmp Fast 96-well reaction plate (0.1 ml) (Applied Biosciences, Life Biosystems) and sealed with an qPCR-compatible optical adhesive cover (Applied Biosystems, Life Technologies) and centrifuged briefly to spin down the contents and eliminate any air bubbles.

TABLE 3.21: qPCR reaction setup.

Component	Volume (10 µl/well)	Volume (20 µl/well)
Power Up SYBR Green Master Mix	5 µl	10 µl
Forward and reverse primers	variable	variable
DNA template + Nuclease-free water	variable	variable
Total	10 µl	20 µl

TABLE 3.22: qPCR reaction setup for STAT3, GAPDH, GMPS and PI3KCA.

Component	Volume (per reaction)
Power Up SYBR Green Master Mix	5 µl
Forward primers (10µM)	0.3 µl (300nM)
Reverse primers (10µM)	0.3 µl (300nM)
DNA template	2 µl
Nuclease-free water	2.4 µl
Total	10 µl

TABLE 3.23: qPCR reaction setup for SOCS3.

Component	Volume (per reaction)
Power Up SYBR Green Master Mix	5 µl
Forward primers (10µM)	0.2 µl (200 nM)
Reverse primers (10µM)	0.2 µl (200 nM)
DNA template	2 µl
Nuclease-free water	2.6 µl
Total	10 µl

3.9.5.4 Setup of the PCR instrument

A ViiA 7 system was programmed with the following settings: fast ramp speed, 96-well (0.1 ml), comparative Ct ($\Delta\Delta$Ct), SYBR Green reagents, reporter SYBR, no quencher, ROX passive reference dye and continuous melt curve ramp increment (Table 3.24). The manufacturer's guidelines were followed for the qPCR experiment using standard cycling mode (primer Tm $\geq$ 60°C) and dissociation curve conditions were as outlined in Table 3.25.

TABLE 3.24: qPCR reaction instrument setup.

Step	Temperature	Duration	Cycles
UDG activation	50°C	2 minutes	Hold
Dual-lock DNA Polymerase	95°C	2 minutes	Hold
Denature	95°C	15 seconds	50
Anneal/extend	60°C	1 minute	

TABLE 3.25: qPCR reaction melt curve analysis setup.

Step	Ramp rate	Temperature	Duration
1	1.6°C/second	95°C	15 seconds
2	1.6°C/second	60°C	1 minute
Dissociation	0.15°C/second	60°C to 95°C	-

3.9.5.5 Analysis of the results

The qPCR output included amplification (ΔRn *v.* cycle; Rn *v.* cycle; C_t *v.* well number) plots, a multicomponent plot, raw data plot, gene expression plot and melt curve plot. In the experiment, it was assumed that the efficiency of the primers was 100%. Therefore, the delta−delta C_t formula ($2^{-\Delta\Delta Ct}$) was used to calculate the relative fold gene expression of the target genes. C_t is the threshold cycle. The formula used was:

$$\Delta C_t = C_t \text{ (gene of interest)} - C_t \text{ (housekeeping/reference gene)}$$
$$\Delta\Delta Ct = \Delta C_t \text{ (Sample)} - \Delta C_t \text{ (Control average)}$$
$$\text{Fold gene expression} = 2^{-(\Delta\Delta Ct)}$$

RT-qPCR was used to provide information on the relative gene expression of target genes in the control and the treated samples, although there was the possibility of detecting non-functional gene expression. Therefore, to determine the relative functional protein expression from the target genes, a western blot experiment was performed.

3.10 Western blot

A western blot is commonly used in biochemistry to identify and separate proteins of interest (Mahmood & Yang, 2012). In this technique a mixture of proteins is separated based on their molecular weight via gel electrophoresis (Mahmood & Yang, 2012). The separated proteins are transferred to a polyvinylidene fluoride membrane that is then incubated with target antibody specific to the protein of interest (Mahmood & Yang, 2012). The unbound antibody is then washed off, leaving the bound antibody, which is visualised using an image developing machine and software (Mahmood & Yang, 2012). The thickness of the band corresponds to the amount of protein present in the sample (Mahmood & Yang, 2012).

3.10.1 Sample preparation

The protocol for sample preparation was identical to Section 3.9.2. The amount of protein amount was estimated following the Pierce BCA protein estimation procedure Section 3.9.3. Using the formula, protein concentration = mass/volume, the volume of total protein extract of each sample was determined to ensure $10\,\mu g$ of total protein was loaded in each well of the gel. NuPAGE LDS sample buffer (4X) was added to the sample at a ratio of 1:3. Each cell lysate in sample buffer was then boiled at 95°C for 5 minutes to denature the protein and the tubes centrifuged at 16,000 g in a microcentrifuge for 1 minute.

3.10.2 Protein separation by gel electrophoresis

After the samples were prepared, they were placed on ice until the gel electrophoresis setup was completed. It was planned to run 10-well gels for samples CAL27 (untreated), LPS treated, LPS+LTA treated; and 12-well gels for CAL27 (untreated), A, B, C, D and E (abbreviations shown in Table 3.11). CAL27 (untreated) was the control in the

experiment. A Novex Sharp Pre-Stained Protein Standard (Life Technologies) ladder was used for the entire experiment. First, 20X NuPAGE MOPS SDS Running Buffer (Invitrogen) was diluted to produce 1X running buffer compatible with the NuPAGE 10% Bis-Tris mini gels used in the project. Then the samples were loaded onto their respective gels and subjected to electrophoresis at 110 V, 5 W, 0.05 Amp for 2 hours, ensuring that the dye front had run off the bottom of the gel.

3.10.3 Electro-transfer

Transfer of proteins from the gel to the membrane was achieved using the iBlot 2 dry blotting system (Invitrogen). The manufacturer's instructions were followed to configure the iBlot 2. For electro-transfer, the 'P0' program was selected.

3.10.4 Blocking and antibody incubation

The blots were rinsed with distilled water and then stained with Ponceau S solution (Sigma-Aldrich) to check the transfer quality. Then the membranes were washed three times with Tris-buffered saline−Tween 20 (TBST) buffer (20 mM Tris, pH 7.5, 150 mM NaCl, 0.1% Tween 20) for 10 minutes on a rocking platform. The membranes were blocked with 5% skim milk in TBST for 1 hour on a rocking platform and then washed three times with TBST buffer for 10 minutes on a rocking platform. They were then incubated with primary antibodies in 5% skim milk overnight on a rocking platform at 4°C. On the following day the membranes were washed three times with TBST buffer for 10 minutes on a rocking platform and further incubated with the respective secondary antibody in 5% skim milk for 2 hours on a rocking platform at room temperature. All primary and secondary antibodies were provided by R&D Systems (Table 3.26). After incubation, membranes were washed like the previous steps and then the chemiluminescent substrate (ECL mix) (Bio-Rad) was prepared following the manufacturer's instructions and added to the membranes; the chemiluminescent signals were then captured.

TABLE 3.26: Primary and secondary antibodies used in the project.

Primary antibody	MW	Concentration used	Source	Secondary antibody	Concentration used
Human/mouse SOCS3 antibody	30 kDa	0.1 µg/ml	Mouse	Anti-mouse IgG HRP conjugate	1:1500 dilution
Human PI 3-kinase p110β antibody	110 kDa	1 µg/ml	Mouse	Anti-mouse IgG HRP conjugate	1:1500 dilution
STAT3 Mouse anti-human, mouse, rat	94 kDa	0.1 µg/ml	Mouse	Anti-mouse IgG HRP conjugate	1:1500 dilution
Human EGFR antibody	175 kDa	1 µg/ml	Goat	Anti-goat IgG HRP conjugate	1:1500 dilution
Human GAPDH	38 kDa	1:1000 dilution	Rabbit	Anti-rabbit IgG HRP conjugate	1:1500 dilution

3.10.5 Imaging

High-resolution (1536 pixels wide $\times$ 1024 pixels high, 345 dpi horizontal and vertical resolution, 32-bit depth, LZW compression, 3-unit resolution, 35-mm focal length) tiff images were acquired after exposure of $1-120$ seconds using the Bio-Rad Chemidoc MP Imaging system, and processed using Image Lab version 6.0.0 build 25, © 2017 (Bio-Rad Laboratories). Densitometric analysis of the images was achieved with the help of Microarray plugin using ImageJ 1.52a (National Institutes of Health; http://imagej.nih.gov.ij Java 1.8.0_112; 64 bit). The band density of the GAPDH and loading control protein (CAL27) were used to normalise the protein expression in the treatments.

Since proteome profiling showed lowering of tumour suppressor proteins and upregulation of some of the proliferating factors, which was also seen with the MT Glo, clonogenic and trypan blue live/dead cell assays, it was concluded that the calcium channel drugs reduced the growth of the CAL27 cells (Sections 4.4, 4.5, and 4.6). Therefore, an apoptotic assay was performed to compare the percentage of apoptosis of CAL27 cells under various treatment conditions.

3.11 Apoptotic assay

CellEvent Caspase-3/7 Green Detection Reagent (Thermo Fisher) was used for live cell imaging and to estimate the total apoptotic cells under each condition. This reagent is a novel fluorogenic substrate for activated caspase 3 and 7, consisting of a four-amino acid peptide (DEVD) conjugated to nucleic acid binding dye. After activation of caspase 3 or 7 in apoptotic cells, the DEVD peptide is cleaved, enabling the dye to bind to the DNA and produce a bright, fluorogenic response with an absorption/emission maximum of ~502/530 nm.

3.11.1 Method

Five thousand cells (CAL27) per 96-well plate (transparent, flat-bottomed) were plated and subjected to different treatments. After the incubation period for each treatment, the medium was carefully removed, and cells were washed once with 1X PBS. Then, a working stock solution of 7.2 µM of CellEvent Caspase-3/7 Green Detection Reagent was prepared from a stock solution of 2 mM in 1X PBS + 5% FBS. Then 100 µl of the diluted reagent was added to each well of the 96-well plate. Plates were incubated at 37°C/5% CO_2 for 30 minutes and then imaged for caspase3/7 apoptotic analysis.

3.11.2 Imaging

For each well, three live cell images were produced with turret position 1, objective lens '10x', capture mode 'find and focus', lighting setting '60%'and exposure 24010, using the capture software EVOS (revision 26133). Tiff images were 1280 pixels wide × 960 pixels high, with 96 dpi horizontal and vertical resolution, 24-bit depth, uncompressed, 35- mm focal length, RGB (photometric interpretation), with filter cube 'transmitted' and filter cube 'GFP', respectively, for bright field and green fluorescent image acquisition.

3.11.3 Analysis of the images

Analysis of the images were done using ImageJ 1.52a software (National Institutes of Health, http://imagej.nih.gov.ij Java 1.8.0_112 (64 bit).

To analyse the percentage of apoptotic cells, the total number of cells and number of apoptotic cells were analysed, and the apoptotic cell percentage calculated using the formula: Caspase 3/7 positive cell% = (Total number of caspase 3/7 positive cells per image ÷ Total number of cells per image) x 100

As the phosphokinase array, RT-qPCR and western blot analyses showed that the bacterial antigens stimulated the oral cancer cells via downregulating tumour suppressor proteins and upregulating some of the proliferating factors, (Section 4.5 and 4.6) the role of tumour necrosis factor α (TNF α) was examined. This 157-amino acid, non-glycosylated polypeptide cytokine has previously been shown to be associated with LPS stimulation. (Parameswaran & Patial, 2010) Also, since SOCS3/STAT3 has previously been shown to affect various cytokines in different cancers (Carow & Rottenberg 2014) and calcium channel drugs have been shown affect the growth of bacterial antigen-stimulated oral cancer cells (CAL27), the study aimed to compare levels of TNF α expression under different treatment conditions.

3.12 TNF α ELISA

A Human TNF α ELISA kit (Invitrogen) (Table 3.27), which employs a solid-phase sandwich ELISA was used to determine TNF α levels under different treatment conditions (Crowther, 1995).

TABLE 3.27: TNF α ELISA reagents used in the project.

Contents	Supplied
Hu TNF α Standard	2 vials
Standard Diluent Buffer	25 ml
Incubation Buffer	11 ml
Antibody coated 96-well plate	1 plate
Hu TNF α Biotin Conjugate	11 ml
Streptavidine-HRP (100X)	0.125 ml
Streptavidine-HRP Diluent	25 ml
Wash Buffer Concentrate (25X)	100 ml
Stabilised chromogen	25 ml
Stop Solution	25 ml
Plate covers and adhesive strips	3

3.12.1 Sample preparation

In the experiment, protein was extracted from different passage numbers of OKF6 (untreated), CAL27 (untreated), LPS treated, LPS+LTA treated, A, B, C and D (abbreviations in Table 3.11). Protein estimation for the samples was performed using the Pierce BCA Protein Assay kit (Thermo Fisher Scientific). Before plating in the 96-well plate with pre-coated antibody wells, the samples were further diluted with their respective cell culture medium to a sample concentration of 2000 pg/ml (according to the manufacturer's instructions, the sample concentration should be within the range of the standard curve).

3.12.2 Preparation of reagents

First, 16 ml of Wash Buffer Concentrate (25X) was diluted to 1X with 384 ml of deionised water. Then, standards were prepared via serial dilution using Standard Diluent Buffer and labelled according to Table 3.28. For a 96-well plate, 120 µl of streptavidin-HRP (100X) was added to 12 ml of streptavidin-HRP Diluent.

TABLE 3.28: Preparation of standards for the ELISA assay.

Vial	Volume of the standard diluent (µl)	Volume and source of BSA (µl)	Final concentration (pg/ml)
A	0	300 of stock	2000
B	300	300 of stock	1000
C	300	300 of B	500
D	300	300 of C	250
E	300	300 of D	125
F	300	300 of E	62.5
G	300	300 of F	31.2
H	300	300 of G	15.6
I	300	0	0

3.12.3 Method

Then 100 µl of standards, controls (OKF6, CAL27) and samples (pre-diluted) were added to the antibody pre-coated appropriate wells. Manufacturer's protocol was followed for the entire assay with the help of the reagents of the supplied Human TNF α ELISA kit (Invitrogen) (Table 3.27).

3.12.4 Plate reading and generating the standard curve

The absorbance of the samples was measured in Greiner 96-well flat-bottomed plates using a BMG Labtech microplate reader PHERAstar with the following settings: 22 flashes per well, excitation of 450 nm, shaking frequency of 300 g, double orbital shaking mode, additional shaking of 1 second before reading, settling time of 0.2 second, bidirectional, horizontal left to right, top to bottom reading, top optic (used to allow comparison of different kinetic windows, all measurement values were normalised to 1 second) and a constant target temperature of 37°C. The background absorbance was subtracted from the standards, unknowns and controls. Then, curve-fitting software Curve Expert version 1.40 (double precision, 32 bit) was used to generate a standard curve (Figure 3.4). The rational function model provided the best standard curve fit, with standard error 12.0317763 and correlation coefficient 0.9999135 (the fit converged to a tolerance of 1e-006 in 28 iterations). The mathematical equation was generated from the rational function model: $y = (a + bx) \div (1 + cx + dx^2)$. Where a = 1.92780332486E+001, b = 3.01059593821E+001, c = 7.25710400933E-001 and d = 1.38081537136E-001.
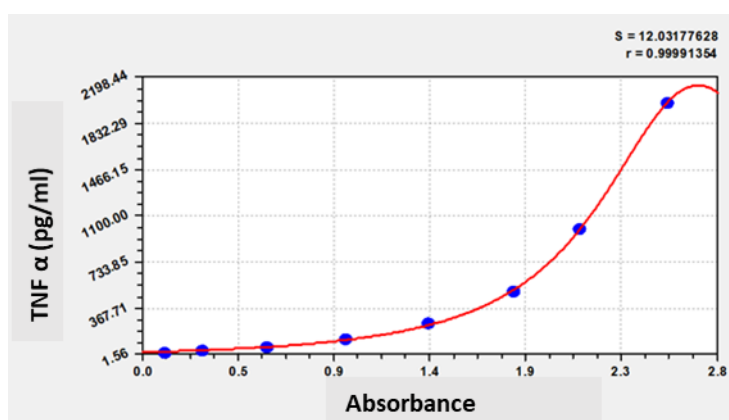
FIGURE 3.4: Standard curve generated by Rational function model. The graph-fitting software generated the formula used for the estimation of the concentration of TNF α (pg/ml) under each treatment condition.

3.13 Statistical analysis

All statistical analyses were performed using GraphPad Prism® version 5.02. The data were tested for normality of distribution using the D'Agostino & Pearson omnibus normality test. To determine the relative gene expressions of calcium channel receptors and genes related to tumour proliferation and suppression, protein expressions of tumour proliferation and suppression, metabolic activity/viability/colony formation responses of CAL27 after bacterial antigen stimulation and calcium channel drug treatment, TNF α ELISA, and percentage of caspase 3/7 positive cells one-way ANOVA with Tukey's Multiple Comparison Test were performed. p-values less than or equal to 0.05 were considered statistically significant.

<div style="text-align: right; font-size: 4em; color: #bbb; font-weight: bold;">4</div>

Results

4.1 Identification of calcium channel receptors

4.1.1 qPCR output

qPCR was performed to identify calcium channel receptor expression in the oral cancer and normal oral cell lines. None of the experiments showed any amplification in the negative control (negative RT control), bad passive reference signal, off-scale fluorescence, high standard deviation for the replicate groups, outliers in the replicate group, baseline algorithm failure, low passive reference signal, C_t algorithm failure or passive reference signal changes near C_t (Figure 4.1).

After normalising (against the gene expression of the reference gene, GAPDH) and calibrating the gene expression in each cell line (five passage numbers at different time points plated in triplicate; i.e. $n = 15$) against that in the normal oral cell line, OKF6, the relative fold gene expression of each of the calcium channel receptors for each cell line was compared.
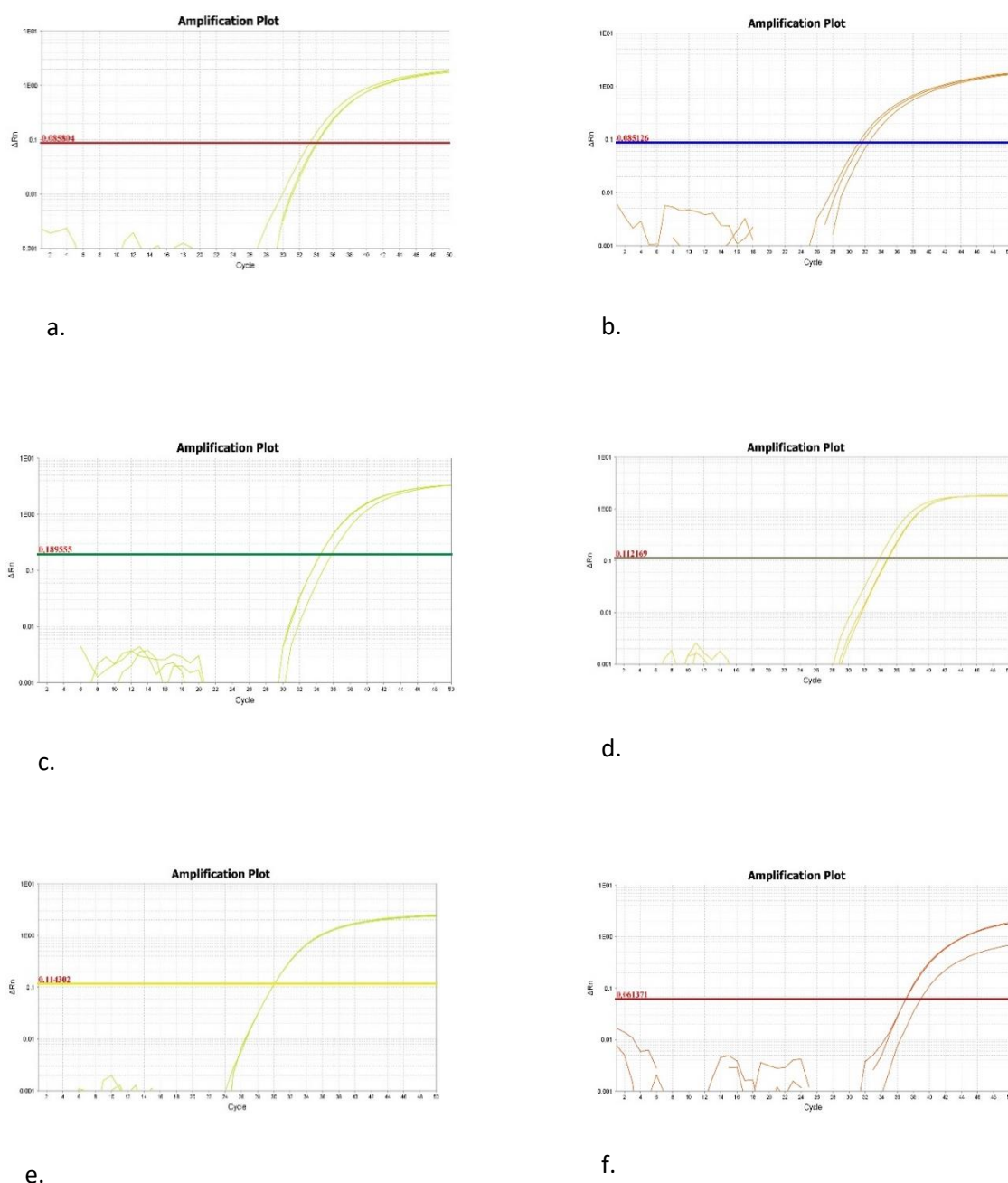
FIGURE 4.1: Amplification curves for calcium channel receptors. a. Cav 3.1 in CAL 27; b. Cav 3.2 in CAL 27; c. Cav 3.3 in CAL 27; d. TRPA1 in OKF6; e. TRPV1 in CAL 27; f. GPR55 in CAL 27. Here, ΔRn is represented on the *y*-axis, and number of cycles is represented on the *x*-axis; ΔRn is the difference in the Rn value for each experiment and the Rn value of the baseline signal generated by the instrument; Rn is the reporter signal normalised to the fluorescence signal of passive reference dye (ROX).

4.1.2 Differential calcium channel gene expression

SCC4 showed the lowest relative fold gene expression of Cav 3.1 among all cell lines (p ≤ 0.05) (Figure 4.2a). The relative fold gene expressions of SCC9 were lower than that in OKF6 (p ≤ 0.05) (Figure 4.2a). SCC25 was the only cell line that showed gene expression of Cav 3.2 (Table A2). CAL27 showed the highest relative fold gene expression of Cav 3.3 among all cell lines (p ≤ 0.005) (Figure 4.2b). Although the difference was not statistically significant, CAL27 showed 20% higher and 20% lower relative fold gene expression of TRPV1 and Cav 3.1 respectively than did OKF6 (Figure 4.2a, c). In contrast, SCC25 showed 20% higher Cav 3.1 gene expression than did OKF6 (Figure 4.2a). Also, SCC25 showed 50% higher TRPV1 expression relative to OKF6 (Figure 4.2c). All oral cancer cell lines showed higher relative fold gene expression of TRPV1 than did OKF6 (Figure 4.2c). SCC9 showed the higher relative fold gene expression of TRPV1 than did OKF6 (p ≤ 0.001) (Figure 4.2c). SCC9 and SCC4 showed higher relative fold gene expression of TRPV1 than did CAL27 (p ≤ 0.005) (Figure 4.2c). Only OKF6 showed expression of TRPA1 (Table A2). No cell lines showed expression of CB1 and CB2 (Table A2). GPR55 expression was seen in all oral cancer cell lines but not OKF6 (Table A2).

a.   b.   c.
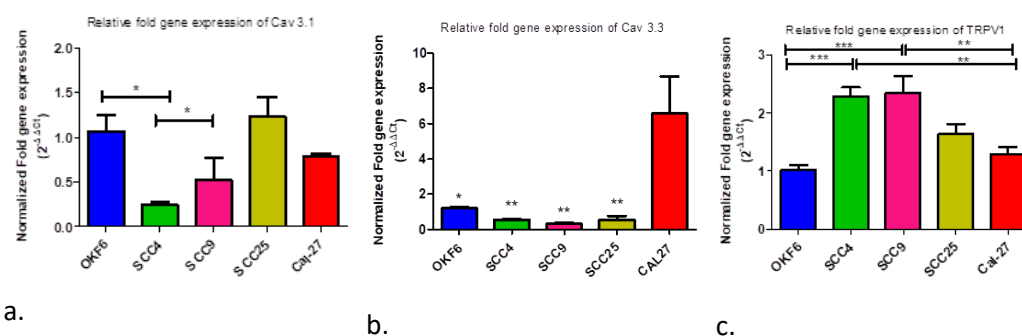
FIGURE 4.2: Relative fold gene expression of calcium channel receptors in oral cancer and normal oral cells. a. Cav 3.1; b. Cav 3.3; c. TRPV1. Normalised fold gene expression is represented on the *y*-axis, the cell line is represented on the *x*-axis. Here, *** p ≤ 0.001, ** p ≤ 0.005, * p ≤ 0.05 are statistically significant at *n* = 15. Here 'n' represents biological replicates. Error bars represent standard error of the mean. Biological replicates were obtained from five cell passages and totalled fifteen.

4.2 Optimisation of bacterial antigens and calcium channel drugs

The optimum cell number per well and bacterial antigen concentration to be used for further bacterial antigen stimulation and combination drug experiments, for all oral cancer and normal oral cells, was determined to be 5000 cells per well of a 96-well plate and 5 µg/ml LPS, PHA and LTA. Capsaicin at 10 µM and 150 µM; ML218 HCl at 1 µM and 100 µM; and capsazepine at 30 µM produced maximum inhibition of oral cancer cells (Figure A3). The conditions for the drug combination experiment was based on these drug concentrations.

4.3 Bacterial stimulation index and effect of calcium channel drugs on OKF6

4.3.1 Bacterial stimulation index

CAL27 showed the highest LPS, LTA and PHA stimulation after 24 hours ($p > 0.05$) and 72 hours among all oral cancer and normal oral cell lines ($p \leq 0.001$) (Figures 4.3 a, b, c, d, e, f).

When CAL27 was treated with 5 µg/ml of LPS, LTA and LPS+LTA stimulation for 24 hours and 72 hours, combined LPS+LTA stimulation was higher compared with either LPS or LTA alone ($p \leq 0.001$) (Figures 4.4 a, b). After 72 hours of bacterial antigen stimulation, CAL27 showed the least stimulation for LTA ($p \leq 0.001$) (Figures 4.4b).
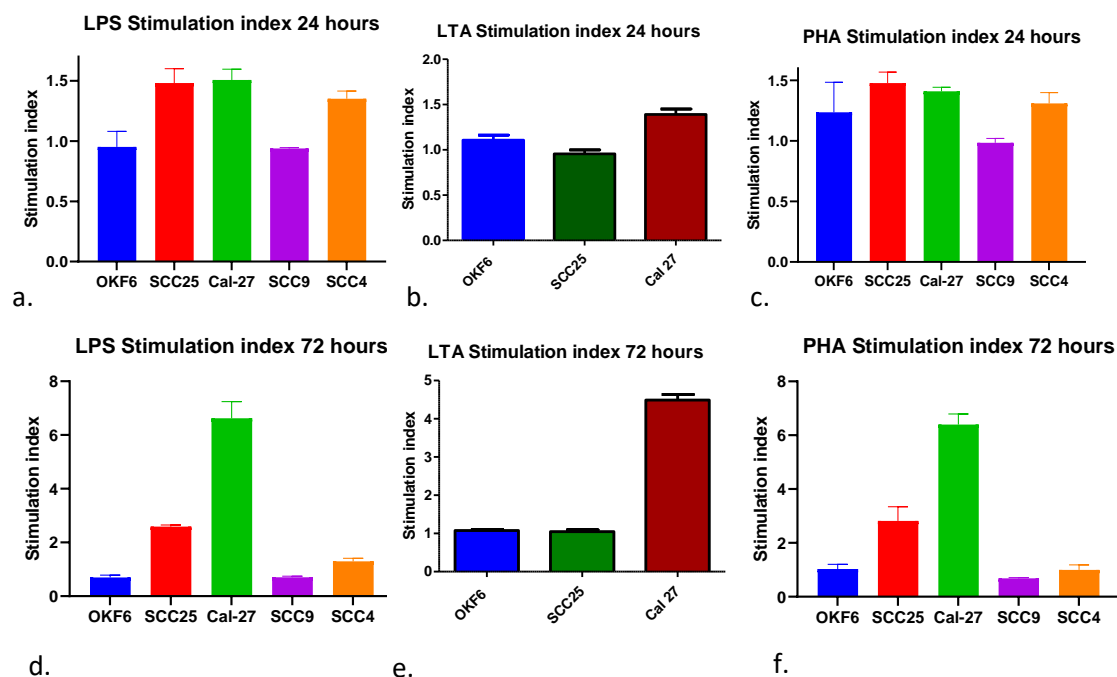
FIGURE 4.3: Stimulation index of normal oral cells and oral cancer cells following stimulation with mitogens. Cells were stimulated with bacterial antigens LPS and LTA and the non-specific mitogen PHA for 24 hrs (a, b, c) or 72hrs (d, e, f) respectively; at $n = 6$; Here 'n' represents biological replicates. Error bars represent standard error of the mean. Statistical significance not shown in figure. Biological replicates were obtained from two cell passages and totalled six.
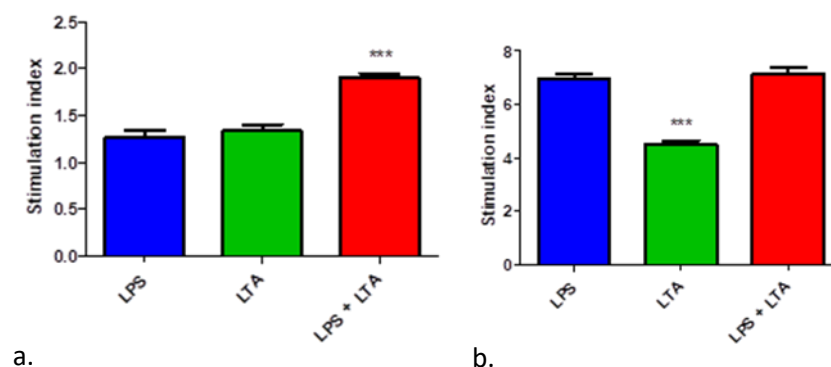
FIGURE 4.4: Stimulation of CAL27 cells with bacterial antigens. LPS, /LTA, and combined LPS+LTA at 5µg/ml. Following a) 24 hours and b) 72 hrs of stimulation. Here, *** p $\leq$ 0.001 are statistically significant at $n = 9$. Here 'n' represents biological replicates. Error bars represent standard error of the mean. Biological replicates were obtained from three cell passages and totalled nine.

4.3.2 Effect of bacterial antigen and calcium channel drugs on OKF6 normal oral cells

There was no significant change in OKF6 cell metabolism when treated with calcium channel drugs—capsaicin, ML218 HCl and LPS+LTA (as determined by MT Glo assay) (Figure 4.5a). As determined by trypan blue assay, cell viability was reduced after capsaicin 150 µM treatment ($p \leq 0.001$) (Figure 4.5b), but there was no significant change in viability with bacterial antigens and ML218 HCl treatment (Figure 4.5b).

a.   b.
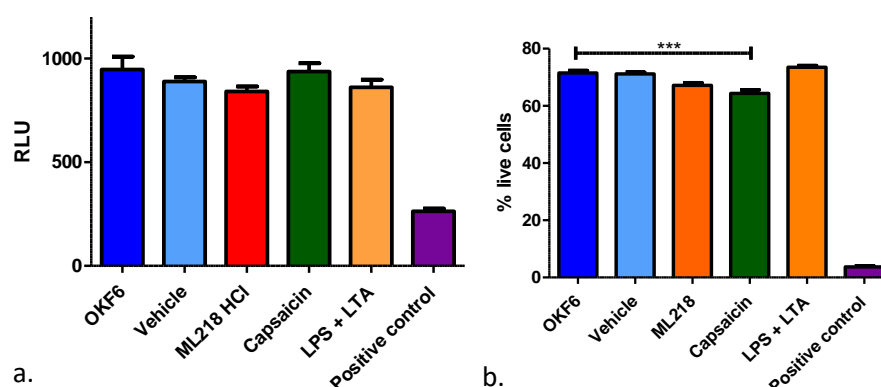
FIGURE 4.5: Metabolic and viability effect of bacterial antigens and calcium channel drugs treatment on OKF6. a. metabolic assay; b. viability assay. Here, OKF6 is untreated normal oral cells, vehicle (0.1% DMSO), ML218 HCl (100 µM), capsaicin (150 µM), LPS+LTA (5 µg/ml), positive control (5% DMSO); *** $p \leq 0.001$ are statistically significant at $n = 6$. Error bars represent standard error of the mean. Here 'n' represents biological replicates. RLU = relative luminescence unit. Biological replicates were obtained from two cell passages and totalled six.

4.4 Drug combination assay

4.4.1 Drug combination MT Glo and Trypan Blue assay

In the drug stimulation assay CAL27 showed the highest level of bacterial antigen stimulation among all cell lines. Also, ML218 HCl, capsaicin and capsazepine reduced cell viability/metabolism more strongly in CAL27 than in the other cell lines; therefore, it was decided to continue the rest of the experiments with CAL27 only. Six biological replicates were plated and treated with capsazepin (Figure A4), capsaicin and ML218 HCl (Figure 4.6).

In the absence of antigenic stimulation capsazepine reduced metabolism of CAL27 cells by 20% (Figure A3) while treatment with ML218 HCl and capsaicin reduced metabolism by 100% (Figure 4.6). In the absence of antigenic stimulation, 50, 70, 65% of cells were killed by the capsazepine, ML218 HCl and capsaicin treatment respectively (Figures A5 and 4.6). Addition of antigens at the same time as anti-cancer drugs without prior antigenic stimulation (0 hour) significantly prevented cell death (Figures A5f, g and 4.7f, g) (p ≤ 0.001) and this effect was significantly greater with LPS+LTA than LPS stimulation alone (p ≤ 0.001). This confirms our earlier finding that CAL27 cells grow quicker in the presence of both Gram-positive and Gram-negative antigens (LPS+LTA) when compared to just Gram-negative antigens (LPS). The degree of metabolic inhibition was also significantly decreased by addition of antigens at time 0 and this protection was also greater with LPS+LTA stimulation than with LPS stimulation alone (p ≤ 0.001) (Figures A4e, f and 4.6c).

Providing antigenic stimulation to cells prior to addition of capsazepine significantly increased the inhibition of metabolism and dead cells seen at 24 and 72 hours (p ≤ 0.001) (Figures A4a, b, c, d and A5a, b, c, d). Providing antigenic stimulation only prior to treatment with ML218 HCl had no effect on metabolism and percentage of killed cells at 24 or 72 hours with metabolism inhibited 100% (Figures 4.6a, b and 4.7b, c, d, e). However, addition of antigen prior to and concurrently with ML218 HCl treatment significantly improved metabolism and reduced the percentage of killed cells (p ≤ 0.001) (Figures 4.6a, b and 4.7b, c, d, e). A similar effect was seen with capsaicin treatment at 72 hours (p ≤ 0.001) (Figures 4.6a and 4.7d, e). In contrast, by 72 hours the addition of antigens prior to capsaicin treatment also proved effective (p ≤ 0.001) (Figure 4.6a and 4.7d, e).

4.4.2 Drug combination clonogenic assay

The effect of calcium channel drugs on bacterial antigen stimulated CAL27 in the presence or absence of bacterial antigens was determined by a clonogenic assay. Cells were stimulated with LPS or combined LPS+LTA for 72 hrs prior to the addition of ML218 HCl or capsaicin with or without additional antigens (Figure 4.8). The percentage colony intensity and number of colonies were significantly higher when CAL27 were stimulated with LPS (p ≤ 0.001) (Figure 4.8b). Stimulating cells with combined LPS+LTA resulted in even greater colony intensity and more colonies (p ≤ 0.001)

confirming our previous finding that bacterial antigens stimulate CAL27 cells and this stimulation is greater when both Gram-positive and Gram-negative antigens are combined. Treating cells with ML218 HCl or capsaicin significantly reduced both colony intensity and number of colonies ($p \leq 0.001$) (Figure 4.8c). Stimulating cells with bacterial antigens prior to drug treatment non-significantly increased the number of colonies and increased colony intensity approximately 2-fold ($p > 0.05$). Addition of more antigens simultaneously with drug treatment increased colony intensity and significantly increased colony counts ($p \leq 0.001$) (Figure 4.8 c, e test sample A, B *v.* C, D). In the presence of bacterial antigens ML218 inhibited CAL27 cells significantly more than capsaicin ($p \leq 0.05$) (Figure 4.8 c, e).
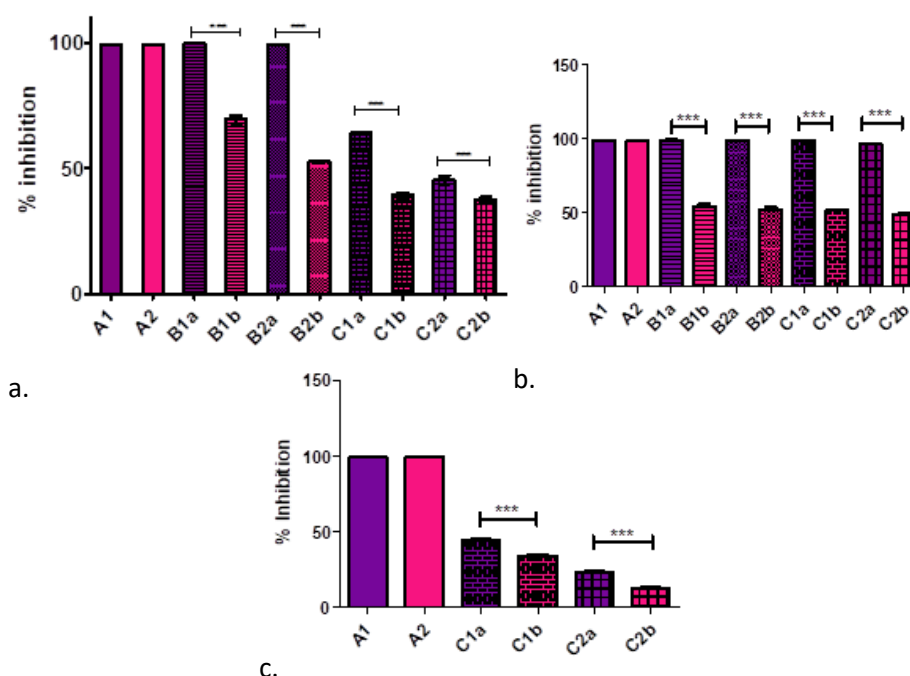
FIGURE 4.6: MT Glo drug ML218 HCl and capsaicin drug combination assay. a. 72-hour stimulation luminescence assay; b. 24-hour stimulation luminescence assay; c. 0-hour stimulation luminescence assay; *** $p \leq 0.001$ are statistically significant at *n* = 6. Here 'n' represents biological replicates. Error bars represent standard error of the mean. A1: ML218 HCl only (purple); A2: capsaicin only (pink); B1a and b: after LPS stimulation, addition of ML218 HCl (purple stippled) and capsaicin (pink stippled), respectively; B2a and b: after LPS+LTA stimulation, addition of ML218 HCl (purple dotted) and capsaicin (pink dotted), respectively; C1a and b: after LPS stimulation, addition of (ML218 HCl+LPS) (purple bricked) and (capsaicin+LPS) (pink bricked) respectively; C2a and b: after LPS+LTA stimulation, addition of (ML218 HCl+LPS+LTA) (purple webbed) and (capsaicin+LPS+LTA) (pink webbed), respectively. Biological replicates were obtained from three cell passages and totalled six.
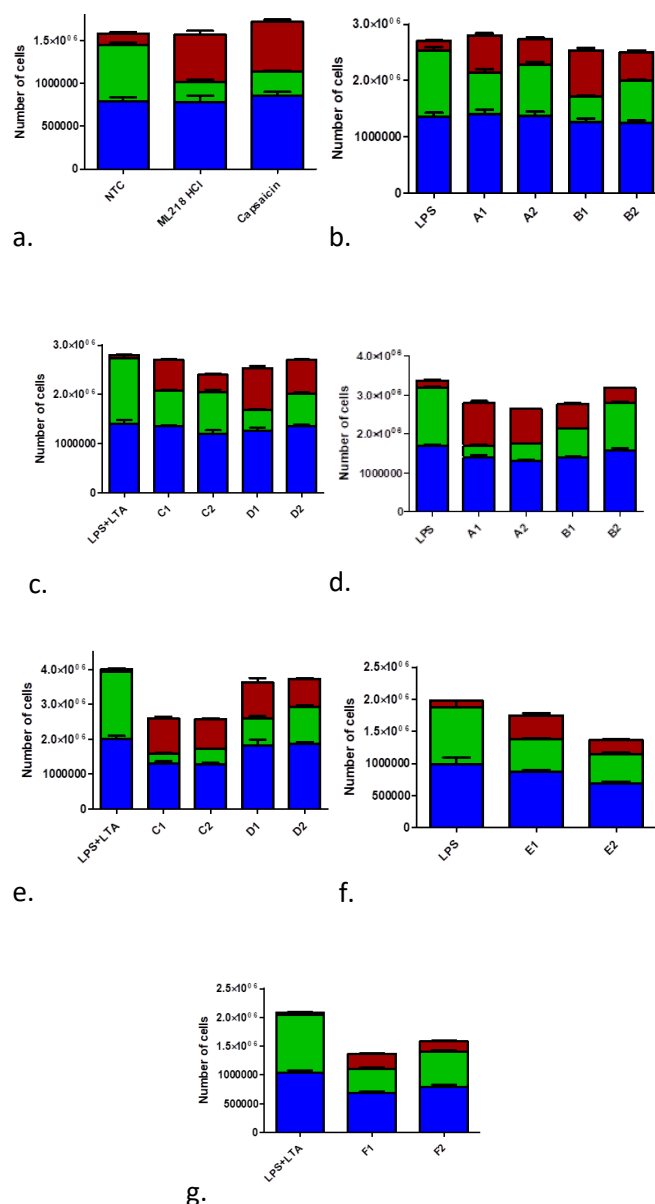
FIGURE 4.7: Trypan Blue ML218 HCl and capsaicin drug combination assay. a. only drug cell viability assay; b. and c. 24-hour stimulation cell viability assay; d. and e. 72-hour stimulation cell viability assay; f. and g. 0-hour stimulation cell viability assay; at $n = 6$. Error bars represent standard error of the mean. Here 'n' represents biological replicates. NTC: no treatment control; A1 and A2: after LPS stimulation, addition of ML218 HCl and capsaicin, respectively; B1 and B2: after LPS stimulation, addition of (ML218 HCl+LPS) and (capsaicin+LPS), respectively; C1 and C2: after LPS+LTA stimulation, addition of ML218 HCl and capsaicin, respectively; D1 and D2: after LPS+LTA stimulation, addition of (ML218 HCl+LPS+LTA) and (capsaicin+LPS+LTA), respectively; E1 and E2: after 0 hour LPS stimulation, addition of (ML218 HCl+LPS) and (Capsaicin+LPS), respectively; F1 and F2: after 0 hour LPS+LTA stimulation, addition of (ML218 HCl+LPS+LTA) and (capsaicin+LPS+LTA), respectively; red represents dead cells; green represents live cells; blue represents total cells; statistical significance not shown in the figure. Biological replicates were obtained from three cell passages and totalled six.
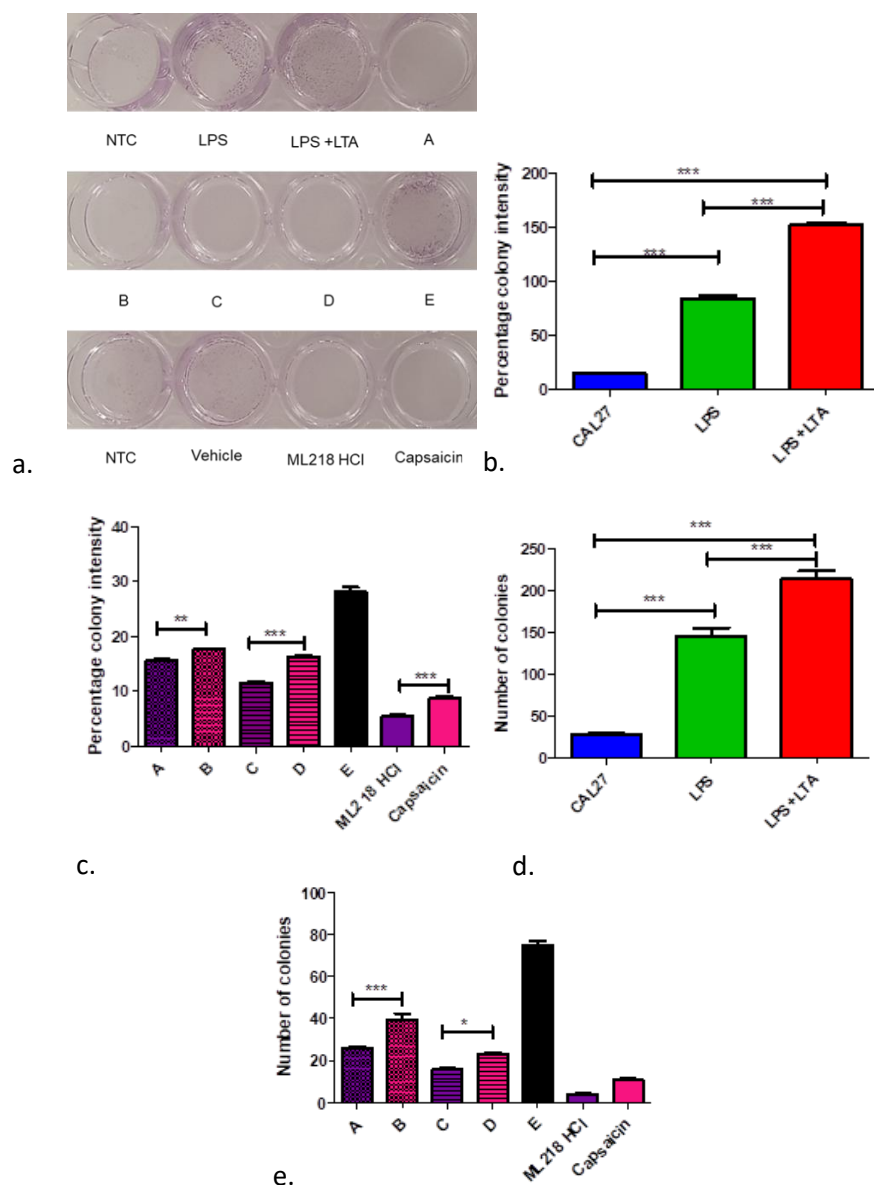
FIGURE 4.8: Clonogenic assay of drug combinations.

 a. Image of clonogenic assay under different drug conditions; b. Percentage colony intensity of CAL27 *v.* different bacterial antigens after 72 hours stimulation; c. Percentage colony intensity of different drug combinations; d. Number of colonies of CAL 27 *v.* different bacterial antigens after 72 hours stimulation; e. Number of colonies of different drug combinations. A: ML218 HCl+LPS+LTA after 72 hours of LPS+LTA stimulation (purple dotted), B: capsaicin+LPS+LTA after 72 hours of LPS+LTA stimulation (pink dotted), C: ML218 HCl after 72 hours of LPS+LTA stimulation (purple stippled), D: capsaicin after 72 hours of LPS+LTA stimulation (pink stippled); E: CaCl$_2$ after 72 hours of LPS+LTA stimulation (black); LPS stimulated (green); LPS+LTA stimulated (red); CAL27 (untreated) (blue).; vehicle: 0.1% DMSO; *** $p \leq 0.001$, ** $p \leq 0.005$, * $p \leq 0.05$ are statistically significant at $n = 6$; Error bars represent standard error of the mean. Here 'n' represents biological replicates. Biological replicates were obtained from three cell passages and totalled six.

4.5 Phosphokinase array

A proteome profiler array of 37 kinases was used to understand the biochemical reason for the differences in cell viability, colony formation and metabolism after bacterial antigen stimulation of CAL27. Positive signals (radiopaque dark circular dots) were identified by placing a transparency overlay on the array image and aligning it with the pairs of reference spots in the corner of each membrane (Figure 4.9e). Densitometric analysis of the array membrane showed greater reduction of EGFR, eNOS, ERK 1/2, Lyn, STAT5 a/b, Yes, p53, p38α, Src, RSK 1/2, β-catenin, HSP 60, Chk2, GSKα/β and GSK3β phosphorylation in CAL27 after combined LPS+LTA antigen stimulation than after stimulation with LPS, after stimulation with LTA and cells without bacterial antigen stimulation (Figure 4.9d). Stimulation with LTA showed increases in Src and HSP 60 phosphorylation relative to cells without bacterial antigen stimulation (Figure 4.9b). There was no difference in EGFR phosphorylation in LPS stimulated and unstimulated cells (Figure 4.9a). However, LPS stimulation, produced increased RSK 1/2 phosphorylation, compared with unstimulated cells (Figure 4.9a). Combined LPS+LTA antigen stimulation, produced lower STAT3 phosphorylation compared with LTA stimulation or with no bacterial antigen stimulation, but did not differ from LPS stimulated cells (Figure 4.9d). LTA stimulation showed increase in the phosphorylation of eNOS, GSK3β, GSK3α/β, STAT3, Src, β-catenin, HSP 60 and Chk2 phosphorylation, relative to LPS stimulated cells (Figure 4.9d).
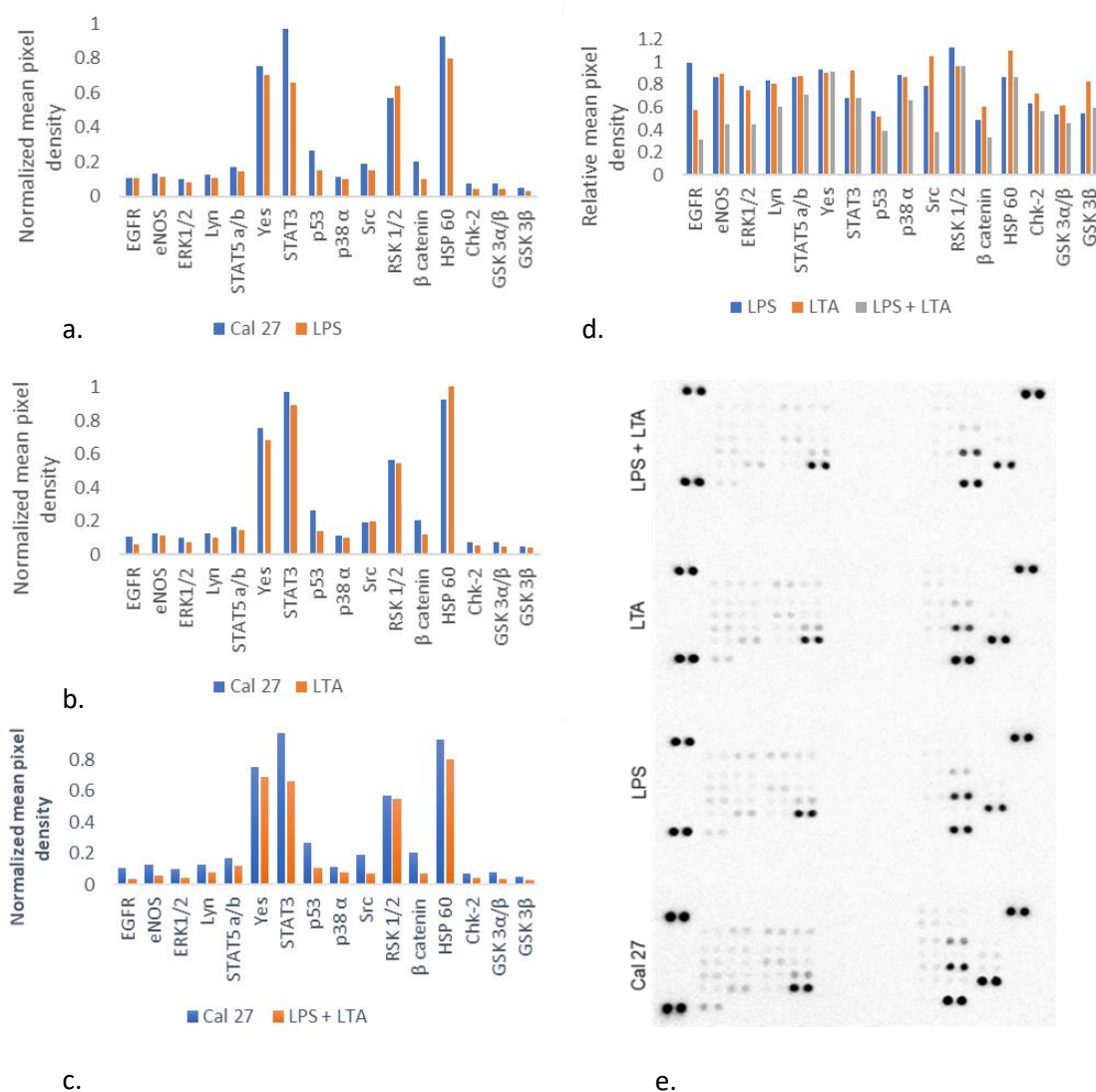
FIGURE 4.9: Comparison in normalised and relative mean pixel density of different kinases under different conditions. a. CAL27 (unstimulated) *v*. CAL27 after 72 hours LPS stimulation; b. CAL27 (unstimulated) *v*. CAL27 after 72 hours LTA stimulation; c. CAL27 (unstimulated) *v*. CAL27 after 72 hours LPS+LTA stimulation; d. CAL27 after 72 hours LPS stimulation *v*. CAL27 after 72 hours LTA stimulation *v*. CAL27 after 72 hours LPS+LTA stimulation; e. Image of the phosphokinase array; at *n* = 2; Here 'n' represents biological replicates. EGFR: epidermal growth factor receptor, eNOS: endothelial nitric oxide synthase, ERK 1/2: extracellular receptor kinase, STAT5 a/b: signal transducer and activator of transcription 5 a/b, STAT3: signal transducer and activator of transcription 3, p53: tumour suppressor protein, p38 α: mitogen-activated protein kinase 14, Src, Lyn and Yes: non-receptor tyrosine kinases, RSK 1/2: p90 ribosomal S6 kinase, β-catenin, HSP 60: heat shock protein 60, Chk-2: checkpoint kinase 2, GSK3α/β: glycogen synthase kinase 3α/β, GSK3β: glycogen synthase kinase 3β. The assay measured phosphorylated protein levels. Biological replicates were obtained from one cell passages and totalled two.

4.6 Identification of tumour proliferation and suppressor proteins

4.6.1 Validation of qPCR products

RT-PCR and western blots were used to quantify gene expression and protein expression for tumour suppressor protein SOCS3 and tumour proliferation-associated proteins EGFR, GMPS, STAT3 and PI3K. RT-qPCR showed no amplification in negative controls, bad passive reference signals, off-scale fluorescence, high standard deviation among replicates, outliers in replicate group, C_t, baseline or exponential algorithm failure, low passive reference signal, passive reference signal changes near C_t or multiple melting temperature (T_m) peaks (Figure 4.11). Melting curve of the RT-qPCR showed specific PCR products and no false amplification (Figure 4.10).

4.6.2 Relative fold gene expression of proliferation related proteins

Relative fold gene expression of SOCS3 was highest when CAL27 were stimulated with LPS ($p \leq 0.001$) (Figure 4.12a). After stimulating cells with bacterial antigens capsaicin increased the relative fold gene expression of SOCS3 significantly more than ML218 HCl ($p \leq 0.05$) (Figure 4.12a). Whereas Gram-negative bacterial antigen stimulation resulted in significantly lower EGFR and GMPS relative fold gene expression than unstimulated CAL27 ($p \leq 0.05$) (Figures 4.12b, c). Stimulating cells with both Gram-positive and Gram-negative bacterial antigen and addition of bacterial antigens simultaneously with ML218 HCl resulted in significant decrease of relative fold gene expression of PI3KCA than unstimulated CAL27 ($p \leq 0.05$) (Figure 4.12e). There was no significant STAT3 relative fold gene expression difference among the treatment groups (Figure 4.12d).
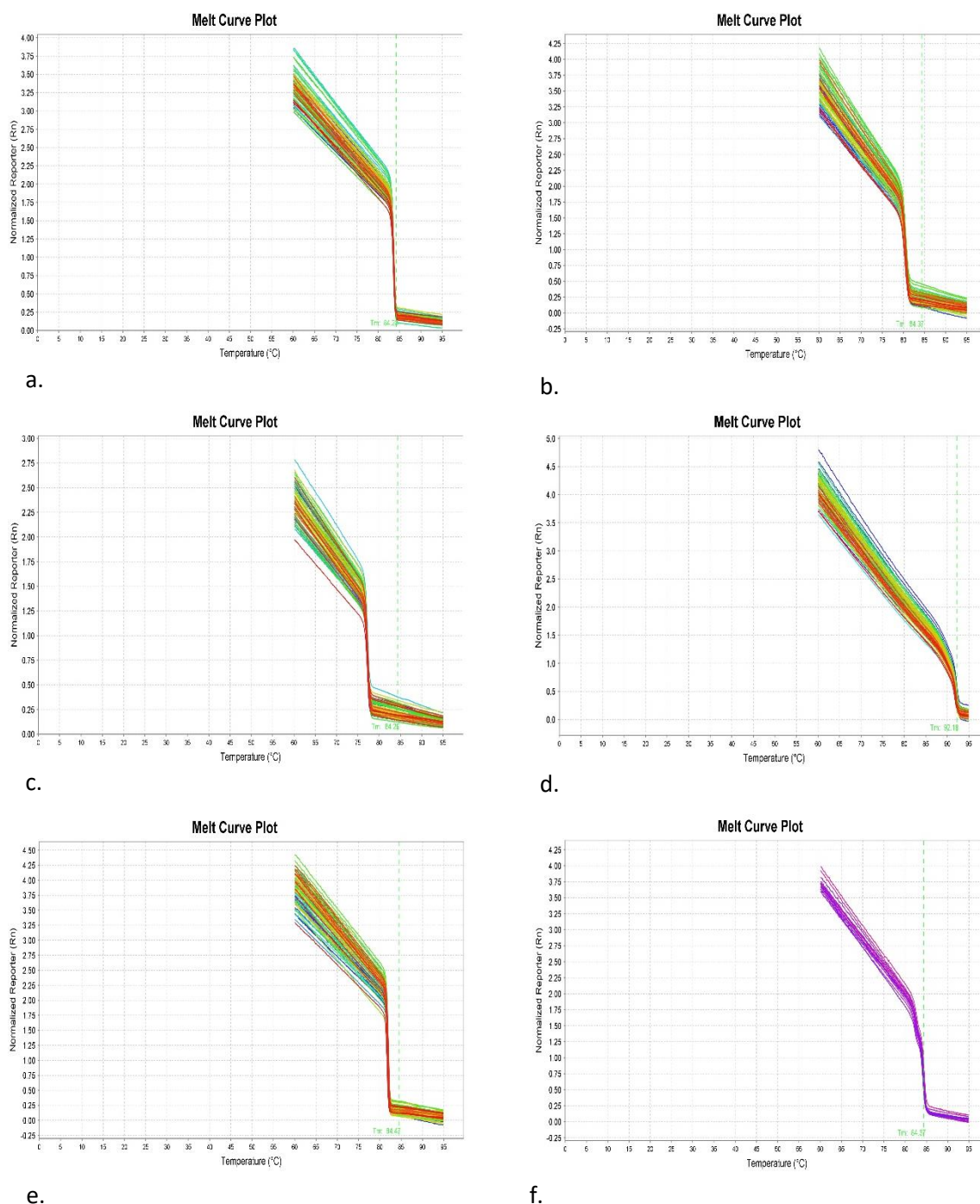
FIGURE 4.10: Melt curve for primers used during the RT-qPCR. a. EGFR with T_m of 84.28°C; b. GMPS with T_m of 84.37°C; c. PI3KCA with T_m of 84.29°C; d. SOCS3 with T_m of 92.18°C; e. STAT3 with T_m of 84.47°C; f. GAPDH with T_m of 84.37°C. Here, Tm is the melting temperature; *y*-axis and *x*-axis represent normalised reporter (Rn) and temperature (°C) respectively.
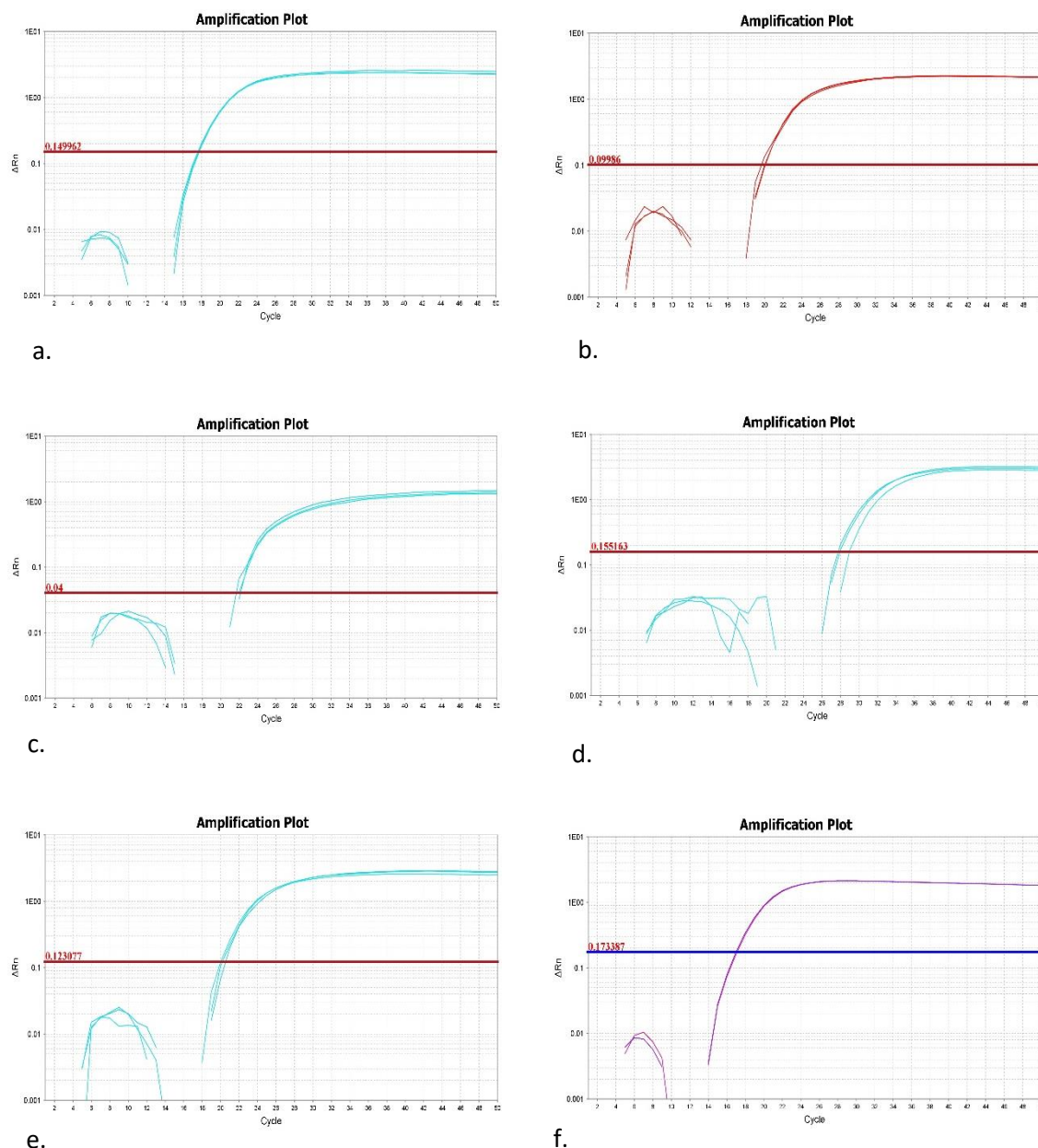
FIGURE 4.11: Amplification curves for tumour proliferation and suppressor proteins from CAL27. a. EGFR; b. GMPS; c. PI3KCA; d. SOCS3; e. STAT3; f. GAPDH. Here, ΔRn is represented on the *y*-axis, and number of cycles is represented on the *x*-axis; ΔRn is the difference in the Rn value of each of the experiments and the Rn value of the baseline signal generated by the instrument; Rn is the reporter signal normalised to the fluorescence signal of passive reference dye (ROX).
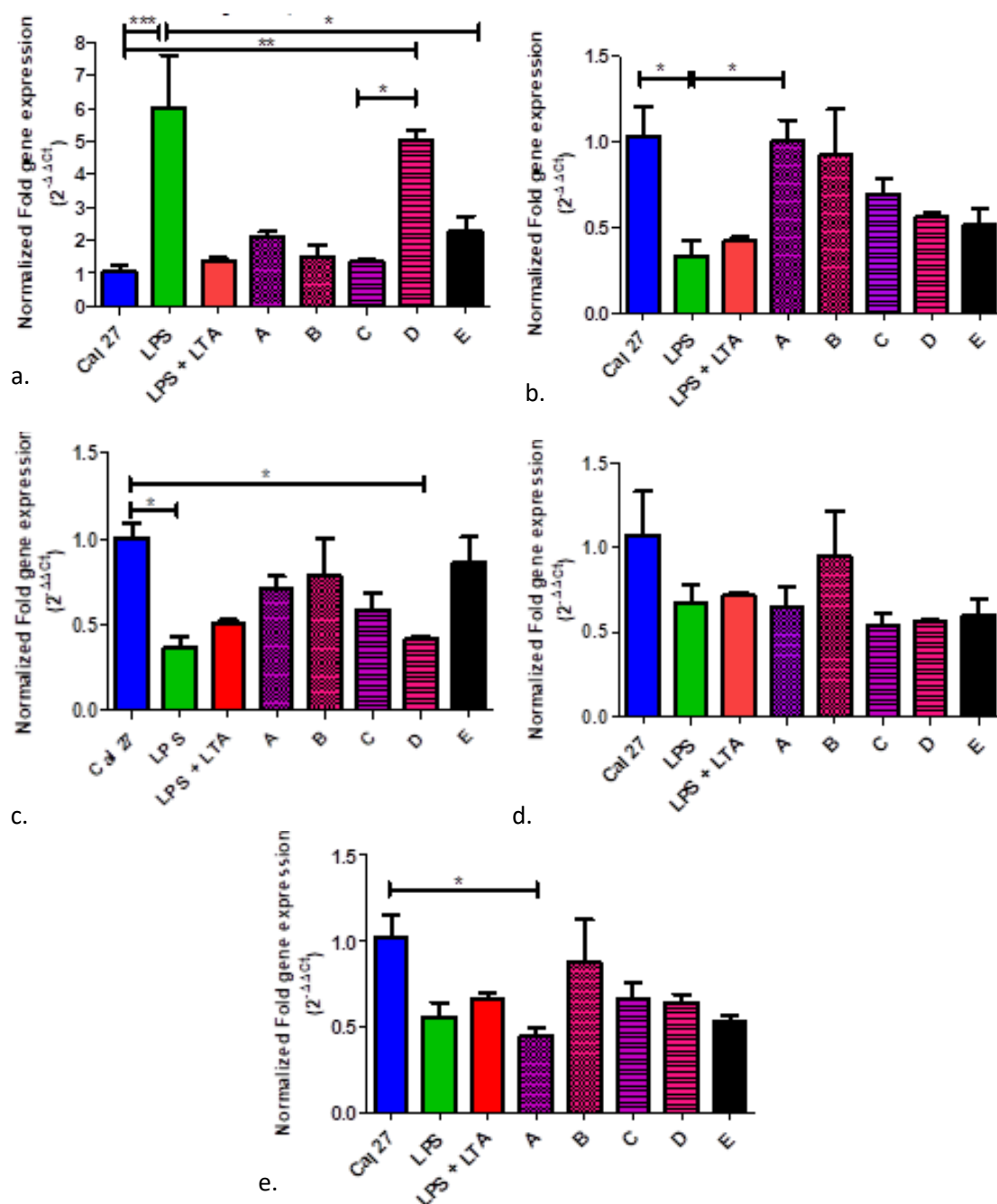
FIGURE 4.12: Relative fold gene expression of tumour proliferation and suppressor proteins in CAL27. a. SOCS3; b. EGFR; c. GMPS; d. STAT3; e. PIK3CA. Normalised fold gene expression is represented on the *y*-axis; treatment condition is represented on the *x*-axis; *** p ≤ 0.001, ** p ≤ 0.005, * p ≤ 0.05 are statistically significant at *n* = 9. Error bars represent standard error of the mean. Here 'n' represents biological replicates. A: ML218 HCl+LPS+LTA after 72 hours of LPS+LTA stimulation (purple dotted), B: capsaicin+LPS+LTA after 72 hours of LPS+LTA stimulation (pink dotted), C: ML218 HCl after 72 hours of LPS+LTA stimulation (purple stippled), D: capsaicin after 72 hours of LPS+LTA stimulation (pink stippled); E: CaCl2 after 72 hours of LPS+LTA stimulation (black); LPS stimulated (green); LPS+LTA stimulated (red); CAL27 (untreated) (blue). Biological replicates were obtained from three cell passages and totalled nine.

4.6.3 Protein expression of proliferation related proteins

Analysis of the western blot images (Figure 4.13) showed STAT3, SOCS3 and EGFR protein expression was significantly higher in CAL27 without bacterial antigen stimulation than bacterial antigen stimulated cells ($p \leq 0.001$) (Figures 4.14a, e, g). Also, STAT3 protein expression was significantly higher in CAL27 after LPS+LTA than after stimulation with LPS ($p \leq 0.05$) (Figure 4.14a). After stimulating cells with bacterial antigens ML218 HCl resulted in highest protein expressions of STAT3 and EGFR protein expression ($p \leq 0.001$) (Figures 4.14b, h). PI3K protein expression was significantly higher after stimulation with LPS+LTA than with no bacterial antigen stimulation, or after stimulation with LPS alone ($p \leq 0.001$) (Figure 4.14c). However, addition of more antigens simultaneously with ML218 HCl increased PI3K protein expression ($p \leq 0.05$) (Figure 4.14d). Similarly, stimulating cells with bacterial antigens prior to capsaicin treatment and addition of more antigens simultaneously with capsaicin resulted in higher SOCS3 protein expression than cells after bacterial antigen stimulation ($p \leq 0.001$) (Figure 4.14f). Interestingly, stimulating cells with bacterial antigens prior to ML218 HCl and capsaicin non-significantly increased the protein expressions of SOCS3 and PI3K with respect to cells after bacterial antigen stimulation ($p > 0.05$) (Figures 4.14d, f). Also, EGFR protein expression was significantly higher in CAL27 after stimulation of LPS+LTA than after stimulation of LPS ($p \leq 0.005$) (Figure 4.14g).
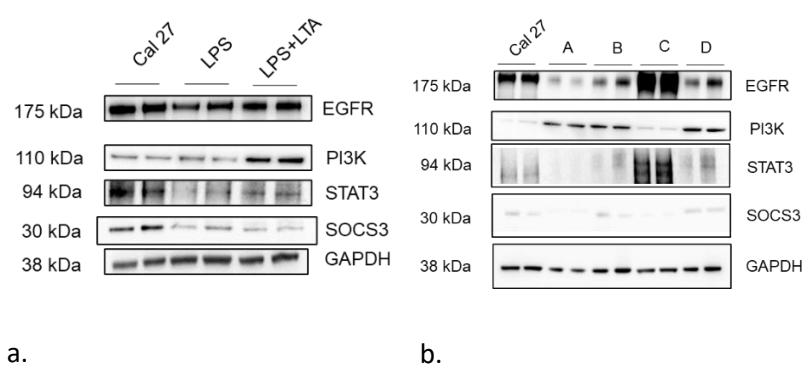
FIGURE 4.13: Western blot images of different treatment conditions. a. 10-well western blot image showing bands of different tumour suppressor and proliferation-related proteins in CAL27 (untreated/control), CAL27 after LPS stimulation, and CAL27 after LPS+LTA stimulation; b. 12-well western blot image showing bands of different tumour suppressor and proliferation-related proteins in CAL27 (untreated/control) and other treatment conditions.
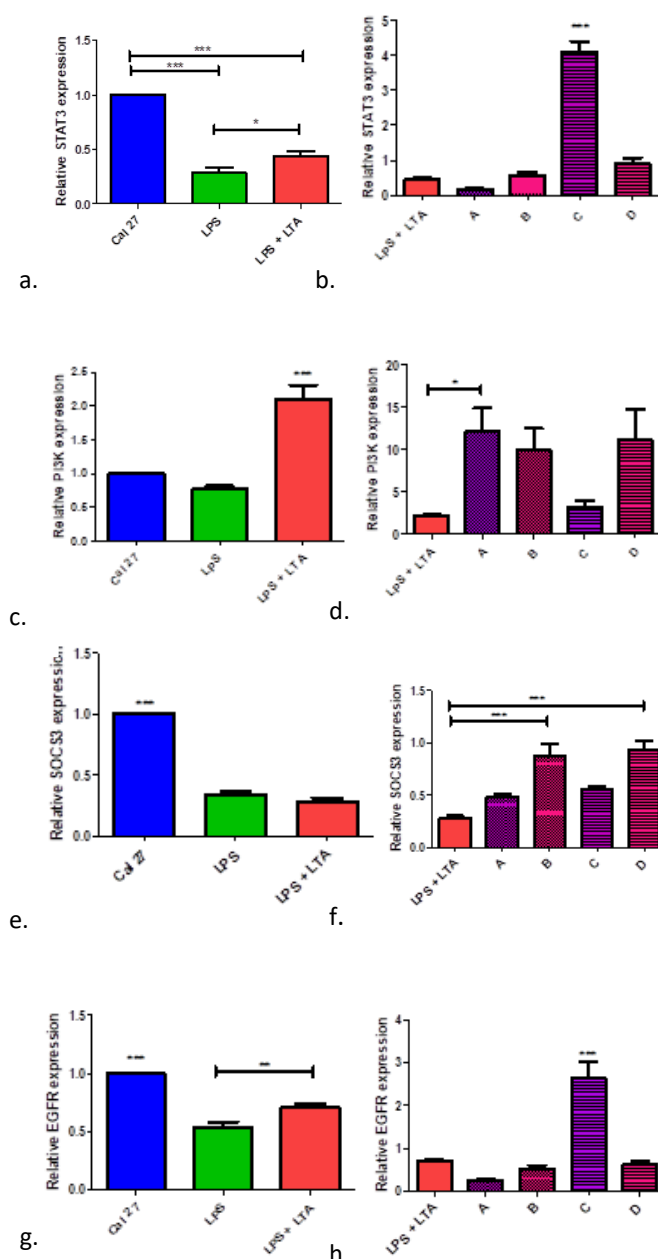
FIGURE 4.14: Western blot analysis of different tumour suppressor and proliferation-related proteins in CAL27. a. and b. Relative STAT3 expression under different conditions; c. and d. Relative PI3K expression under different conditions; e. and f. Relative SOCS3 expression under different conditions; g. and h. Relative EGFR expression under different conditions; *** $p \leq 0.001$, ** $p \leq 0.005$, * $p \leq 0.05$ are statistically significant at $n = 6$. Error bars represent standard error of the mean. Here 'n' represents biological replicates. All the protein expressions are relative to CAL27. A: ML218 HCl+LPS+LTA after 72 hours of LPS+LTA stimulation (purple dotted), B: capsaicin+LPS+LTA after 72 hours of LPS+LTA stimulation (pink dotted), C: ML218 HCl after 72 hours of LPS+LTA stimulation (purple stippled), D: capsaicin after 72 hours of LPS+LTA stimulation (pink stippled); LPS stimulated (green); LPS+LTA stimulated (red); CAL27 (untreated) (blue). Biological replicates were obtained from three cell passages and totalled six.

4.7 Apoptosis assay

CellEvent Caspase 3/7 Green Detection Reagent produced bright, opaque, green fluorescent circular or oval shaped bodies that denoted caspase 3/7-positive cells (Figure 4.15a). Comparing the caspase 3/7-positive cells to the total number of cells per image under each condition, the percentage of cells undergoing apoptosis was higher in CAL27 cells without bacterial antigen stimulation ($p \leq 0.001$) (Figure 4.15b). Combined LPS+LTA antigen stimulation, produced the smallest percentage of caspase 3/7-positive cells ($p \leq 0.001$) (Figure 4.15b). Treatment with ML218 HCl resulted in a higher percentage of caspase 3/7-positive cells than treatment with capsaicin irrespective of whether or not the cells received antigen stimulation prior to treatment or if additional antigen was added during drug treatment ($p \leq 0.001$) (Figure 4.15c). Similarly, treatment of LPS+LTA stimulated cells with $CaCl_2$ for 24 hours produced a higher percentage of caspase 3/7-positive cells than untreated stimulated cells ($p \leq 0.001$), but a lower percentage than ML218 HCl ($p \leq 0.001$) or capsaicin treatment ($p \leq 0.005$) (Figure 4.15c).
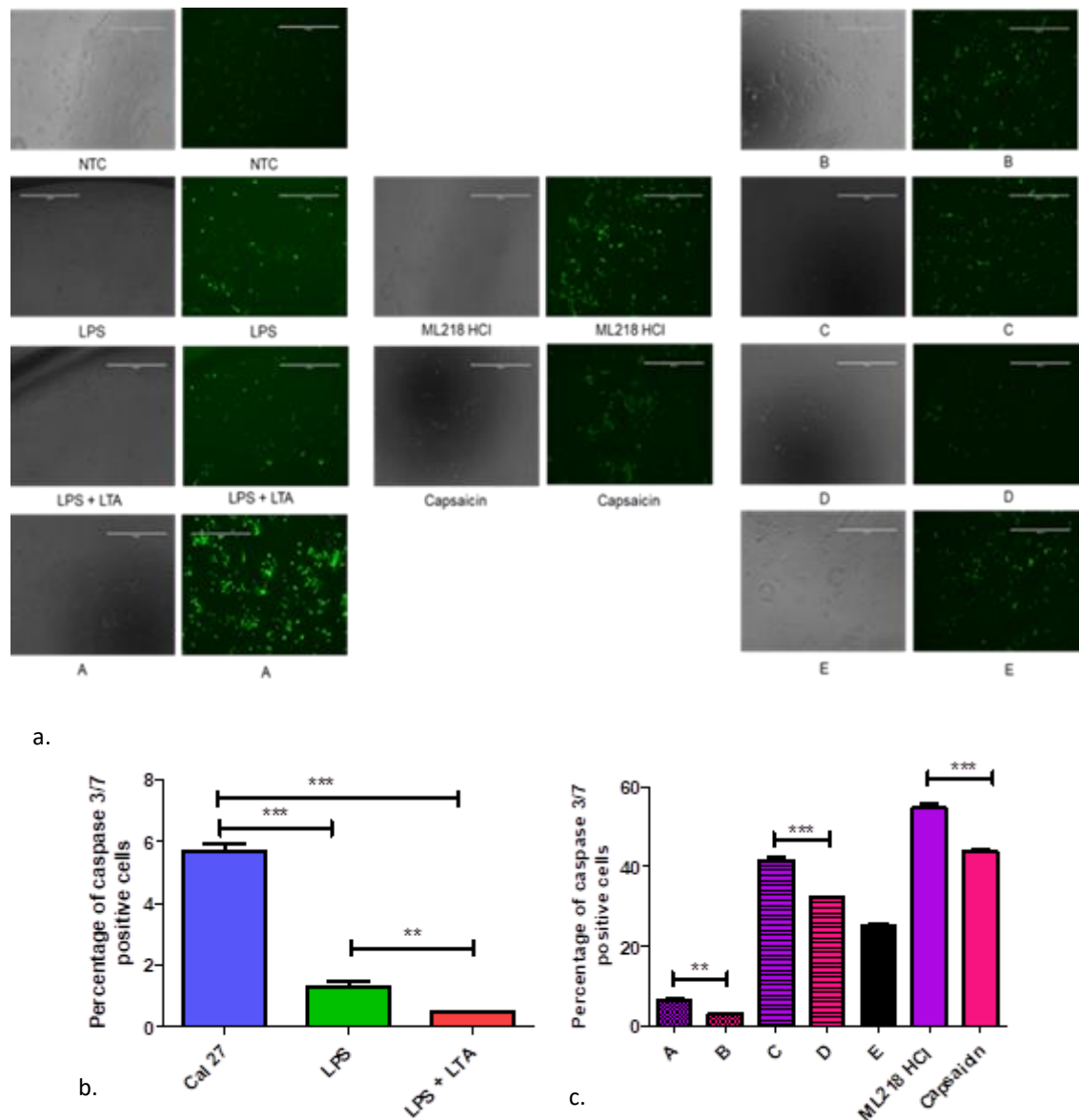
FIGURE 4.15: Caspase 3/7 assay. a. Caspase 3/7 green fluorescent and bright field images of each treatment condition; b. and c. Percentage of caspase 3/7-positive cells under different conditions; *** $p \leq 0.001$, ** $p \leq 0.005$ are statistically significant at $n = 6$. Error bars represent standard error of the mean. Here 'n' represents biological replicates. A: ML218 HCl+LPS+LTA after 72 hours of LPS+LTA stimulation (purple dotted), B: capsaicin+LPS+LTA after 72 hours of LPS+LTA stimulation (pink dotted), C: ML218 HCl after 72 hours of LPS+LTA stimulation (purple stippled), D: capsaicin after 72 hours of LPS+LTA stimulation (pink stippled); LPS stimulated (green); LPS+LTA stimulated (red); CAL27 (untreated) (blue). Biological replicates were obtained from three cell passages and totalled six.

4.8 TNFα ELISA

The concentration of TNFα (pg/ml) was significantly higher in OKF6 (without any treatment) than in CAL27 (without any treatment) (p ≤ 0.001) (Figure 4.16a). In CAL27, TNFα (pg/ml) was significantly higher after stimulation with LPS than after stimulation with LPS+LTA (p ≤ 0.001) (Figure 4.16b). Stimulating cells with combined LPS+LTA resulted in significantly higher TNFα (pg/ml) than did stimulating cells with bacterial antigens prior to ML218 HCl or capsaicin treatment, and addition of more antigens simultaneously with drug treatments (p ≤ 0.001) (Figure 4.16c). Moreover, addition of more antigens simultaneously with ML218 HCl significantly produced higher TNFα (pg/ml) than did stimulating cells with bacterial antigens prior to ML218 HCl (p ≤ 0.005) (Figure 4.16c). Contrastingly the results are opposite in capsaicin treatment (p ≤ 0.001) (Figure 4.16c). Also, after stimulating cells with bacterial antigens capsaicin produced TNFα (pg/ml) significantly more than ML218 HCl (p ≤ 0.001) (Figure 4.16c).
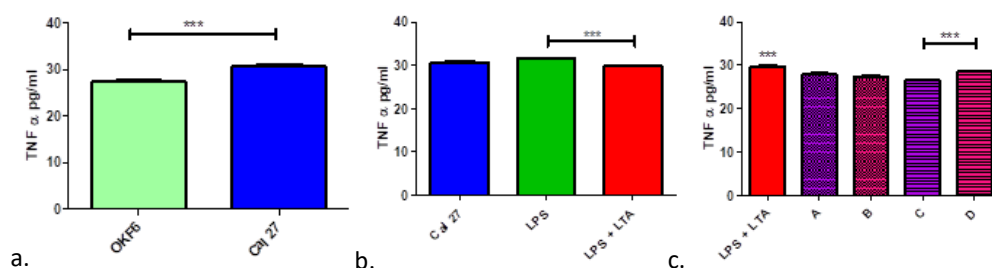
FIGURE 4.16: TNFα ELISA. a. Comparison of TNFα (pg/ml) in OKF6 (untreated) (light green) and CAL27 (untreated) (blue); b. and c. Comparison of TNFα (pg/ml) under different treatment conditions; *** p ≤ 0.001, ** p ≤ 0.005, * p ≤ 0.05 are statistically significant at *n* = 9; Error bars represent standard error of the mean. Here 'n' represents biological replicates. A: ML218 HCl+LPS+LTA after 72 hours of LPS+LTA stimulation (purple dotted), B: capsaicin+LPS+LTA after 72 hours of LPS+LTA stimulation (pink dotted), C: ML218 HCl after 72 hours of LPS+LTA stimulation (purple stippled), D: capsaicin after 72 hours of LPS+LTA stimulation (pink stippled); LPS stimulated (green); LPS+LTA stimulated (red). Biological replicates were obtained from three cell passages and totalled nine.

Discussion

5.1 Selection and optimisation of calcium channel drugs

5.1.1 Selection of calcium channel drugs

Change in calcium signalling affects cancer cell proliferation (Cui et al., 2017). Influx of calcium upregulates various proliferation pathways (Varghese et al., 2019). Relative gene expression of calcium channels showed that CAL27 had higher Cav 3.3 and TRPV1 than normal oral cells, but lower expression of another T-type voltage-gated calcium channel, Cav 3.1. This may reflect that Cav 3.3 and TRPV1 caused increased entry and accumulation of calcium in CAL27 cells, which may aid proliferation of CAL27 cells, as it has been shown that VDCC and RDC increased entry of calcium into cancer cells and leads to their proliferation (Capiod, 2016) (Figure 1.3). Also, there might crosstalk among calcium channel receptors since TRPV1 activation has been shown to downregulate voltage-gated calcium channels (Wu, Chen & Pan, 2005).

Capsaicin is a TRPV1 agonist (Yang & Zheng, 2017) reported to reduce the proliferation of an oral squamous cancer cell line of Asian origin, ORL-48 (Kamaruddin et al., 2019). Also, capsaicin induces apoptosis in SCC4 via mitochondria-dependent and independent pathways (Ip et al., 2012). Capsaicin has also been shown to induce apoptosis in SCC4

and SCC25 independent of TRPV1; that is TRPV1 is non-functional in SCC4 and SCC25 (Gonzales et al., 2014). Capsazepine has also been shown to be a TRPV1 antagonist (Nguyen et al., 2010) effective in reducing the proliferation of oral cancer cells (De La Chapa et al., 2019).

In the current study, most of the oral cancer cell lines showed lower expression of Cav 3.1 than Cav 3.3. Consequently, ML218 HCl was used rather ML218 because ML218 is a T-type (Cav 3.1, Cav 3.2, Cav 3.3) selective voltage-gated calcium channel blocker (Xiang et al., 2011) whereas ML218 HCl is a T-type (Cav 3.2 and Cav 3.3) selective voltage-gated calcium channel blocker, that does not block Cav 3.1 (Li et al., 2017).

5.1.2 Optimization of calcium channel drugs

Having applied various concentrations of a range of calcium channel drugs based on the literature, capsaicin (10 µM and 150 µM), capsazepine (30 µM) and ML218 HCl (1 µM and 100 µM) were found to decrease proliferation and viability of oral cancer cells (SCC25, and CAL27) the most. SCC25 and CAL27 were cultured in KSFM (with calcium chloride at a final concentration of 0.02 Mm) and DMEM (containing 1.2mM calcium ion concentration) respectively. CID16020046, a GPR55 antagonist (Stancic et al., 2015) was found to have no effect on oral cancer cell proliferation/viability.

5.2 Effect of bacterial antigen on oral cancer cells and proliferation-related proteins

5.2.1 Selection of CAL27 for the drug combination assay

SCC4, SCC9, SCC25, CAL27 and OKF6 cells were stimulated with LPS, LTA, PHA and LPS+LTA. CAL27 showed the highest bacterial antigen stimulation response among all the cell lines. During optimisation of the oral cancer cells to bacterial antigens, LPS, LTA and PHA at 5 µg/ml concentration induced the strongest stimulation effect of all concentrations of bacterial antigen.

Cancer cells are more active than their normal counterparts (Hanahan & Weinberg, 2011). TLR4 (considered a potent activator of LPS stimulation) is upregulated in cancer cells,

([Oblak & Jerala, 2011](#)) which may explain the finding in this study that OKF6 was not affected by LPS and LTA treatment.

All bacterial antigens showed more stimulation of CAL27 after 72 hours than only 24 hours. However, LPS and PHA were associated with similar stimulation index values after 24 hours and 72 hours stimulation. This probably reflects the lower number of receptors available for antigens compared with PHA, that may require further investigation in future.

5.2.2 LPS and LTA combination is more potent that LPS alone

Based on the results of the MT Glo assay, trypan blue live/dead cell count and the clonogenic assay, LPS+LTA increased CAL27 cell metabolism, viability and colony formation, all of which suggests higher proliferation compared with LPS treatment alone. This further signifies that not only LPS, but LPS+LTA promotes proliferation of CAL27.

5.2.3 Possible biochemical reason for LPS and LTA stimulation

Further analysis of the proliferation-related proteins that may be affected by bacterial antigens involved a phosphokinase array (Table 5.1) and western blot. This showed that LPS+LTA stimulation CAL27 showed lower levels of phosphorylation of p53 (at serine 15, serine 46, serine 392), Chk2 (threonine 68), β-catenin, p38α (threonine 180, tyrosine 182), GSK 3α/β (serine 21, serine 9), GSK 3β (serine 9) and HSP 60 than it did after stimulation with either LPS or LTA alone (Figure 4.9) (Table 5.2). This likely indicates downregulation of tumour suppressor protein activity of p53, p38α and Chk2 (major activator of p53), which are activated by phosphorylation ([DeNicola et al., 2013](#); [Jenkins et al., 2012](#); [Xu, Tsvetkov & Stern, 2002](#)); and downregulation of inactivated β-catenin, which is inactivated by phosphorylation ([Liu et al., 2002](#)). Also, lower levels of phosphorylated (activated) GSK 3α/β and GSK 3β likely reflects the activity of GSK required for binding to inactivated β-catenin for β-catenin degradation and ubiquitination ([Liu et al., 2002](#)). Also, downregulation of phosphorylated HSP 60, which has previously been shown to have a tumour suppressor-like function by inducing cell differentiation and inhibiting invasion in hepatocellular carcinoma ([Zhang et al., 2016](#)), may further

explain the current findings for CAL27. However, phosphorylation of other proliferation-related proteins such as Yes-associated proteins (tyrosine 426), Src (tyrosine 419), EGFR (tyrosine 1086), eNOS (serine 1177), ERK 1/2 (threonine 202/tyrosine 204 and threonine 185/tyrosine 187) and STAT3 (tyrosine 705) was higher in untreated cells than in LPS+LTA stimulated cells (Figure 4.9). This finding is paradoxical and may require further investigation to explain the reduction in the abovementioned proliferation-related protein; although it has previously been shown that phosphorylation at tyrosine 705 of STAT3 may inactivate STAT3 by co-deactivation of serine 727 of STAT3 (Yang et al., 2020). Contrastingly, LTA induced proliferation (that was found in the project) may be due to the phosphorylation of HSP60 (Co expression of HSP60 and nuclear β catenin), Src and GSK3β (Figure 4.9) (Table 5.2).

RSK 1/2 has previously been seen to promote invasion and metastasis of head and neck squamous cell carcinoma cells (Kang et al., 2010) (Table 5.2). RSK 1/2 in its phosphorylated (activated) form was seen to be at higher levels in CAL27 following LPS stimulation than in either after LTA or LPS+LTA stimulation (Figure 4.9). Phosphorylated RSK 1/2 has been seen to be associated with cell survival, proliferation and metastasis (Kang et al., 2010). This may suggest that proliferation caused by LPS stimulation of CAL27 using RSK 1/2 uses pathways other than Ras/MAPK/ERK 1/2 or that it occurs via upregulation resulting from a positive feedback loop involving other unknown pathways. Paradoxically, EGFR, eNOS, ERK 1/2, Src and RSK 1/2 expression associated with proliferation was found to be lowest after LPS+LTA stimulation (Figure 4.9), which showed the highest proliferation.

TABLE 5.1: Phosphokinases and the role in cancer.

Phosphokinase	Phosphorylation site	Effect on cancer	References
Akt 1/2/3	T308, S473	Aberrant activation of Akt activation is prevalent across human cancer lineages	(Wang et al., 2018)
CREB	S133	Controls the cancer cell viability and proliferation	(Sakamoto & Frank, 2009)
EGFR	Y1086	It is the driver of tumorigenesis	(Sigismund, Avanzato & Lanzetti, 2018)
eNOS	S1177	Related to chronic inflammation,	(Lim et al., 2008)

Phosphokinase	Phosphorylation site	Effect on cancer	References
		apoptosis and maintains tumour microenvironment	
ERK 1/2	T202/Y204, T185/Y187	Key regulators of cell cycle progression	(Meloche & Pouyssegur, 2007)
Chk2	T68	Key regulator of tumour suppressor proteins	(Craig & Hupp, 2004)
c-Jun	S63	Associated with proliferation and angiogenesis	(Vleugel et al., 2006)
Fgr	Y412	Growth of cancer	(Stransky et al., 2014)
GSK3α/β	S21/S9	Both pro-apoptotic and anti-apoptotic activity	(McCubrey et al., 2014)
HSP 27	S78/S82	Associated with poor prognosis	(Acunzo et al., 2014)
p53	S15, S46, S392	Tumour suppressor protein	(Harris, 1996)
JNK 1/2/3	T183/Y185, T221/Y223	Regulates inflammatory responses	(Bubici & Papa, 2014)
Lck	Y394	Affects cellular energetics and proliferation	(Shi et al., 2015)
Lyn	Y397	Mediator of epithelial-mesenchymal transition	(Choi et al., 2010)
MSK 1/2	S376/S360	Involved in the phosphorylation of several proliferation related proteins	(Duncan et al., 2006)
p70 S6 kinase	T389/T421/S424	Promotes epithelial mesenchymal transition	(Pon et al., 2008)
PRAS40	T246	Deregulates apoptosis	(Madhunapantula, Sharma & Robertson, 2007)
p38α	T180/Y182	Dysregulation of p38α is related to progression of cancer	(Koul, Pal & Koul, 2013)

Phosphokinase	Phosphorylation site	Effect on cancer	References
PDGF Rβ	Y751	Regulate tumour stroma fibroblasts and angiogenesis	(Pietras et al., 2003)
PLC-γ1	Y783	Required for metastasis	(Sala et al., 2008)
Src	Y419	Strongly implicated in the cancer progression	(Wheeler, Iida & Dunn, 2009)
PYK2	Y402	Involved in the process of metastasis	(Lipinski et al., 2005)
RSK 1/2/3	S221/S227/S380/S386/S377	Involved in the process of progression and metastasis	(Sulzmaier & Ramos, 2013)
STAT2	Y689	Promotes progression of cancer	(Gamero et al., 2010)
STAT5a/b	Y694/Y699	Suppression of anti-tumour immunity	(Rani & Murphy, 2016)
WNK1	T60	Stimulates angiogenesis	(Sie et al., 2020)
Yes	Y426	Drives growth and progression of cancer	(Garmendia et al., 2019)
STAT1	Y701	Anti-proliferative, pro-apoptotic and anti-angiogenic activity	(Meissl et al., 2017)
STAT3	Y705/S727	Related to the progression of cancer	(Yu, Pardoll & Jove, 2009)
β-catenin	—	Related to the progression of cancer	(Morin, 1999)
STAT6	Y641	Induction of apoptosis	(Gooch, Christy & Yee, 2002)
HSP 60	—	Promotes the progression of cancer	(Wu et al., 2017)

TABLE 5.2: Phosphokinases found related to the bacterial antigens.

Phosphokinase	Effect on head and neck cancer proliferation	References
LPS		
EGFR	Activation leads to phosphorylation of various proliferating mechanisms in SCC	(Bossi et al., 2016)
RSK1/2	RSK1/2 promotes invasion and metastasis of SCC	(Kang et al., 2010)
LTA		
HSP60	Co expression of HSP60 and nuclear β catenin predicts a worse prognosis of SCC	(Tsai et al., 2009)
Src	Activation of Src results in proliferation of SCC	(Egloff & Grandis, 2008)
GSK3β	GSK3βtrigger proliferation of SCC by activating β catenin	(Schulz et al., 2018)
LPS + LTA		
β catenin	β catenin activity regulates the tumour microenvironment of SCC by regulating extracellular matrix remodelling	(Alamoud & Kukuruzinska, 2018)
PI3K	Promotes progression of SCC	(Psyrri, Seiwert & Jimeno, 2013)

5.2.4 Further validation with RT-qPCR and western blot

The relative fold gene expression of SOCS3 and PI3KCA were higher in CAL27 whether untreated or following LPS stimulation than other treatment conditions. However, western blot analysis, showed that SOCS3 protein expression was lowest and PI3K expression highest after LPS+LTA stimulation compared with untreated and LPS stimulated cells. This may indicate the lack of translation of SOCS3 and PI3K proteins (Gsponer & Babu, 2012). Since SOCS3 is known to be a tumour suppressor protein (Inagaki-Ohara et al., 2013) and PI3K is a tumour proliferation-related protein (Arcaro & Guerreiro, 2007), this result further supports the finding that CAL27 after LPS+LTA stimulation produced the highest proliferation among all treatment conditions.

Like the proteome profiling results, the western blot showed lower STAT3 and EGFR expression in CAL27 after LPS+LTA stimulation compared with untreated cells. This may be because of lower expression of SOCS3, which might have a positive feedback loop with STAT3 for CAL27 (Carow & Rottenberg, 2014). Also, it has been found that hyperactivation of TRPV1 downregulates EGFR in skin cancer (Bode et al., 2009). LPS sensitises and activates TRPV1 (Diogenes et al., 2011), and upregulates calcium concentration in mouse uterine smooth muscle cells through T-type calcium channels (Zhang et al., 2015). Since CAL27 showed hyperactivity of TRPV1 and Cav 3.3, and higher stimulation of LPS compared with other oral cancer cell lines, hyperactivity of TRPV1 may explain the lowering of EGFR in CAL27 after bacterial antigen stimulation (Huang, Liu & Qiu, 2020). However, this is the opposite of previous findings, where LPS has always been shown to transactivate EGFR, which results in the proliferation of cancer cells (McElroy et al., 2012).

The western blot revealed lower EGFR protein expression in CAL27 after LPS stimulation than in untreated cells. In contrast, there was no difference among the two groups in expression levels of phosphorylated EGFR. This implies a difference in phosphorylated (activated) and total protein expression (Hunter, 2000). Therefore, total protein expression does not predict the activity of proliferation proteins in response to the bacterial antigen. Further, the tyrosine 1086 phosphorylation site of EGFR was examined in this study, but other EGFR phosphorylation sites might be activated more in CAL27 after LPS stimulation (Tong et al., 2009).

PI3K expression was higher in LPS+LTA stimulated cells than in untreated and LPS stimulated cells. These findings are in line with previous findings that the PI3K signalling pathway is activated by LTA (Kao et al., 2005). Interestingly, the phosphokinase array did not show any appreciable expression of Akt 1/2/3 (serine 473, threonine 308) under any treatment condition, although expression of PI3K was detected in both the RT-qPCR and western blot. This likely indicates that PI3K induced proliferation of CAL27, rather than activating the downstream Akt pathway (Faes & Dormond, 2015).

5.3 Effect of calcium channel drugs and bacterial antigens on proliferation and proliferation-related proteins

There were five major groups of treatment that were further divided into two groups in each treatment group. The rationale for the drug combination treatment was to determine the effect of calcium channel drugs in the presence and absence of bacterial antigens after bacterial antigen stimulation for certain length of times.

5.3.1 Cell viability assay

Based on the MT Glo assay and trypan blue live/dead cell count results, capsaicin (150 µM) and ML218 HCl (100 µM) showed the highest percentage inhibition of CAL27. However, incremental lowering of inhibition of CAL27 was observed following addition of more antigens simultaneously with calcium channel drugs. Similarly, after stimulation with bacterial antigen, capsaicin gave a lower inhibition percentage than did ML218 HCl. After 24 hours of bacterial antigen stimulation, ML218 HCl and capsaicin showed no difference in inhibition percentage. At 0 hours of stimulation, both ML28 HCl and capsaicin showed lower inhibition percentages after treatment with LPS than after treatment with LPS+LTA. There was little difference in the ML218 HCl and capsaicin treatment groups after 24 hours of stimulation, but after 0 hours and 72 hours of stimulation, both the drugs showed lower inhibition percentage in the presence of LPS+LTA than in the presence of LPS. Taken together, these results suggest that the presence of bacterial antigen lowered the inhibition percentage of calcium channel drugs and combined LPS+LTA acted synergistically to lower the effect of calcium channel drugs on CAL27 that is similar to the previous findings of other researchers (Lehouritis et al., 2015).

5.3.2 Colony formation assay

Based on the MT Glo assay and trypan blue live/dead cell count, treatment conditions were further narrowed down and the clonogenic assay was performed for different treatment conditions after 72 hours of LPS+LTA stimulation only. The clonogenic assay revealed the lowest colony intensity and number of colonies when the drugs were used

without bacterial antigens or pre-stimulation with bacterial antigen. The clonogenic assay showed lower colony intensity and number of colonies after ML218 HCl treatment under different conditions than was seen for capsaicin. Also, both the calcium channel drugs were associated with higher colony intensity and number of colonies when used alongside the bacterial antigen. This further suggests that the bacterial antigens reduced the inhibitory effect of the drugs on the cells.

5.3.3 Proliferation related gene and protein expression assay

Based on the RT-qPCR results, the relative fold gene expression of PI3KCA, EGFR, GMPS and STAT3 did not differ significantly among the treatment groups, although SOCS3 was higher in capsaicin treated bacterial antigen pre-stimulated cells than with ML218 HCl.

In the western blot analysis, cells treated with ML218 HCl after bacterial antigen stimulation showed the highest STAT3 and EGFR protein expression among treatments but there was no difference between SOCS3 expression in ML218 HCl and capsaicin treated pre-stimulated cells. This again supports that upregulated non-functional proteins were amplified during the RT-qPCR that was done previous to western blot.

Previous research has reported that overexpression of STAT3 turns STAT3 from anti-apoptotic to pro-apoptotic (Lu et al., 2006). The current findings suggest that EGFR and STAT3 may be engaged in crosstalk in CAL27 cells. Similar observations have been reported previously, where hyperactivation of EGFR mediates apoptosis via STAT3 (Jackson & Ceresa, 2017). Further, none of the treatments showed any difference in PI3K protein expression. This may corroborate previous finding that EGFR hyperactivation may result in lowering of cell viability, independent of the PI3K/Akt pathway (Treda et al., 2016).

5.4 Effect of calcium channel drugs and bacterial antigens on apoptosis

Differences in tumour suppressor protein expression by CAL27, including of p53, Chk2, p38α, and SOCS3, and proliferation-related proteins including EGFR, β-actin, PI3K, and STAT3 under various treatments were consistent with previous findings of the study. Therefore, a caspase 3/7 green detection reagent assay was performed.

Caspases are the central component of the apoptotic machinery (Shi, 2002). Apoptosis, or programmed cell death, plays a pivotal role in the progression of all types of cancers (Shi, 2002). Insufficient apoptosis leads to uncontrolled proliferation of cancer cells (Shi, 2002) and is one of the hallmarks of the progression of cancer (Hanahan & Weinberg, 2011). There are various types of caspases (McIlwain, Berger & Mak, 2013). The apoptotic cascade is generally executed by initiator (caspase 8, caspase 9) and executioner caspases (caspase 3, caspase 6, caspase 7) (McIlwain et al., 2013). Initiator caspases are required for the appropriate formation of functional mature protease (executioner caspases), which are required for the programmed cell death of cancer cells (McIlwain et al., 2013). Caspase 3 plays the primary executioner caspase role, whereas caspase 7 plays a supportive role in the executioner phase of apoptosis (McIlwain et al., 2013; Walsh et al., 2008). Both caspase 3 and caspase 7 are part of the intrinsic apoptosis pathway; thus, both caspase 3 and caspase 7 are important indicators of apoptosis (Brentnall et al., 2013; McIlwain et al., 2013; Porter & Janicke, 1999).

5.4.1 LPS and LTA combination showed lower caspase positive cells

The assay showed that the percentage of caspase 3/7-positive cells was higher in untreated CAL27 than in bacterial antigen stimulated cells. CAL27 after LPS+LTA stimulation had the lowest percentage of caspase 3/7-positive cells among these groups. These results are concordant with earlier findings in the study that showed the highest proliferation in CAL27 after LPS+LTA stimulation.

5.4.2 ML218 HCl produced the maximum caspase positive cells

Based on the percentages of caspase 3/7-positive cells, ML218 HCl was associated with the highest level of apoptosis among all of the calcium channel drug treatment conditions applied. Also, ML218 HCl showed higher apoptosis compared with capsaicin under different bacterial antigen treatment conditions. This suggests that the voltage-gated calcium channel blocker was more potent in restricting the proliferation of CAL27 than was the TRPV1 agonist.

5.4.3 Calcium oscillation restricting the proliferation

Functional T-type calcium channels are required for tumour growth and proliferation (Santoni, Santoni & Nabissi, 2012). Previously it was reported that the blockade of T-type calcium channels in glioblastoma resulted in restriction of the progression of glioblastoma (Sallan et al., 2018). Also, capsaicin induces apoptosis in gastric cancer cells, various types of breast cancer as well as pancreatic, oesophageal, colonic, prostrate, skin, endothelial cell and lung cancer (Lin et al., 2013). The findings of the current study along with the literature support the notion that calcium oscillations (perturbations in calcium signalling) result in apoptosis of cancer cells by reducing the influx of calcium (Varghese et al., 2019) by ML218 HCl (T-type calcium channel blocker) and an overload of calcium (Pinton et al., 2008) as a result of excessive influx of calcium by the TRPV1 agonist capsaicin. However, to date no study has compared the apoptotic efficiency of both calcium channel drugs in the same cell line.

The lowering of tumour suppressor proteins like SOCS3, p53, Chk2 and p38α is also consistent with the apoptotic percentage findings in this study, as all the tumour suppressor proteins were directly or indirectly related to the upregulation of intrinsic pathway proteases, caspase 3 and caspase 7 (Olsson & Zhivotovsky, 2011). Also, as previously mentioned, hyperactivation of EGFR and STAT3 has also been associated with increased functioning of the apoptotic machinery, which also upregulates caspase 3/7 activity (Lu et al., 2006; Jackson & Ceresa, 2017). This is also consistent with the caspase 3/7 percentage findings for CAL27 treated with ML218 HCl after LPS+LTA stimulation.

5.5 TNF α ELISA

5.5.1 Analysis of TNF α without the presence of immune cells

TNF α is the earliest activator of LPS to cause inflammation-induced cancer cell proliferation (Parameswaran & Patial, 2010). It is also associated with the proliferation and progression of cancer cells (Wang & Lin, 2008). It has been previously shown that TNF α cross-talks with other proliferation and tumour suppression proteins (Wang & Lin, 2008). TNF α ELISA in the current study showed that untreated CAL27 had higher TNF α concentrations than did OKF6 (non-cancerous oral) cells. This is consistent with the literature for other cancer cells compared with their normal counterparts (Szlosarek et al., 2006).

5.5.2 Possible relation of TNF α, apoptosis and proliferation in CAL27

There was no difference in TNF α concentration among untreated and LPS stimulated CAL27. However, LPS stimulated cells showed higher TNF α concentration than LPS+LTA stimulated cells. This may suggest that LTA had a dampening effect on TNF α or that may suffice the lowest expression of SOCS3, p38α and p53 that results in the lowering of apoptosis in LPS+LTA stimulated cells, since SOCS3, p38α and p53 stabilisation and activation have been previously shown to be mediated by TNF α (Ehlting et al., 2007; Ladiwala et al., 1999; Zhou et al., 2006). Lowering of STAT3 is consistent with the TNF α findings in that STAT3 has previously been found to be activated by TNF α (Chung et al., 2017). Although several studies have reported PI3K/Akt to be one of the major tumour proliferation proteins activated by TNF α (Smith et al., 2007), in the current study contrasting results were found: LPS+LTA stimulated cells showed higher PI3K protein expression and lower TNF α concentration than did both untreated and LPS (only) stimulated cells. Nonetheless, similar observations have been reported by other researchers who found that PI3K limits LPS activation of ERK 1/2, p38, JNK and JAK/STAT pathway in monocytes (Guha & Mackman, 2002). Thus, with reference to proteome profiling, it can be hypothesised that in the CAL27 cell line after LPS+LTA treatment, proliferation was largely due to PI3K blocking LPS-induced TNF α activity,

resulting in suppression of tumour proliferation proteins. Another consistent result with previous studies is related to downregulation of inactivated β-catenin in LPS+LTA treated CAL27, due to low TNF α concentration in the same subset. Previously it was reported that TNF α induce apoptosis that is reversed by stabilized β-catenin that promotes proliferation of cancer cells (Shang et al., 2004). In the current study, β-catenin may have been stabilised by PI3K, similar to some of the previous findings (Brown et al., 2011).

This study also showed that cells treated with ML218 HCl after bacterial antigen stimulation had the lowest TNF α, which may be attributed to overexpression of STAT3 and loss of function of SOCS3. This is similar to previous findings that abrogation of SOCS3 function results in hyperactivation of STAT3 in macrophages (Lu et al., 2006).

5.6 Epithelial cancer differentiation

Differentiation is the process where one cell transforms to another different phenotype (Blagosklonny, 2003). Previously several proliferation factors have been related to the proliferation, differentiation and apoptosis (Blagosklonny, 2003). Impeding the growth factors precede apoptosis (Blagosklonny, 2003). Also, hyperactivity of the differentiation machinery may lead to apoptosis (Blagosklonny, 2003). Therefore, in the project, calcium chloride was used to induce CAL27 differentiation after bacterial antigen stimulation. It was found that the colony formation and apoptotic cells were less in $CaCl_2$ treated pre-stimulated cells compared to bacterial antigen stimulated cells, but more than the bacterial antigen stimulated calcium channel drugs treated cells. That may suggest that the calcium channel drugs like capsaicin that has previously shown to induce differentiation (Baboota et al., 2014), and although ML218 HCl have not shown to induce differentiation, but alteration in calcium signalling cause differentiation, may not only cause differentiation (Varghese et al., 2019) but the hyperactivity of STAT3, EGFR and suppression of SOCS3 that lowers the TNF α may have resulted in the lowering of the proliferation of CAL27 after the treatment with different calcium channel drug after bacterial antigen stimulation.

<div align="right">

6

</div>

Limitations of the study

As with any study, the project was subject to limitations, as follows:

The entire project was based on the effect of calcium channel drugs on their specific receptors. The drug experiment began after the expression analysis using qPCR. However, no functionality assay for the receptors was performed. The functionality of the receptors could have been determined using a calcium 5 (TRPV1 or TRPA1) (Hu et al., 2011) or patch clamp assay (T-type voltage-gated calcium channel) (Leech & Holz, 1994). If in future it is found that the receptors are non-functional, then investigations could be made to find the exact receptors targeted by the drug to achieve the outcome. Also, gene knockout or suppression studies using genetic tools can be performed.

The project used LTA and LPS to simulate Gram-positive and Gram-negative bacterial infection, respectively. However, components of bacteria other than their bacterial cell wall antigens may be responsible for the progression of oral squamous cell carcinomas.

The project only investigated T-type calcium channel receptors. Other calcium channel receptors may affect calcium metabolism of oral cancer cells (Monteith et al., 2012). In future R., L. and P- type calcium channel receptor expression and functionality should also be examined.

The project was not carried out in a co-culture model setup (i.e. oral bacteria and oral cancer cells were cultured together) that incorporated immune cells. Bacterial antigens have been found to mostly target immune cells for cancer progression (Kurago et al., 2008). The project found that bacterial antigens can stimulate oral cancer cells without the presence of immune cells, but this does not help to identify the effect of bacterial antigens in the real world, where there are confounding factors like immune cells and cytokines.

The determination of calcium channel drug concentrations was done with the help of a RealTime MT Glo cell viability assay. The cells were treated with drugs for 24 hours. The major limitations to this approach are that:

1. It is not known whether treating the cells with a lower concentration, or the same concentration for a shorter time, would have been more effective in producing more apoptotic cells. Other assays such as Annexin V flow cytometry could have been done to determine the duration and concentration of the drug to achieve the best outcome (Vermes et al., 1995).
2. The RealTime MT Glo cell viability assay is primarily a metabolic assay. It has inherent limitations including that it could not predict the percentage of live or dead cells after treatment with drugs and antigens.

The later stages of the project only used one oral cancer cell line (CAL27), which is an aggressive cancer cell line. Other cancer cell lines that did not show a high stimulation index or were slow growing might have resulted in different inhibition percentages due to the drug combination treatment compared. It should be noted that cancer tissues are heterogeneous in nature (Meacham & Morrison, 2013). The general effect of bacterial antigens and calcium channel drugs cannot be concluded based on one cell line alone.

The percentage cell death caused by the drug in the presence and absence of stimulants was mainly based on trypan blue assay. Since oral cancer cells are of the epithelial-like adherent type, trypsin was used to detach the cells. Two drawbacks of this procedure that might have affected the overall outcome are that:

1. trypsin alone can disrupt the cell membrane of attached cells (Besingi & Clark, 2015)

2. live/dead cell counting under different conditions may result in incomplete detachment of the attached cells.

Phosphokinase array proteome profiling was used to identify interactions between the proliferating factors and bacterial antigens. The proteome profiler did not include anti-apoptotic factors. An apoptotic profiler could have been used to identify anti-apoptotic factors that might have contributed to the proliferation of the cells (Elmore, 2007).

A clonogenic assay was used to confirm the proliferation of the oral cancer cells under different conditions. This assay is primarily a colony formation assay and some researchers argue against its use to identify proliferation of cancer cells. According to them, performing a clonogenic assay after cells have been seeded on alginate (a non-attaching surface) should be used to determine the proliferation of cancer cells (Read et al., 2018).

The project could not establish a temporal relationship in the effect of different bacterial antigens on the proliferation of the oral cancer cells. During the formation of a biofilm, Gram-positive bacteria are the initial colonisers. Gram-positive bacterial antigen may result in the upregulation or downregulation of various proliferating, apoptotic or anti apoptotic factors before Gram-negative bacterial antigens have any effect on oral cancer cells.

Caspase 3/7 was analysed in the project, but other apoptotic markers may be involved in the antigen-oral cancer cell-drug interaction (McIlwain, Berger & Mak, 2013).

The project used LPS from *E. coli*. Previous research has used LPS from *P. gingivalis*, which might have been more appropriate for an LPS-oral cancer cell project (Goncalves et al., 2016).

The differentiation experiment focused on colony formation and apoptosis, although different differentiation markers were not explored. Further, the expression of calcium channel receptors after the addition of $CaCl_2$ could have been examined to elucidate more convincingly the role of calcium channel drugs in the differentiation and apoptosis of CAL27 cells. Future differentiation experiments might focus on identifying the phenotypic changes that could have occurred after the addition of calcium channel drugs and $CaCl_2$. A differentiation-apoptosis cascade is also identified by the expression of different proliferating and tumour suppressor proteins (Blagosklonny, 2003).

Experiments to identify the relative protein expression of different proliferation and tumour suppressor proteins should be done after the addition of calcium channel drugs and CaCl$_2$.

The phosphokinase array included only phosphorylated proteins. In future, total protein expression of p53, Chk2, GSK3β and β-catenin ought to be checked to identify actual protein expression differences among the various CAL27 treatment groups. Also, western blot analyses should be done to determine phosphorylation status in addition to the protein expression levels of the target proteins STAT3, SOCS3, PI3K, and EGFR.

All oral cancer cell lines used in the project were from Caucasian subjects. Epigenetically, oral cancer cell lines of Asian or Indian subcontinent origin may differ (Giuliani et al., 2016). Given the preponderance of oral cancer among the Indian subcontinent population (Coelho, 2012), oral cancer cells of Indian subcontinent or Asian origin should also be used in future research.

7

Conclusion and future directions

The project was initiated based on the idea of stimulating oral cancer cells with LPS. It was found during the project that CAL27 produced the highest stimulation index among all the oral cancer cell lines tested. Also, LTA showed stimulation. This led to the use of both bacterial antigens to demonstrate real-world-like, biofilm-related bacterial antigen stimulation of oral cancer cells. The findings of differential expression of calcium channel drugs helped in the selection of capsaicin and ML218 HCl. The project measured 20% higher and 20% lower levels respectively of TRPV1 and Cav 3.1 in CAL27 compared with normal oral cells. At first glance, such a minor change in expression of a calcium channel receptor may not support the further use of calcium channel drugs in the project. However, the project only determined gene expression levels; it did not conduct functionality assays. In the same way that the western blot provided very different results from RT-qPCR, a functionality assay may have revealed larger differences in functional receptors among cell lines. After treatment with calcium channel drugs, CAL27 exhibited an appreciable reduction in metabolism and viability, which may confirm the role of functional calcium channels in oral cancer cells. However, future investigations involving other calcium channels are required.

However, the most challenging aspect of the project was to design a drug combination treatment that could mimic the real-world challenge of anti-cancer drugs in the presence of bacterial antigens that themselves mimic the presence of Gram-negative and Gram-positive bacteria. To achieve a real-world-like scenario, calcium channel drug treatment was performed under different bacterial antigen treatment conditions. Biofilm formation is a continuous process. Even after proper extirpation/elimination of a bacterial plaque via surgical manoeuvre or antibiotic treatment, oral cancer patients generally experience unhygienic oral conditions, leading to continuous formation of bacterial biofilm. Also, elimination of a bacterial plaque does not necessarily remove already-bacterial antigen-stimulated oral cancer cells. Therefore, combination drug treatment may be an appropriate approach to elucidate the confounding effects of bacterial antigens on chemotherapeutic drugs. The combination drug treatment helped to understand the reduction in the effect of calcium channel drugs in the presence of bacterial antigens. It also showed that LPS along with LTA was more potent in producing CAL27 proliferation than LPS treatment alone. This is an important and novel finding of the project.

The successful reduction in cell viability, metabolism and colony formation by a voltage-gated calcium channel blocker is a second novel finding of the project. To date there have been no reports on the effect of ML218 HCl on oral cancer cell proliferation.

The literature supports the upregulation of certain proliferation-related proteins due to LPS-induced oral cancer cell proliferation. This project showed, for the first time, that not only upregulation of the proliferation protein, but also lowering of tumour suppressors is responsible for bacterial antigen-related oral cancer cell proliferation. The project also showed that calcium channel drugs overexpress certain proliferation proteins, which also results in lowering of tumour suppressor proteins and causes apoptosis (Figure 7.1).

Finally, the project demonstrated definitively that bacterial antigens played a confounding role during the action of calcium channel drugs on CAL27 (under different bacterial antigen treatment conditions). These findings may benefit other cancer researchers considering the presence of bacterial antigens when developing novel pharmacological strategies for cancer (not only head and neck but also colorectal cancer where commensal bacteria may affect chemotherapeutic drugs), as well as implant researchers designing implants to replace diseased or non-functional parts of body, where bacteria antigens may affect the longevity of implant success.
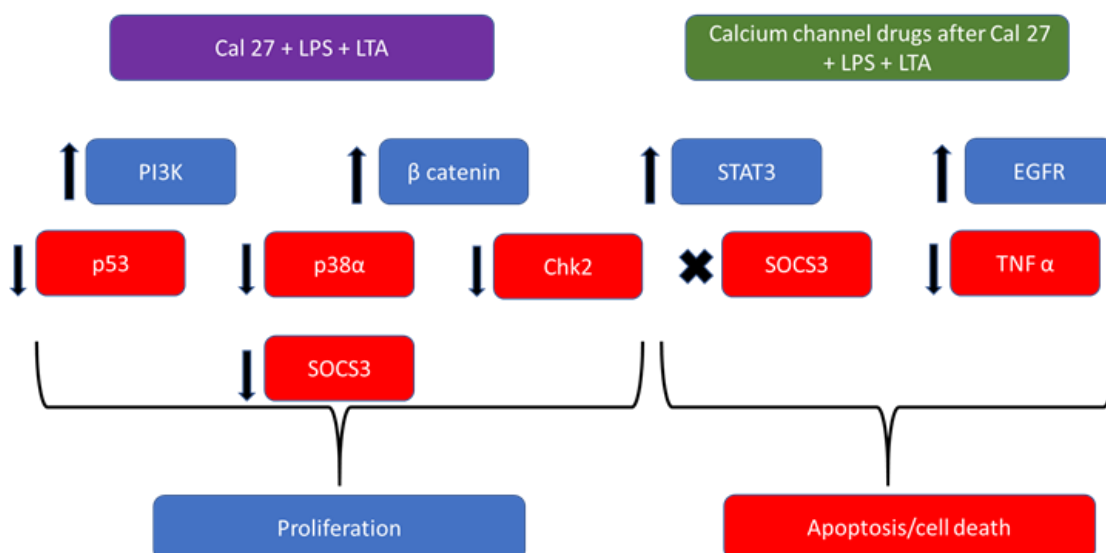
FIGURE 7.1: Schematic representation of the possible mechanistic overview of the effect of bacterial antigen and calcium channel drugs on CAL27 proliferation and apoptosis.

In future, despite the low bacterial antigen stimulation, the drug combination strategy used here might be employed to determine similar effects of other calcium channel drugs in the presence and absence of bacterial antigens. Also, a bacterial co-culture model should be developed. This may provide a better picture of the role of bacterial antigens and calcium channel drugs. In future, if other calcium channel receptors are found to be functional in oral cancer cells, other calcium channel drugs could be investigated for their effect on inhibition of oral cancer cells. Also, LPS from *P. gingivalis* should be trialled to identify any differences in the stimulation of oral cancer cells. LPS from different bacterial serotypes might have different effects on cell types of different origins. If, after further experimentation, drugs are found to affect oral cancer cells, then tissue samples from cancerous and precancerous lesions should be examined. The plausible and possible role of newer pharmacological drugs is not only to restrict the growth of cancer cells but also to decrease the chances of progression of precancerous lesions to cancerous phenotypes. Therefore, experiments should be done on precancerous cell lines.

A functionality assay for TRPA1 in OKF6 cells should be done in future because the project showed lack of expression of TRPA1 in cancer cell lines, despite its presence in OKF6. If found to be functional, then the relative gene expression of TRPA1 in OKF6, along with other cell lines from different stages of dysplasia (precancerous lesions), should be quantified. This may help to identify a newer prognostic tool for oral squamous

cell carcinoma. Also, a novel pharmacological treatment strategy could be developed based on functional TRPA1 expression.

CAL27 treated with ML218 HCl after bacterial antigen stimulation showed higher STAT3/EGFR protein expression and lowest SOCS3 protein expression than it did with other calcium channel drug treatment conditions. Similarly, TNF α concentration was lowest in CAL27 treated with ML218 HCl after bacterial antigen stimulation. Previously it has been reported that TNF α stabilises SOCS3 and assists in its function. It is possible that the abovementioned scenario was orchestrated by TNF α or STAT3/EGFR interaction. Therefore, in future, a co-immunoprecipitation experiment could be performed to identify protein–protein interactions involving these proteins. Finally, since bacterial antigens have mostly been seen to affect immune cells, future studies using an immune cell-cancer cell co-culture model, or a tissue study on T-cell phenotypic changes should be undertaken to more thoroughly elucidate the role of bacterial antigens and calcium channel drugs.

References

Aas, J. A., Paster, B. J., Stokes, L. N., Olsen, I., & Dewhirst, F. E. (2005). Defining the normal bacterial flora of the oral cavity. *Journal of Clinical Microbiology, 43*(11), 5721-5732. doi:10.1128/JCM.43.11.5721-5732.2005

Aoki, K., & Taketo, M. M. (2007). Adenomatous polyposis coli (APC): A multi-functional tumor suppressor gene. *Journal of Cell Science, 120*(Pt 19), 3327-3335. doi:10.1242/jcs.03485

Acunzo, J., Andrieu, C., Baylot, V., So, A., & Rocchi, P. (2014). Hsp27 as a therapeutic target in cancers. *Current Drug Targets, 15*(4), 423-431. doi:10.2174/13894501113146660230

Alamoud, K. A., & Kukuruzinska, M. A. (2018). Emerging Insights into Wnt/beta-catenin Signaling in Head and Neck Cancer. *Journal of Dental Research, 97*(6), 665-673. doi:10.1177/0022034518771923

Arcaro, A., & Guerreiro, A. S. (2007). The phosphoinositide 3-kinase pathway in human cancer: genetic alterations and therapeutic implications. *Current Genomics, 8*(5), 271-306. doi:10.2174/138920207782446160

Ardito, F., Giuliani, M., Perrone, D., Troiano, G., & Lo Muzio, L. (2017). The crucial role of protein phosphorylation in cell signaling and its use as targeted therapy (Review). *International Journal of Molecular Medicine, 40*(2), 271-280. doi:10.3892/ijmm.2017.3036

Arya, M., Shergill, I. S., Williamson, M., Gommersall, L., Arya, N., & Patel, H. R. (2005). Basic principles of real-time quantitative PCR. *Expert Review of Molecular Diagnosis, 5*(2), 209-219. doi:10.1586/14737159.5.2.209

Banwell, J. G., Boldt, D. H., Meyers, J., & Weber, F. L., Jr. (1983). Phytohemagglutinin derived from red kidney bean (Phaseolus vulgaris): a cause for intestinal malabsorption associated with bacterial overgrowth in the rat. *Gastroenterology, 84*(3), 506-515.

Bickenbach, J. R., Vormwald-Dogan, V., Bachor, C., Bleuel, K., Schnapp, G., & Boukamp, P. (1998). Telomerase is not an epidermal stem cell marker and is

downregulated by calcium. *Journal of Investigative Dermatology, 111*(6), 1045-1052. doi:10.1046/j.1523-1747.1998.00420.x

Bode, A. M., Cho, Y. Y., Zheng, D., Zhu, F., Ericson, M. E., Ma, W. Y., Dong, Z. (2009). Transient receptor potential type vanilloid 1 suppresses skin carcinogenesis. *Cancer Research, 69*(3), 905-913. doi:10.1158/0008-5472.CAN-08-3263

Bode, J. G., Nimmesgern, A., Schmitz, J., Schaper, F., Schmitt, M., Frisch, W.,Graeve, L. (1999). LPS and TNF alpha induce SOCS3 mRNA and inhibit IL-6-induced activation of STAT3 in macrophages. *FEBS Letters, 463*(3), 365-370. doi:10.1016/s0014-5793(99)01662-2

Bossi, P., Resteghini, C., Paielli, N., Licitra, L., Pilotti, S., & Perrone, F. (2016). Prognostic and predictive value of EGFR in head and neck squamous cell carcinoma. *Oncotarget, 7*(45), 74362-74379. doi:10.18632/oncotarget.11413

Baram, L., Peled, E., Berman, P., Yellin, B., Besser, E., Benami, M., Meiri, D. (2019). The heterogeneity and complexity of Cannabis extracts as antitumor agents. *Oncotarget, 10*(41), 4091-4106. doi:10.18632/oncotarget.26983

Buchanan, P. J., & McCloskey, K. D. (2016). CaV channels and cancer: canonical functions indicate benefits of repurposed drugs as cancer therapeutics. *European Biophysics Journal, 45*(7), 621-633. doi:10.1007/s00249-016-1144-z

Bubici, C., & Papa, S. (2014). JNK signalling in cancer: in need of new, smarter therapeutic targets. *British Journal of Pharmacology, 171*(1), 24-37. doi:10.1111/bph.12432

Buchanan, P. J., & McCloskey, K. D. (2016). CaV channels and cancer: Canonical functions indicate benefits of repurposed drugs as cancer therapeutics. *European Biophysics Journal*, *45*(7), 621-633. doi:10.1007/s00249-016-1144-z

Besingi, R. N., & Clark, P. L. (2015). Extracellular protease digestion to evaluate membrane protein cell surface localization. *Nature Protocols, 10*(12), 2074-2080. doi:10.1038/nprot.2015.131

Baboota, R. K., Singh, D. P., Sarma, S. M., Kaur, J., Sandhir, R., Boparai, R. K., Bishnoi, M. (2014). Capsaicin induces "brite" phenotype in differentiating 3T3-L1 preadipocytes. *PLoS One, 9*(7), e103093. doi: 10.1371/journal.pone.0103093

Blagosklonny, M. V. (2003). Apoptosis, proliferation, differentiation: in search of the order. *Seminar of Cancer Biology, 13*(2), 97-105. doi:10.1016/s1044-579 x (02)00127-x

Brentnall, M., Rodriguez-Menocal, L., De Guevara, R. L., Cepero, E., & Boise, L. H. (2013). Caspase-9, caspase-3 and caspase-7 have distinct roles during intrinsic apoptosis. *BMC Cell Biology, 14*, 32. doi:10.1186/1471-2121-14-32

Brown, J. B., Cheresh, P., Goretsky, T., Managlia, E., Grimm, G. R., Ryu, H., Barrett, T. A. (2011). Epithelial phosphatidylinositol-3-kinase signaling is required for beta-catenin activation and host defense against Citrobacter rodentium infection. *Infection Immunology, 79*(5), 1863-1872. doi:10.1128/IAI.01025-10

Capiod, T. (2016). Extracellular calcium has multiple targets to control cell proliferation. *Advances in Experimental Medicine & Biology, 898*, 133-156. doi:10.1007/978-3-319-26974-0_7

Chakraborty, P. K., Mustafi, S. B., Xiong, X., Dwivedi, S. K. D., Nesin, V., Saha, S., Mukherjee, P. (2017). MICU1 drives glycolysis and chemoresistance in ovarian cancer. *Nature Communications, 8*, 14634. doi:10.1038/ncomms14634

Choi, Y. L., Bocanegra, M., Kwon, M. J., Shin, Y. K., Nam, S. J., Yang, J. H., Pollack, J. R. (2010). LYN is a mediator of epithelial-mesenchymal transition and a target of dasatinib in breast cancer. *Cancer Research, 70*(6), 2296-2306. doi:10.1158/0008-5472.CAN-09-3141

Craig, A. L., & Hupp, T. R. (2004). The regulation of CHK2 in human cancer. *Oncogene, 23*(52), 8411-8418. doi:10.1038/sj.onc.1208035

Coelho, K. R. (2012). Challenges of the oral cancer burden in India. *Journal of Cancer Epidemiology, 2012*, 701932. doi:10.1155/2012/701932

Cotran, R. S., Kumar, V., Robbins, S. L., & Collins, T. (1999). *Pathologic basis of disease*. Philadelphia, PA: Saunders.

Croker, B. A., Kiu, H., & Nicholson, S. E. (2008). SOCS regulation of the JAK/STAT signalling pathway. *Seminars in Cell & Developmental Biology, 19*(4), 414-422. doi:10.1016/j.semcdb.2008.07.010

Cui, C., Merritt, R., Fu, L., & Pan, Z. (2017). Targeting calcium signaling in cancer therapy. *Acta Pharmacological Sinica B, 7*(1), 3-17. doi:10.1016/j.apsb.2016.11.001

Carow, B., & Rottenberg, M. E. (2014). SOCS3, a Major Regulator of Infection and Inflammation. *Frontiers of Immunology, 5*, 58. doi:10.3389/fimmu.2014.00058

Chung, S. S., Wu, Y., Okobi, Q., Adekoya, D., Atefi, M., Clarke, O., Vadgama, J. V. (2017). Proinflammatory Cytokines IL-6 and TNF-alpha Increased Telomerase

Activity through NF-kappaB/STAT1/STAT3 Activation, and Withaferin A Inhibited the Signaling in Colorectal Cancer Cells. *Mediators of Inflammation, 2017*, 5958429. doi:10.1155/2017/5958429

Crowther, J. R. (1995). ELISA. Theory and practice. *Methods of Molecular Biology, 42*, 1-218. doi:10.1385/0-89603-279-5:1

Das, B. R., & Nagpal, J. K. (2002). Understanding the biology of oral cancer. *Medical Science Monitor, 8*(11), RA258-267.

Davis, F. M., Azimi, I., Faville, R. A., Peters, A. A., Jalink, K., Putney, J. W., Jr., Monteith, G. R. (2014). Induction of epithelial-mesenchymal transition (EMT) in breast cancer cells is calcium signal dependent. *Oncogene, 33*(18), 2307-2316. doi:10.1038/onc.2013.187

De La Chapa, J. J., Singha, P. K., Self, K. K., Sallaway, M. L., McHardy, S. F., Hart, M. J., Gonzales, C. B. (2019). The novel capsazepine analog, CIDD-99, significantly inhibits oral squamous cell carcinoma in vivo through a TRPV1-independent induction of ER stress, mitochondrial dysfunction, and apoptosis. *Journal of Oral Pathology & Medicine, 48*(5), 389-399. doi:10.1111/jop.12843

Diogenes, A., Ferraz, C. C., Akopian, A. N., Henry, M. A., & Hargreaves, K. M. (2011). LPS sensitizes TRPV1 via activation of TLR4 in trigeminal sensory neurons. *Journal of Dental Research, 90*(6), 759-764. doi:10.1177/0022034511400225

Dowty, J. G., Win, A. K., Buchanan, D. D., Lindor, N. M., Macrae, F. A., Clendenning, M., Jenkins, M. A. (2013). Cancer risks for MLH1 and MSH2 mutation carriers. *Human Mutation, 34*(3), 490-497. doi:10.1002/humu.22262

Du, W., & Searle, J. S. (2009). The Rb pathway and cancer therapeutics. *Current Drug Targets, 10*(7), 581-589.

Duncan, E. A., Anest, V., Cogswell, P., & Baldwin, A. S. (2006). The kinases MSK1 and MSK2 are required for epidermal growth factor-induced, but not tumor necrosis factor-induced, histone H3 Ser10 phosphorylation. *Journal of Biological Chemistry, 281*(18), 12521-12525. doi:10.1074/jbc.M513333200

DeNicola, G. F., Martin, E. D., Chaikuad, A., Bassi, R., Clark, J., Martino, L., Marber, M. S. (2013). Mechanism and consequence of the autoactivation of p38alpha mitogen-activated protein kinase promoted by TAB1. *Nature Structural Molecular Biology, 20*(10), 1182-1190. doi:10.1038/nsmb.2668

Egloff, A. M., & Grandis, J. R. (2008). Targeting epidermal growth factor receptor and SRC pathways in head and neck cancer. *Seminars in Oncology, 35*(3), 286-297. doi:10.1053/j.seminoncol.2008.03.008

Ehlting, C., Lai, W. S., Schaper, F., Brenndorfer, E. D., Matthes, R. J., Heinrich, P. C., Bode, J. G. (2007). Regulation of suppressor of cytokine signaling 3 (SOCS3) mRNA stability by TNF-alpha involves activation of the MKK6/p38MAPK/MK2 cascade. *Journal of Immunology, 178*(5), 2813-2826. doi:10.4049/jimmunol.178.5.2813

Elmore, S. (2007). Apoptosis: a review of programmed cell death. *Toxicologic Pathology, 35*(4), 495-516. doi:10.1080/01926230701320337

Elwood, J. M., Youlden, D. R., Chelimo, C., Ioannides, S. J., & Baade, P. D. (2014). Comparison of oropharyngeal and oral cavity squamous cell cancer incidence and trends in New Zealand and Queensland, Australia. *Cancer Epidemiology, 38*(1), 16-21. doi:10.1016/j.canep.2013.12.004

Endo, Y., Uzawa, K., Mochida, Y., Shiiba, M., Bukawa, H., Yokoe, H., & Tanzawa, H. (2004). Sarcoendoplasmic reticulum Ca(2+) ATPase type 2 downregulated in human oral squamous cell carcinoma. *Internation Journal of Cancer, 110*(2), 225-231. doi:10.1002/ijc.20118

Faehling, M., Kroll, J., Fohr, K. J., Fellbrich, G., Mayr, U., Trischler, G., & Waltenberger, J. (2002). Essential role of calcium in vascular endothelial growth factor A-induced signaling: Mechanism of the antiangiogenic effect of carboxyamidotriazole. *FASEB Journal, 16*(13), 1805-1807. doi:10.1096/fj.01-0938fje

Faes, S., & Dormond, O. (2015). PI3K and AKT: Unfaithful Partners in Cancer. *International of Journal of Molecular Sciences, 16*(9), 21138-21152. doi:10.3390/ijms160921138

Franken, N. A., Rodermond, H. M., Stap, J., Haveman, J., & van Bree, C. (2006). Clonogenic assay of cells in vitro. *Nature Protocols, 1*(5), 2315-2319. doi:10.1038/nprot.2006.339

Francipane, M. G., Eterno, V., Spina, V., Bini, M., Scerrino, G., Buscemi, G., Stassi, G. (2009). Suppressor of cytokine signaling 3 sensitizes anaplastic thyroid cancer to

standard chemotherapy. *Cancer Research, 69*(15), 6141-6148. doi:10.1158/0008-5472.CAN-09-0994

Gelebart, P., Kovacs, T., Brouland, J. P., van Gorp, R., Grossmann, J., Rivard, N., Papp, B. (2002). Expression of endomembrane calcium pumps in colon and gastric cancer cells. Induction of SERCA3 expression during differentiation. *Journal of Biological Chemistry, 277*(29), 26310-26320. doi:10.1074/jbc.M201747200

Ghilardi, J. R., Rohrich, H., Lindsay, T. H., Sevcik, M. A., Schwei, M. J., Kubota, K.,... Mantyh, P. W. (2005). Selective blockade of the capsaicin receptor TRPV1 attenuates bone cancer pain. *Journal of Neuroscience, 25*(12), 3126-3131. doi:10.1523/JNEUROSCI.3815-04.2005

Goncalves, M., Cappellari, A. R., dos Santos, A. A., Macchi, F. S., Antunes, K. H., de Souza, A. P. D., Marchi, F. O. (2016). Effect of LPS on the viability and proliferation of human oral and esophageal cancer cell lines. *Brazilian Archives of Biology & Technology*, *59* e16150485. Epub March 22, 2016. https://doi.org/10.1590/1678-4324-2016150485

Gonzales, C. B., Kirma, N. B., De La Chapa, J. J., Chen, R., Henry, M. A., Luo, S., & Hargreaves, K. M. (2014). Vanilloids induce oral cancer apoptosis independent of TRPV1. *Oral Oncology, 50*(5), 437-447. doi:10.1016/j.oraloncology.2013.12.023

Gamero, A. M., Young, M. R., Mentor-Marcel, R., Bobe, G., Scarzello, A. J., Wise, J., & Colburn, N. H. (2010). STAT2 contributes to promotion of colorectal and skin carcinogenesis. *Cancer prevention research (Philadelphia), 3*(4), 495-504. doi:10.1158/1940-6207.CAPR-09-0105

Garmendia, I., Pajares, M. J., Hermida-Prado, F., Ajona, D., Bertolo, C., Sainz, C., Agorreta, J. (2019). YES1 Drives Lung Cancer Growth and Progression and Predicts Sensitivity to Dasatinib. *American Journal of Respiratory and Critical Care Medicine, 200*(7), 888-899. doi:10.1164/rccm.201807-1292OC

Gooch, J. L., Christy, B., & Yee, D. (2002). STAT6 mediates interleukin-4 growth inhibition in human breast cancer cells. *Neoplasia, 4*(4), 324-331. doi:10.1038/sj.neo.7900248

Gsponer, J., & Babu, M. M. (2012). Cellular strategies for regulating functional and non-functional protein aggregation. *Cell Report, 2*(5), 1425-1437. doi: 10.1016/j.celrep.2012.09.036

Guha, M., & Mackman, N. (2002). The phosphatidylinositol 3-kinase-Akt pathway limits lipopolysaccharide activation of signaling pathways and expression of inflammatory mediators in human monocytic cells. *Journal of Biological Chemistry, 277*(35), 32124-32132. doi:10.1074/jbc.M203298200

Giuliani, C., Sazzini, M., Bacalini, M. G., Pirazzini, C., Marasco, E., Fontanesi, E., Garagnani, P. (2016). Epigenetic Variability across Human Populations: A Focus on DNA Methylation Profiles of the KRTCAP3, MAD1L1 and BRSK2 Genes. *Genome Biology and Evolution, 8*(9), 2760-2773. doi:10.1093/gbe/evw186

Hu, H., Bandell, M., Grandl, J., & Petrus, M. (2011). High-Throughput Approaches to Studying Mechanisms of TRP Channel Activation. In M. X. Zhu (Ed.), TRP Channels. Boca Raton (FL): *CRC Press/Taylor & Francis, Chapter 12*.

Hanahan, D., & Weinberg, R. A. (2011). Hallmarks of cancer: The next generation. *Cell, 144*(5), 646-674. doi:10.1016/j.cell.2011.02.013

Harris, C. C. (1996). Structure and function of the p53 tumor suppressor gene: clues for rational cancer therapeutic strategies. *The Journal of the National Cancer Institute, 88*(20), 1442-1455. doi:10.1093/jnci/88.20.1442

Hassid, A., & Oudinet, J. P. (1986). Relationship between cellular calcium and prostaglandin synthesis in cultured vascular smooth muscle cells. *Prostaglandins, 32*(3), 457-478. doi:10.1016/0090-6980(86)90012-2

Hattar, K., Reinert, C. P., Sibelius, U., Gokyildirim, M. Y., Subtil, F. S. B., Wilhelm, J.,... Grandel, U. (2017). Lipoteichoic acids from *Staphylococcus aureus* stimulate proliferation of human non-small-cell lung cancer cells in vitro. *Cancer Immunology & Immunotherapy, 66*(6), 799-809. doi:10.1007/s00262-017-1980-4

Hsu, R. Y., Chan, C. H., Spicer, J. D., Rousseau, M. C., Giannias, B., Rousseau, S., & Ferri, L. E. (2011). LPS-induced TLR4 signaling in human colorectal cancer cells increases beta1 integrin-mediated cell adhesion and liver metastasis. *Cancer Research, 71*(5), 1989-1998. doi:10.1158/0008-5472.CAN-10-2833

Huang, R., Li, M., & Gregory, R. L. (2011). Bacterial interactions in dental biofilm. *Virulence, 2*(5), 435-444. doi:10.4161/viru.2.5.16140

Huang, J., Liu, J., & Qiu, L. (2020). Transient receptor potential vanilloid 1 promotes EGFR ubiquitination and modulates EGFR/MAPK signalling in pancreatic cancer cells. *Cell Biochemistry and Function*. doi:10.1002/cbf.348

Hunter, T. (2000). Signaling--2000 and beyond. *Cell, 100*(1), 113-127. doi:10.1016/s0092-8674(00)81688-8

Inagaki-Ohara, K., Kondo, T., Ito, M., & Yoshimura, A. (2013). SOCS, inflammation, and cancer. *JAKSTAT, 2*(3), e24053. doi:10.4161/jkst.24053

Ip, S. W., Lan, S. H., Huang, A. C., Yang, J. S., Chen, Y. Y., Huang, H. Y., Chung, J. G. (2012). Capsaicin induces apoptosis in SCC-4 human tongue cancer cells through mitochondria-dependent and -independent pathways. *Environmental Toxicology, 27*(6), 332-341. doi:10.1002/tox.20646

Jackson, N. M., & Ceresa, B. P. (2017). EGFR-mediated apoptosis via STAT3. *Experimental Cell Research, 356*(1), 93-103. doi:10.1016/j.yexcr.2017.04.016

Jiang, R., Wei, L., Zhu, M., Wu, J., & Wang, L. (2016). Aspirin inhibits LPS-induced expression of PI3K/Akt, ERK, NF-kappaB, CX3CL1, and MMPs in human bronchial epithelial cells. *Inflammation, 39*(2), 643-650. doi:10.1007/s10753-015-0289-8

Johnson, D. E., O'Keefe, R. A., & Grandis, J. R. (2018). Targeting the IL-6/JAK/STAT3 signalling axis in cancer. *Nature Reviews Clinical Oncology, 15*(4), 234-248. doi:10.1038/nrclinonc.2018.8

Jones, K. B., & Klein, O. D. (2013). Oral epithelial stem cells in tissue maintenance and disease: The first steps in a long journey. *International Journal of Oral Science, 5*(3), 121-129. doi:10.1038/ijos.2013.46

Jenkins, L. M., Durell, S. R., Mazur, S. J., & Appella, E. (2012). p53 N-terminal phosphorylation: a defining layer of complex regulation. *Carcinogenesis, 33*(8), 1441-1449. doi:10.1093/carcin/bgs145

Kamaruddin, M. F., Hossain, M. Z., Mohamed Alabsi, A., & Mohd Bakri, M. (2019). The antiproliferative and apoptotic effects of capsaicin on an oral squamous cancer cell line of Asian origin, ORL-48. *Medicina (Kaunas), 55*(7). doi:10.3390/medicina55070322

Kang, S., Elf, S., Lythgoe, K., Hitosugi, T., Taunton, J., Zhou, W., Chen, J. (2010). p90 ribosomal S6 kinase 2 promotes invasion and metastasis of human head and

neck squamous cell carcinoma cells. *Journal of Clinical Investigation, 120*(4), 1165-1177. doi:10.1172/JCI40582

Koul, H. K., Pal, M., & Koul, S. (2013). Role of p38 MAP Kinase Signal Transduction in Solid Tumors. *Genes Cancer, 4*(9-10), 342-359. doi:10.1177/1947601913507951

Karpinski, T. M. (2019). Role of oral microbiota in cancer development. *Microorganisms, 7*(1). doi:10.3390/microorganisms7010020

Kim, W. Y., & Kaelin, W. G. (2004). Role of VHL gene mutation in human cancer. *Journal of Clinical Oncology, 22*(24), 4991-5004. doi:10.1200/JCO.2004.05.061

Kiuru, M., & Busam, K. J. (2017). The NF1 gene in tumor syndromes and melanoma. *Laboratory Investigation, 97*(2), 146-157. doi:10.1038/labinvest.2016.142

Kurago, Z. B., Lam-ubol, A., Stetsenko, A., De La Mater, C., Chen, Y., & Dawson, D. V. (2008). Lipopolysaccharide-squamous cell carcinoma-monocyte interactions induce cancer-supporting factors leading to rapid STAT3 activation. *Head & Neck Pathology, 2*(1), 1-12. doi:10.1007/s12105-007-0038-x

Kao, S. J., Lei, H. C., Kuo, C. T., Chang, M. S., Chen, B. C., Chang, Y. C., Lin, C. H. (2005). Lipoteichoic acid induces nuclear factor-kappaB activation and nitric oxide synthase expression via phosphatidylinositol 3-kinase, Akt, and p38 MAPK in RAW 264.7 macrophages. *Immunology, 115*(3), 366-374. doi:10.1111/j.1365-2567.2005.02160.x

Laplante, M., & Sabatini, D. M. (2009). mTOR signaling at a glance. *Journal of Cell Science, 122*(Pt 20), 3589-3594. doi:10.1242/jcs.051011

Lee, S. H., Rigas, N. K., Lee, C. R., Bang, A., Srikanth, S., Gwack, Y., Shin, K. H. (2016). Orai1 promotes tumor progression by enhancing cancer stemness via NFAT signaling in oral/oropharyngeal squamous cell carcinoma. *Oncotarget, 7*(28), 43239-43255. doi:10.18632/oncotarget.9755

Li, Z., Li, S., Hu, L., Li, F., Cheung, A. C., Shao, W., Yang, C. (2017). Mechanisms underlying action of xinmailong injection, a traditional Chinese medicine in cardiac function improvement. *African Journal of Traditional, Complementarey & Alternative Medicines, 14*(2), 241-252. doi:10.21010/ajtcam.v14i2.26

Lim, K. H., Ancrile, B. B., Kashatus, D. F., & Counter, C. M. (2008). Tumour maintenance is mediated by eNOS. *Nature, 452*(7187), 646-649. doi:10.1038/nature06778

Lipinski, C. A., Tran, N. L., Menashi, E., Rohl, C., Kloss, J., Bay, R. C., Loftus, J. C. (2005). The tyrosine kinase pyk2 promotes migration and invasion of glioma cells. *Neoplasia, 7*(5), 435-445. doi:10.1593/neo.04712

Liu, P., Cheng, H., Roberts, T. M., & Zhao, J. J. (2009). Targeting the phosphoinositide 3-kinase pathway in cancer. *Nature Reviews Drug Discovery, 8*(8), 627-644. doi:10.1038/nrd2926

Lory, P., Bidaud, I., & Chemin, J. (2006). T-type calcium channels in differentiation and proliferation. *Cell Calcium, 40*(2), 135-146. doi:10.1016/j.ceca.2006.04.017

Lu, Y., Fukuyama, S., Yoshida, R., Kobayashi, T., Saeki, K., Shiraishi, H., Takaesu, G. (2006). Loss of SOCS3 gene expression converts STAT3 function from anti-apoptotic to pro-apoptotic. *Journal of Biological Chemistry, 281*(48), 36683-36690. doi:10.1074/jbc.M607374200

Ladiwala, U., Li, H., Antel, J. P., & Nalbantoglu, J. (1999). p53 induction by tumor necrosis factor-alpha and involvement of p53 in cell death of human oligodendrocytes. *Journal of Neurochemistry, 73*(2), 605-611. doi:10.1046/j.1471-4159. 1999.0730605

Lallemant, B., Evrard, A., Combescure, C., Chapuis, H., Chambon, G., Raynal, C., Brouillet, J. P. (2009). Reference gene selection for head and neck squamous cell carcinoma gene expression studies. *BMC Molecular Biology, 10*, 78. doi:10.1186/1471-2199-10-78

Lawyer, F. C., Stoffel, S., Saiki, R. K., Chang, S. Y., Landre, P. A., Abramson, R. D., & Gelfand, D. H. (1993). High-level expression, purification, and enzymatic characterization of full-length Thermus aquaticus DNA polymerase and a truncated form deficient in 5' to 3' exonuclease activity. *PCR Methods Applications, 2*(4), 275-287. doi:10.1101/gr.2.4.275

Lehouritis, P., Cummins, J., Stanton, M., Murphy, C. T., McCarthy, F. O., Reid, G., Tangney, M. (2015). Local bacteria affect the efficacy of chemotherapeutic drugs. *Science Report, 5*, 14554. doi:10.1038/srep14554

Li, H., Wawrose, J. S., Gooding, W. E., Garraway, L. A., Lui, V. W., Peyser, N. D., & Grandis, J. R. (2014). Genomic analysis of head and neck squamous cell carcinoma cell lines and human tumors: a rational approach to preclinical model selection. *Molecular Cancer Research, 12*(4), 571-582. doi: 10.1158/1541-7786.MCR-13-0396

Lin, C. H., Lu, W. C., Wang, C. W., Chan, Y. C., & Chen, M. K. (2013). Capsaicin induces cell cycle arrest and apoptosis in human KB cancer cells. *BMC Complement Alternative Medicine,* 13, 46. doi:10.1186/1472-6882-13-46

Liu, C., Li, Y., Semenov, M., Han, C., Baeg, G. H., Tan, Y., He, X. (2002). Control of beta-catenin phosphorylation/degradation by a dual-kinase mechanism. *Cell, 108*(6), 837-847. doi:10.1016/s0092-8674(02)00685-2

Leech, C. A., & Holz, G. G. t. (1994). Application of patch clamp methods to the study of calcium currents and calcium channels. *Methods in Cell Biology, 40*, 135-151. doi:10.1016/s0091-679x(08)61113-9

Meacham, C. E., & Morrison, S. J. (2013). Tumour heterogeneity and cancer cell plasticity. *Nature, 501*(7467), 328-337. doi:10.1038/nature12624

Madhunapantula, S. V., Sharma, A., & Robertson, G. P. (2007). PRAS40 deregulates apoptosis in malignant melanoma. *Cancer Research, 67*(8), 3626-3636. doi:10.1158/0008-5472.CAN-06-4234

Marini, P., Moriello, A. S., Cristino, L., Palmery, M., De Petrocellis, L., & Di Marzo, V. (2009). Cannabinoid CB1 receptor elevation of intracellular calcium in neuroblastoma SH-SY5Y cells: interactions with muscarinic and delta-opioid receptors. *Biochimica et Biophysica Acta, 1793*(7), 1289-1303. doi:10.1016/j.bbamcr.2009.05.002

McCubrey, J. A., Steelman, L. S., Bertrand, F. E., Davis, N. M., Sokolosky, M., Abrams, S. L., Cervello, M. (2014). GSK-3 as potential target for therapeutic intervention in cancer. *Oncotarget, 5*(10), 2881-2911. doi:10.18632/oncotarget.2037

Meissl, K., Macho-Maschler, S., Muller, M., & Strobl, B. (2017). The good and the bad faces of STAT1 in solid tumours. *Cytokine, 89*, 12-20. doi:10.1016/j.cyto.2015.11.011

Meloche, S., & Pouyssegur, J. (2007). The ERK1/2 mitogen-activated protein kinase pathway as a master regulator of the G1- to S-phase transition. *Oncogene, 26*(22), 3227-3239. doi:10.1038/sj.onc.1210414

Morin, P. J. (1999). beta-catenin signaling and cancer. *Bioessays, 21*(12), 1021-1030. doi:10.1002/(SICI)1521-1878(199912)22:1<1021::AID-BIES6>3.0.CO;2-P

Mahmood, T., & Yang, P. C. (2012). Western blot: technique, theory, and trouble shooting. *North American Journal of Medical Sciences, 4*(9), 429-434. doi:10.4103/1947-2714.100998

McElroy, S. J., Hobbs, S., Kallen, M., Tejera, N., Rosen, M. J., Grishin, A., Weitkamp, J. H. (2012). Transactivation of EGFR by LPS induces COX-2 expression in enterocytes. *PLoS One, 7*(5), e38373. doi: 10.1371/journal.pone.0038373

McIlwain, D. R., Berger, T., & Mak, T. W. (2013). Caspase functions in cell death and disease. *Cold Spring Harbour Perspective Biology, 5*(4), a008656. doi:10.1101/cshperspect.a008656

Marini, F., Falchetti, A., Luzi, E., Tonelli, F., & Maria Luisa, B. (2009). Multiple Endocrine Neoplasia Type 1 (MEN1) syndrome. In D. L. Riegert-Johnson, L. A. Boardman, T. Hefferon, & M. Roberts (Eds.), *Cancer syndromes*. Bethesda, MD.

Martini, M., De Santis, M. C., Braccini, L., Gulluni, F., & Hirsch, E. (2014). PI3K/AKT signaling pathway and cancer: An updated review. *Annals of Medicine, 46*(6), 372-383. doi:10.3109/07853890.2014.912836

Matsumoto, K., Umitsu, M., De Silva, D. M., Roy, A., & Bottaro, D. P. (2017). Hepatocyte growth factor/MET in cancer progression and biomarker discovery. *Cancer Science, 108*(3), 296-307. doi:10.1111/cas.13156

McElroy, S. J., Hobbs, S., Kallen, M., Tejera, N., Rosen, M. J., Grishin, A., Weitkamp, J. H. (2012). Transactivation of EGFR by LPS induces COX-2 expression in enterocytes. *PLoS One, 7*(5), e38373. doi:10.1371/journal.pone.0038373

Medina, D. L., Di Paola, S., Peluso, I., Armani, A., De Stefani, D., Venditti, R., Ballabio, A. (2015). Lysosomal calcium signalling regulates autophagy through calcineurin and TFEB. *Nature Cell Biology, 17*(3), 288-299. doi:10.1038/ncb3114

Millet, C., & Zhang, Y. E. (2007). Roles of Smad3 in TGF-beta signaling during carcinogenesis. *Critical Reviews in Eukaryotic Gene Expression, 17*(4), 281-293.

Molina, J. R., & Adjei, A. A. (2006). The Ras/Raf/MAPK pathway. *Journal of Thoracic Oncology, 1*(1), 7-9.

Monteith, G. R., Davis, F. M., & Roberts-Thomson, S. J. (2012). Calcium channels and pumps in cancer: Changes and consequences. *Journal of Biological Chemistry, 287*(38), 31666-31673. doi:10.1074/jbc.R112.343061

Mu, D., Zhang, W., Chu, D., Liu, T., Xie, Y., Fu, E., & Jin, F. (2008). The role of calcium, P38 MAPK in dihydroartemisinin-induced apoptosis of lung cancer PC-14 cells. *Cancer Chemotherapy & Pharmacology, 61*(4), 639-645. doi:10.1007/s00280-007-0517-5

Neuhaus, F. C., & Baddiley, J. (2003). A continuum of anionic charge: structures and functions of D-alanyl-teichoic acids in gram-positive bacteria. *Microbiology & Molecular Biology Reviews, 67*(4), 686-723. doi:10.1128/mmbr.67.4.686-723.2003

Nong, L., Newton, C., Friedman, H., & Klein, T. W. (2001). CB1 and CB2 receptor mRNA expression in human peripheral blood mononuclear cells (PBMC) from various donor types. *Advances in Experimental Medicine and Biology, 493*, 229-233. doi:10.1007/0-306-47611-8_27

Nguyen, T. L., Nam, Y. S., Lee, S. Y., Kim, H. C., & Jang, C. G. (2010). Effects of capsazepine, a transient receptor potential vanilloid type 1 antagonist, on morphine-induced antinociception, tolerance, and dependence in mice. *British Journal of Anaesthesia, 105*(5), 668-674. doi:10.1093/bja/aeq212

Okamoto, Y., Ohkubo, T., Ikebe, T., & Yamazaki, J. (2012). Blockade of TRPM8 activity reduces the invasion potential of oral squamous carcinoma cell lines. *International Journal of Oncology, 40*(5), 1431-1440. doi:10.3892/ijo.2012.1340

Ozaki, T., & Nakagawara, A. (2011). Role of p53 in cell death and human cancers. *Cancers (Basel), 3*(1), 994-1013. doi:10.3390/cancers3010994

Oblak, A., & Jerala, R. (2011). Toll-like receptor 4 activation in cancer progression and therapy. *Clinical Development of Immunology, 2011*, 609579. doi:10.1155/2011/609579

Olsson, M., & Zhivotovsky, B. (2011). Caspases and cancer. *Cell Death and Differentiation, 18*(9), 1441-1449. doi:10.1038/cdd.2011.30

Parameswaran, N., & Patial, S. (2010). Tumor necrosis factor-alpha signaling in macrophages. *Critical Review of Eukaryotic Gene Expression, 20*(2), 87-103. doi:10.1615/critreveukargeneexpr.v20.i2.10

Pedersen, R. W. C. C. A. (1989). An Immunocytochemical Technique Offering Increased Sensitivity and Lowered Cost with a Streptavidin-Horseradish Peroxidase Conjugate. *Journal of Histotechnology, 12*(4), 273-277. doi:10.1179/his.1989.12.4.273

Pinton, P., Giorgi, C., Siviero, R., Zecchini, E., & Rizzuto, R. (2008). Calcium and apoptosis: ER-mitochondria Ca2+ transfer in the control of apoptosis. *Oncogene, 27*(50), 6407-6418. doi:10.1038/onc.2008.308

Porter, A. G., & Janicke, R. U. (1999). Emerging roles of caspase-3 in apoptosis. *Cell Death and Differentiation, 6*(2), 99-104. doi: 10.1038/sj.cdd.4400476

Phan, N. N., Wang, C. Y., Chen, C. F., Sun, Z., Lai, M. D., & Lin, Y. C. (2017). Voltage-gated calcium channels: Novel targets for cancer therapy. *Oncology Letters, 14*(2), 2059-2074. doi:10.3892/ol.2017.6457

Populo, H., Lopes, J. M., & Soares, P. (2012). The mTOR signalling pathway in human cancer. *International Journal of Molecular Science, 13*(2), 1886-1918. doi:10.3390/ijms13021886

Pietras, K., Sjoblom, T., Rubin, K., Heldin, C. H., & Ostman, A. (2003). PDGF receptors as cancer drug targets. *Cancer Cell, 3*(5), 439-443. doi:10.1016/s1535-6108(03)00089-8

Pon, Y. L., Zhou, H. Y., Cheung, A. N., Ngan, H. Y., & Wong, A. S. (2008). p70 S6 kinase promotes epithelial to mesenchymal transition through snail induction in ovarian cancer cells. *Cancer Research, 68*(16), 6524-6532. doi:10.1158/0008-5472.CAN-07-6302

Psyrri, A., Seiwert, T. Y., & Jimeno, A. (2013). Molecular pathways in head and neck cancer: EGFR, PI3K, and more. *American Society of Clinical Oncology Educational Book*, 246-255. doi:10.1200/EdBook_AM.2013.33.24610.14694/EdBook_AM.2013.33.246

Qi, X. W., Zhang, F., Wu, H., Liu, J. L., Zong, B. G., Xu, C., & Jiang, J. (2015). Wilms' tumor 1 (WT1) expression and prognosis in solid cancer patients: A systematic review and meta-analysis. *Scientific Reports, 5*, 8924. doi:10.1038/srep08924

Raetz, C. R., & Whitfield, C. (2002). Lipopolysaccharide endotoxins. *Annual Review of Biochemistry, 71*, 635-700. doi:10.1146/annurev.biochem.71.110601.135414

Rani, A., & Murphy, J. J. (2016). STAT5 in Cancer and Immunity. *Journal of Interferon Cytokine Research, 36*(4), 226-237. doi:10.1089/jir.2015.0054

Reibel, J. (2003). Prognosis of oral pre-malignant lesions: Significance of clinical, histopathological, and molecular biological characteristics. *Critical Reviews in Oral Biology & Medicine, 14*(1), 47-62. doi:10.1177/154411130301400105

Rosset, C., Netto, C. B. O., & Ashton-Prolla, P. (2017). TSC1 and TSC2 gene mutations and their implications for treatment in Tuberous Sclerosis Complex: A review. *Genetetics & Molecular Biology, 40*(1), 69-79. doi:10.1590/1678-4685-GMB-2015-0321

Ruparel, S., Bendele, M., Wallace, A., & Green, D. (2015). Released lipids regulate transient receptor potential channel (TRP)-dependent oral cancer pain. *Molecular Pain, 11*, 30. doi:10.1186/s12990-015-0016-3

Riss, T., Niles, A., Moravec, R., Karassina, N., & Vidugiriene, J. (2004). Cytotoxicity Assays: In Vitro Methods to Measure Dead Cells. In G. S. Sittampalam, A. Grossman, K. Brimacombe, M. Arkin, D. Auld, C. P. Austin, J. Baell, B. Bejcek, J. M. M. Caaveiro, T. D. Y. Chung, N. P. Coussens, J. L. Dahlin, V. Devanaryan, T. L. Foley, M. Glicksman, M. D. Hall, J. V. Haas, S. R. J. Hoare, J. Inglese, P. W. Iversen, S. D. Kahl, S. C. Kales, S. Kirshner, M. Lal-Nag, Z. Li, J. McGee, O. McManus, T. Riss, P. Saradjian, O. J. Trask, Jr., J. R. Weidner, M. J. Wildey, M. Xia, & X. Xu (Eds.), *Assay Guidance Manual*. Bethesda (MD).

Riss, T. L., Moravec, R. A., Niles, A. L., Duellman, S., Benink, H. A., Worzella, T. J., & Minor, L. (2004). Cell Viability Assays. In G. S. Sittampalam, A. Grossman, K. Brimacombe, M. Arkin, D. Auld, C. P. Austin, J. Baell, B. Bejcek, J. M. M. Caaveiro, T. D. Y. Chung, N. P. Coussens, J. L. Dahlin, V. Devanaryan, T. L. Foley, M. Glicksman, M. D. Hall, J. V. Haas, S. R. J. Hoare, J. Inglese, P. W. Iversen, S. D. Kahl, S. C. Kales, S. Kirshner, M. Lal-Nag, Z. Li, J. McGee, O. McManus, T. Riss, P. Saradjian, O. J. Trask, Jr., J. R. Weidner, M. J. Wildey, M. Xia, & X. Xu (Eds.), *Assay Guidance Manual*. Bethesda (MD).

Read, G. H., Miura, N., Carter, J. L., Kines, K. T., Yamamoto, K., Devasahayam, N., Kesarwala, A. H. (2018). Three-dimensional alginate hydrogels for radiobiological and metabolic studies of cancer cells. *Colloids and Surfaces B: Biointerfaces, 171*, 197-204. doi:10.1016/j.colsurfb.2018.06.018

Sallan, M. C., Visa, A., Shaikh, S., Nager, M., Herreros, J., & Canti, C. (2018). T-type Ca(2+) Channels: T for Targetable. *Cancer Research, 78*(3), 603-609. doi:10.1158/0008-5472.CAN-17-3061

Santoni, G., Santoni, M., & Nabissi, M. (2012). Functional role of T-type calcium channels in tumour growth and progression: prospective in cancer therapy. *British Journal of Pharmacology, 166*(4), 1244-1246. doi:10.1111/j.1476-5381.2012.01908.x

Shang, X. Z., Zhu, H., Lin, K., Tu, Z., Chen, J., Nelson, D. R., & Liu, C. (2004). Stabilized beta-catenin promotes hepatocyte proliferation and inhibits TNF alpha-induced apoptosis. *Laboratory Investigations, 84*(3), 332-341. doi:10.1038/labinvest.3700043

Shi, Y. (2002). Mechanisms of caspase activation and inhibition during apoptosis. *Molecular Cell, 9*(3), 459-470. doi:10.1016/s1097-2765(02)00482-3

Smith, M. V., Lee, M. J., Islam, A. S., Rohrer, J. L., Goldberg, V. M., Beidelschies, M. A., & Greenfield, E. M. (2007). Inhibition of the PI3K-Akt signaling pathway reduces tumor necrosis factor-alpha production in response to titanium particles in vitro. *The Journal of bone and joint surgery. American volume, 89*(5), 1019-1027. doi:10.2106/JBJS.F.00615

Szlosarek, P. W., Grimshaw, M. J., Kulbe, H., Wilson, J. L., Wilbanks, G. D., Burke, F., & Balkwill, F. R. (2006). Expression and regulation of tumor necrosis factor alpha in normal and malignant ovarian epithelium. *Molecular Cancer Therapeutics, 5*(2), 382-390. doi: 10.1158/1535-7163.MCT-05-0303

Saito, K., Uzawa, K., Endo, Y., Kato, Y., Nakashima, D., Ogawara, K.,... Tanzawa, H. (2006). Plasma membrane Ca2+ ATPase isoform 1 down-regulated in human oral cancer. *Oncology Reports, 15*(1), 49-55.

Scotto, C., Deloulme, J. C., Rousseau, D., Chambaz, E., & Baudier, J. (1998). Calcium and S100B regulation of p53-dependent cell growth arrest and apoptosis. *Molecular & Cellular Biology, 18*(7), 4272-4281. doi:10.1128/mcb.18.7.4272

Seol, M. A., Park, J. H., Jeong, J. H., Lyu, J., Han, S. Y., & Oh, S. M. (2017). Role of TOPK in lipopolysaccharide-induced breast cancer cell migration and invasion. *Oncotarget, 8*(25), 40190-40203. doi:10.18632/oncotarget.15360

Shao, X., Lv, N., Liao, J., Long, J., Xue, R., Ai, N., Fan, X. (2019). Copy number variation is highly correlated with differential gene expression: A pan-cancer study. *BMC Medical Genetics, 20*(1), 175. doi:10.1186/s12881-019-0909-5

Sopik, V., Phelan, C., Cybulski, C., & Narod, S. A. (2015). BRCA1 and BRCA2 mutations and the risk for colorectal cancer. *Clinical Genetics, 87*(5), 411-418. doi:10.1111/cge.12497

Squier, C. A., & Kremer, M. J. (2001). Biology of oral mucosa and esophagus. *Journal of the National Cancer Institute. Monographs*, (29), 7-15. doi:10.1093/oxfordjournals.jncimonographs.a003443

Stancic, A., Jandl, K., Hasenohrl, C., Reichmann, F., Marsche, G., Schuligoi, R., Schicho, R. (2015). The GPR55 antagonist CID16020046 protects against intestinal inflammation. *Neurogastroenterology & Motility, 27*(10), 1432-1445. doi:10.1111/nmo.12639

Stewart, T. A., Yapa, K. T., & Monteith, G. R. (2015). Altered calcium signaling in cancer cells. *Biochimica et Biophysica Acta, 1848*(10 Pt B), 2502-2511. doi:10.1016/j.bbamem.2014.08.016

Sugiyama, A., Arakaki, R., Ohnishi, T., Arakaki, N., Daikuhara, Y., & Takada, H. (1996). Lipoteichoic acid and interleukin 1 stimulate synergistically production of hepatocyte growth factor (scatter factor) in human gingival fibroblasts in culture. *Infection & Immunity, 64*(4), 1426-1431.

Sakamoto, K. M., & Frank, D. A. (2009). CREB in the pathophysiology of cancer: implications for targeting transcription factors for cancer therapy. *Clinical Cancer Research, 15*(8), 2583-2587. doi:10.1158/1078-0432.CCR-08-1137

Sala, G., Dituri, F., Raimondi, C., Previdi, S., Maffucci, T., Mazzoletti, M., Falasca, M. (2008). Phospholipase Cgamma1 is required for metastasis development and progression. *Cancer Research, 68*(24), 10187-10196. doi:10.1158/0008-5472.CAN-08-1181

Schulz, L., Pries, R., Lanka, A. S., Drenckhan, M., Rades, D., & Wollenberg, B. (2018). Inhibition of GSK3alpha/beta impairs the progression of HNSCC. *Oncotarget, 9*(45), 27630-27644. doi:10.18632/oncotarget.25250

Shi, M., Cooper, J. C., & Yu, C. L. (2006). A constitutively active Lck kinase promotes cell proliferation and resistance to apoptosis through signal transducer and activator of transcription 5b activation. *Molecular Cancer Research, 4*(1), 39-45. doi:10.1158/1541-7786.MCR-05-0202

Sie, Z. L., Li, R. Y., Sampurna, B. P., Hsu, P. J., Liu, S. C., Wang, H. D., Yuh, C. H. (2020). WNK1 Kinase Stimulates Angiogenesis to Promote Tumor Growth and Metastasis. *Cancers (Basel), 12*(3). doi:10.3390/cancers12030575

Sigismund, S., Avanzato, D., & Lanzetti, L. (2018). Emerging functions of the EGFR in cancer. *Molecular Oncology, 12*(1), 3-20. doi:10.1002/1878-0261.12155

Stransky, N., Cerami, E., Schalm, S., Kim, J. L., & Lengauer, C. (2014). The landscape of kinase fusions in cancer. *Nature Communications, 5*, 4846. doi:10.1038/ncomms5846

Sulzmaier, F. J., & Ramos, J. W. (2013). RSK isoforms in cancer cell invasion and metastasis. *Cancer Research, 73*(20), 6099-6105. doi:10.1158/0008-5472.CAN-13-1087

Thaker, A. I., Rao, M. S., Bishnupuri, K. S., Kerr, T. A., Foster, L., Marinshaw, J. M., Ciorba, M. A. (2013). IDO1 metabolites activate beta-catenin signaling to promote cancer cell proliferation and colon tumorigenesis in mice. *Gastroenterology, 145*(2), 416-425 e411-414. doi:10.1053/j.gastro.2013.05.002

Thomas, S. J., Snowden, J. A., Zeidler, M. P., & Danson, S. J. (2015). The role of JAK/STAT signalling in the pathogenesis, prognosis and treatment of solid tumours. *British Journal of Cancer, 113*(3), 365-371. doi:10.1038/bjc.2015.233

Tong, J., Taylor, P., Peterman, S. M., Prakash, A., & Moran, M. F. (2009). Epidermal growth factor receptor phosphorylation sites Ser991 and Tyr998 are implicated in the regulation of receptor endocytosis and phosphorylations at Ser1039 and Thr1041. *Molecular Cell Proteomics, 8*(9), 2131-2144. doi:10.1074/mcp.M900148-MCP200

Toyota, M., Ho, C., Ohe-Toyota, M., Baylin, S. B., & Issa, J. P. (1999). Inactivation of CACNA1G, a T-type calcium channel gene, by aberrant methylation of its 5' CpG island in human tumors. *Cancer Research, 59*(18), 4535-4541.

Treda, C., Popeda, M., Ksiazkiewicz, M., Grzela, D. P., Walczak, M. P., Banaszczyk, M., Rieske, P. (2016). EGFR activation leads to cell death independent of PI3K/AKT/mTOR in an AD293 cell line. *PLoS One, 11*(5), e0155230. doi:10.1371/journal.pone.0155230

Trevisan, G., Materazzi, S., Fusi, C., Altomare, A., Aldini, G., Lodovici, M., Nassini, R. (2013). Novel therapeutic strategy to prevent chemotherapy-induced persistent sensory neuropathy by TRPA1 blockade. *Cancer Research, 73*(10), 3120-3131. doi:10.1158/0008-5472.CAN-12-4370

Tsai, Y. P., Yang, M. H., Huang, C. H., Chang, S. Y., Chen, P. M., Liu, C. J., Wu, K. J. (2009). Interaction between HSP60 and beta-catenin promotes metastasis. *Carcinogenesis, 30*(6), 1049-1057. doi:10.1093/carcin/bgp087

Utispan, K., Pugdee, K., & Koontongkaew, S. (2018). Porphyromonas gingivalis lipopolysaccharide-induced macrophages modulate proliferation and invasion of head and neck cancer cell lines. *Biomedicine & Pharmacotherapy, 101*, 988-995. doi:10.1016/j.biopha.2018.03.033

Varghese, E., Samuel, S. M., Sadiq, Z., Kubatka, P., Liskova, A., Benacka, J., Busselberg, D. (2019). Anti-Cancer Agents in Proliferation and Cell Death: The Calcium Connection. *International Journal of Molecular Sciences, 20*(12). doi:10.3390/ijms20123017

Vahedi, S., Chueh, F. Y., Chandran, B., & Yu, C. L. (2015). Lymphocyte-specific protein tyrosine kinase (Lck) interacts with CR6-interacting factor 1 (CRIF1) in mitochondria to repress oxidative phosphorylation. *BMC Cancer, 15*, 551. doi:10.1186/s12885-015-1520-6

Vercelli, C., Barbero, R., Cuniberti, B., Odore, R., & Re, G. (2015). Expression and functionality of TRPV1 receptor in human MCF-7 and canine CF.41 cells. *Veterinary and Comparative Oncology, 13*(2), 133-142. doi:10.1111/vco.12028

Vermes, I., Haanen, C., Steffens-Nakken, H., & Reutelingsperger, C. (1995). A novel assay for apoptosis. Flow cytometric detection of phosphatidylserine expression on early apoptotic cells using fluorescein labelled Annexin V. *Journal of Immunological Methods, 184*(1), 39-51. doi:10.1016/0022-1759(95)00072-i

Vleugel, M. M., Greijer, A. E., Bos, R., van der Wall, E., & van Diest, P. J. (2006). c-Jun activation is associated with proliferation and angiogenesis in invasive breast cancer. *Human Pathology, 37*(6), 668-674. doi:10.1016/j.humpath.2006.01.022

Wu, Z. Z., Chen, S. R., & Pan, H. L. (2005). Transient receptor potential vanilloid type 1 activation down-regulates voltage-gated calcium channels through calcium-dependent calcineurin in sensory neurons. *Journal of Biological Chemistry, 280*(18), 18142-18151. doi:10.1074/jbc.M501229200

Walker, J. M. (1994). The bicinchoninic acid (BCA) assay for protein quantitation. *Methods of Molecular Biology, 32*, 5-8. doi:10.1385/0-89603-268-X:5

Walsh, J. G., Cullen, S. P., Sheridan, C., Luthi, A. U., Gerner, C., & Martin, S. J.
    (2008). Executioner caspase-3 and caspase-7 are functionally distinct proteases.
    *Proceedings of the National Academy of Sciences of the United States of
    America, 105*(35), 12815-12819. doi:10.1073/pnas.0707715105

Wang, X., & Lin, Y. (2008). Tumor necrosis factor and cancer, buddies or foes? *Acta
    Pharmacologica Sinica, 29*(11), 1275-1288. doi:10.1111/j.1745-
    7254.2008.00889.x

Wang, J., Zhao, W., Guo, H., Fang, Y., Stockman, S. E., Bai, S., Ding, Z. (2018). AKT
    isoform-specific expression and activation across cancer lineages. *BMC Cancer,
    18*(1), 742. doi:10.1186/s12885-018-4654-5

Wheeler, D. L., Iida, M., & Dunn, E. F. (2009). The role of Src in solid tumors.
    Oncologist, 14(7), 667-678. doi:10.1634/theoncologist.2009-0009

Wu, J., Liu, T., Rios, Z., Mei, Q., Lin, X., & Cao, S. (2017). Heat Shock Proteins and
    Cancer. *Trends in Pharmacological Sciences, 38*(3), 226-256.
    doi:10.1016/j.tips.2016.11.009

Xiang, Z., Thompson, A. D., Brogan, J. T., Schulte, M. L., Melancon, B. J., Mi, D.,
    Lindsley, C. W. (2011). The discovery and characterization of ML218: A novel,
    centrally active T-type calcium channel inhibitor with robust effects in STN
    neurons and in a rodent model of Parkinson's Disease. *ACS Chemical
    Neuroscience, 2*(12), 730-742. doi:10.1021/cn200090z

Xu, X., Tsvetkov, L. M., & Stern, D. F. (2002). Chk2 activation and phosphorylation-
    dependent oligomerization. *Molecular Cell Biology, 22*(12), 4419-4432.
    doi:10.1128/mcb.22.12.4419-4432.2002

Yang, F., & Zheng, J. (2017). Understand spiciness: mechanism of TRPV1 channel
    activation by capsaicin. *Protein & Cell, 8*(3), 169-177. doi:10.1007/s13238-016-
    0353-7

Yang, L., & Karin, M. (2014). Roles of tumor suppressors in regulating tumor-
    associated inflammation. *Cell Death & Differentiation, 21*(11), 1677-1686.
    doi:10.1038/cdd.2014.131

Yu, C. R., Mahdi, R. M., Ebong, S., Vistica, B. P., Gery, I., & Egwuagu, C. E. (2003).
    Suppressor of cytokine signaling 3 regulates proliferation and activation of T-

helper cells. *Journal of Biological Chemistry, 278*(32), 29752-29759. doi:10.1074/jbc.M300489200

Yu, H., & Jove, R. (2004). The STATs of cancer—new molecular targets come of age. *Nature Reviews Cancer, 4*(2), 97-105. doi:10.1038/nrc1275

Yang, J., Kunimoto, H., Katayama, B., Zhao, H., Shiromizu, T., Wang, L., Nakajima, K. (2020). Phospho-Ser727 triggers a multistep inactivation of STAT3 by rapid dissociation of pY705-SH2 through C-terminal tail modulation. *International Immunology, 32*(2), 73-88. doi:10.1093/intimm/dxz061

Yuan, J. S., Reed, A., Chen, F., & Stewart, C. N., Jr. (2006). Statistical analysis of real-time PCR data. *BMC Bioinformatics, 7*, 85. doi:10.1186/1471-2105-7-85

Yu, H., Pardoll, D., & Jove, R. (2009). STATs in cancer inflammation and immunity: a leading role for STAT3. *Nature Reviews Cancer, 9*(11), 798-809. doi:10.1038/nrc2734

Zhan, T., Rindtorff, N., & Boutros, M. (2017). Wnt signaling in cancer. *Oncogene, 36*(11), 1461-1473. doi:10.1038/onc.2016.304

Zhang, L., Wang, L., Jiang, J., Zheng, D., Liu, S., & Liu, C. (2015). Lipopolysaccharides upregulate calcium concentration in mouse uterine smooth muscle cells through the T-type calcium channels. *International Journal of Molecular Medicine, 35*(3), 784-790. doi:10.3892/ijmm.2014.2054

Zhao, M., Mishra, L., & Deng, C. X. (2018). The role of TGF-beta/SMAD4 signaling in cancer. *International Journal of Biological Sciences, 14*(2), 111-123. doi:10.7150/ijbs.23230

Zhang, J., Zhou, X., Chang, H., Huang, X., Guo, X., Du, X., Xing, J. (2016). Hsp60 exerts a tumor suppressor function by inducing cell differentiation and inhibiting invasion in hepatocellular carcinoma. *Oncotarget, 7*(42), 68976-68989. doi:10.18632/oncotarget.12185

Zhou, F. H., Foster, B. K., Zhou, X. F., Cowin, A. J., & Xian, C. J. (2006). TNF-alpha mediates p38 MAP kinase activation and negatively regulates bone formation at the injured growth plate in rats. *The Journal of Bone and Mineral Research, 21*(7), 1075-1088. doi:10.1359/jbmr.060410

Abbreviations

A LPS+LTA+ML218 HCl after LPS+LTA 72-hour stimulation

A:T:G:C Adenine (A), Cytosine (C), Guanine (G) and Thymine (T)

A1 ML218 HCl only

A2 capsaicin only

ATCC American Type Culture Collection

B LPS+LTA+capsaicin after LPS+LTA 72-hour stimulation

B1a After LPS stimulation, addition of ML218 HCl

B1b After LPS stimulation, addition of Capsaicin

B2a After LPS+LTA stimulation, addition of ML218 HCl

B2b After LPS+LTA stimulation, addition of Capsaicin

Bp Base pair

BPE Bovine pituitary extract

C ML218 HCl after LPS+LTA 72-hour stimulation of CAL27

C1a After LPS stimulation, addition of ML218 HCl+LPS

C1b After LPS stimulation, addition of Capsaicin+LPS

C2a After LPS+LTA stimulation, addition of ML218 HCl+LPS+LTA

C2b After LPS+LTA stimulation, addition of Capsaicin+LPS+LTA

Cav T type voltage gated calcium channel

Chk2 Checkpoint kinase 2

D capsaicin after LPS + LTA 72-hour stimulation of CAL27

DMEM Dulbecco's Modified Eagle Medium

DMSO Dimethyl sulfoxide

DST Desalt purification

E LPS + LTA for 72 hours then $CaCl_2$ for 24 hours

EDTA Ethylenediaminetetraacetic acid

EGFR Epidermal growth factor receptor

ELISA Enzyme-linked immunosorbent assay

Epsilon Extinction coefficient

FBS Fetal bovine serum

GAPDH Glyceraldehyde 3-phosphate dehydrogenase

GMPS Guanosine 5′-monophosphate synthase

GPR55 G protein-coupled receptor 55

HRP Horseradish peroxidase

JAK Janus kinases

KSFM Keratinocyte Serum-Free Growth Medium

LPS Lipopolysaccharide

LTA Lipoteichoic acid

Oligo Oligonucleotides

P/S Penicillin-Streptomycin

p53 transformation-related protein 53

PBMC Peripheral blood mononuclear cell

PHA Phytohemagglutinin

PI3K Phosphoinositide 3-kinase

Pur Purification

qPCR Quantitative polymerase chain reaction

SCC Squamous cell carcinoma

SOCS3 Suppressor of Cytokine Signaling-3

STAT Signal transducer and activator of transcription proteins

Taq PCR enzyme isolated from *Thermus aquaticus*

T$_m$ Melting temperature

TRPA1 Transient receptor potential ankyrin 1

TRPV1 Transient receptor potential vanilloid 1

Wnt Wingless and Int-1

Awards and Journals

Thesis Publication

Role of calcium channel drugs ML218 HCl and capsaicin on lipopolysaccharide and lipoteichoic acid stimulated oral cancer cell CAL 27

Chakraborty, R[1]., Hu, H[1]., Darido, C[2]., Mangani, A[1]., Santiago, M[1]., Jabeen, A[1]., Bai, Y[2]., Mempin, M[1]., Deva, A[1]., Ranganathan, S[1]., Vickery, K[1]

[1]Macquarie University, Sydney, NSW, Australia

[2]Skin, Head & Neck and Solid Cancer, Peter MacCallum Cancer Centre, Melbourne, Victoria, Australia

(Under preparation)

Poster presentations

Chakraborty, R. The role of calcium channel drugs in lipopolysaccharide (LPS) induced oral cancer cell proliferation. 32nd Lorne Cancer Conference, 2020, Lorne, Australia, February 2020.

Awards

[1] Lorne Cancer Conference Travel Bursary 2020 (awarded AUD 350 for Lorne Cancer conference travel)

[2] International Macquarie University Research Excellence Scholarship (MQRES-MRES) holder, 2019-2020.

[3] Sydney Vital Translational Cancer Research Award Round 9, 2019-2020 (awarded AUD 9700 for the oral cancer project).

A.1 Ethics approval

OFFICE OF THE DEPUTY VICE-CHANCELLOR (RESEARCH)
Research Office | Biosafety

MACQUARIE
University
SYDNEY·AUSTRALIA

21/05/2019

Dear Associate Professor Vickery,

Re: "Mammalian Cell Culture " 5215

Your Risk Group 2 project has been approved effective 21/05/2019. The risk
assessment portion of this project is valid for 5 years. Please ensure a
hard copy of this project is made available in your laboratory for reference. A
final report for this project will be required by 21/05/2024.

Kind Regards,

Biosafety Secretariat
Research Office
Level 3, Research Hub, Building C5C East
Macquarie University, NSW 2109 Australia
T: +61 2 9850 4063
E: biosafety@mq.edu.au
W: mq.edu.au/research

A.2 Details of Materials and cell lines used during the project

TABLE A1: List of Materials used during the project.

Reagent/kit	Manufacturer	LOT	Catalogue No.	Description
Growth medium and buffers for the cell culture				
Keratinocyte-Serum Free Medium (K-SFM)	Life Technologies	-	1700504	Contains 2.5 µg human recombinant epithelial growth factor (EGF) (0.035 µg/µl), catalogue No. 10450-013, LOT 1969988 and 25 mg bovine pituitary extract (15.1 mg/ml), catalogue No. 13028-014, LOT 2014313
Foetal bovine serum (FBS)	Life Technologies	-	10099141	Endotoxin level: $\leq$ 5 EU/ml. Haemoglobin level: $\leq$ 30 mg/dL (levels routinely $\leq$ 25 mg/dL).
1X phosphate buffered saline (PBS)	Gibco	-	20012-027	1.5 mM KH_2PO_4; 155.2 mM Cl; 2.7 mM $Na_2HPO_4.7H_2O$ (pH 7.2)
Trypsin-EDTA	Sigma Life Sciences	T4049	SLBZ7364	0.25%, bioreagent 2.5 gm porcine trypsin and 0.2 gm EDTA; 4 Na per litre of Hank's balanced salt solution with phenol red

Reagent/kit	Manufacturer	LOT	Catalogue No.	Description
Dulbeccos Modified Eagles Medium (DMEM)	Gibco	-	11960-044	4,500 mg/L glucose, sodium pyruvate and sodium bicarbonate
Penicillin–streptomycin (P/S) solution	Life Technologies	2068825	15140-148	10,000 units/ml penicillin and 10,000 µg/ml streptomycin
Rosewell Park Memorial Institute (RPMI) 1640 medium	Gibco	1394048	21879-076	Without L-glutamine, and HEPES, with phenol red. Contains biotin, vitamin B12, PABA, vitamin inositol and choline. Used sodium bicarbonate buffer (2.0 g/L), and therefore required 5–10% CO_2 environment to maintain physiological pH
Freezing of the cells				
Tenak Slim tube cryogenic vials	Fisher Scientific	290992017	TE78315	RNAse–DNAse-free, 2-ml cryogenic vials
Dimethyl sulfoxide (DMSO)	Sigma Life Sciences	RNBH8443	D2650	Organic solvent, $(CH_3)_2SO$
Determination of gene expression of calcium channel receptor				
TaqMan Fast Advanced Cells-to-CT Kit	Thermo Fisher Scientific	00737298	A35374	TaqMan Fast Advanced RT enzyme mix, TaqMan Fast Advanced Master mix
Drugs and bacterial antigens				

Reagent/kit	Manufacturer	LOT	Catalogue No.	Description
LPS 25 mg	Sigma-Aldrich	-	L2630	Lipopolysaccharides from *Escherichia coli* O111:B4, water soluble
PHA 20 mg	Sigma-Aldrich	37614100	11082132001	Phytohemagglutinin-M (PHA-M) from *Phaseolus vulgaris*, water soluble
LTA 5 mg	Sigma-Aldrich	049M4155V	L3140	Lipoteichoic acid from *Streptococcus pyogenes*, water soluble
Capsazepine 5 mg	Sigma-Aldrich	039K4615	C191	N-[2-(4-Chlorophenyl) ethyl]-1,3,4,5-tetrahydro-7,8-dihydroxy-2H-2-benzazepine-2-carbothioamide, polar compound soluble in organic solvent
ML218 HCl (hydrochloride) 10 mg	Tocris	1A/226248	RDS450710	3,5-Dichloro-N-[[(1α,5α,6-exo,6α)-3-(3,3-dimethylbutyl)-3-azabicyclo [3.1.0] hex-6-yl] methyl]-benzamide hydrochloride, polar compound soluble in organic solvent
Capsaicin 250 mg	Sigma-Aldrich	MKBV4243V	360376	8-Methyl-N-vanillyl-trans-6-nonenamide, polar compound soluble in organic solvent

Reagent/kit	Manufacturer	LOT	Catalogue No.	Description
CID16020046 5 mg	Sigma-Aldrich	093M4730V	SML0805	4-[4,6-Dihydro-4-(3-hydroxyphenyl)-3-(4-methylphenyl)-6-oxopyrrolo[3,4-c] pyrazol-5(1H)-yl]-benzoic acid, polar compound soluble in organic solvent
Calcium chloride	Univar	D3247	127/500 g	$CaCl_2.2H_2O$ supplied as white powder. Water soluble; pH 5% solution at 25°C– 4.5–8.5
Proliferation assay				
RealTime-Glo MT Cell Viability Assay	Promega	0000383765	G9712	10 ×100 reactions
MT Cell Viability Substrate, 1000X	Promega	0000362418	G971A	10 µl solution supplied in opaque tubes
NanoLuc Enzyme, 1000X	Promega	0000362418	E499A	0.4 mg/ml
Trypan blue stain 0.4%	Invitrogen	2117644	T10282	Trypan blue 0.4% to identify dead cells via colorimetric detection; supplied as 21 ml vials
Crystal violet acetate	Sigma Aldrich	69H3634	C5042	9(amino-5-imino-5H-benzo[a] phenoxyazine acetate salt suppled as powder
Methanol	Chem-Supply	UN1230	MA004-2.5L-P	Analytical reagent

Reagent/kit	Manufacturer	LOT	Catalogue No.	Description
Cell Countess cell-counting chamber slides	Invitrogen	I31A9 Q422	C10283	For live cell and dead cell percentage via calorimetric detection
Protein estimation				
Pierce BCA Protein Assay kit	Thermo Fisher Scientific	UD2969	23225	Two-component, high-precision, detergent-compatible protein assay for determination of protein concentration
Kinase profiling				
Proteome Profiler Human Phospho-Kinase Array kit	R&D Systems	P236166	ARY003C	8 arrays (4 Part A, and 4 Part B), 1 transparency overlay, 1 8-well multi-dish and reagents
Human Phosphokinase array	R&D Systems	1569148	899190	8 nitrocellulose membranes (4 Part A, 4 Part B) each containing antibodies printed in duplicate
Array Buffer 1	R&D Systems	P173293	895477	21 ml of buffered protein base with preservatives
Array Buffer 2 5X Concentrate	R&D Systems	P200594	895478	21 ml of concentrated buffered protein base with preservatives
Array Buffer 3	R&D Systems	P184800	895008	21 ml of buffered protein base with preservatives

Reagent/kit	Manufacturer	LOT	Catalogue No.	Description
Wash Buffer Concentrate	R&D Systems	P230760	895003	2 vials (21 ml/vial) of a 25-fold concentrated solution of buffered surfactant with preservative
Detection Antibody Cocktail A	R&D Systems	1568310	899188	1 vial of biotinylated antibody cocktail; lyophilised
Detection Antibody Cocktail B	R&D Systems	1568313	899189	1 vial of biotinylated antibody cocktail; lyophilised
Streptavidin-HRP	R&D Systems	1549191	893019	200 µl of streptavidin conjugated to horseradish peroxidase (HRP)
Chemi Reagent 1	R&D Systems	P222081	894287	2.5 ml of stabilised hydrogen peroxide with preservative
Chemi Reagent 2	R&D Systems	P222083	894288	2.5 ml of stabilised luminol with preservative
8-well multi-dish	R&D Systems	-	607591	Clear 8-well rectangular multi-dish
Transparency overlay template	R&D Systems	-	608281	1 transparency overlay template for coordinate reference
Determination of proliferation related gene expression				
Pure Link RNA mini kit	Invitrogen	2137737	12183018A	Total RNA extraction
Trizol reagent	Invitrogen	260702	15596026	Total RNA extraction
Ethyl alcohol	Sigma Aldrich	SHBH7551	E7023-1L	CH_3CH_2OH; pure

Reagent/kit	Manufacturer	LOT	Catalogue No.	Description
SSIV VILO Master mix W/ EzDNASE	Invitrogen	00831746	11766050	DNA digestion and Reverse transcription PCR
POWRUP SYBR Master Mix, 5 ml	Invitrogen	00799448	A25742	Real-time PCR Master Mix
Chloroform	BDH AnalaR	19073	VWRC22711.260	$CHCl_3$, contains 1% v/v of ethanol as preservative
MicroAmp Fast plate	Applied Biosciences, Life Biosystems	-	4346907	96-well reaction plate (0.1 ml)
Optical adhesive cover	Applied Biosystems, Life Technologies	-	4360954	qPCR-compatible optical adhesive covers
Western blot				
Human/Mouse SOCS-3 MAb (Clone 516919), 25 µg	R&D Systems	CCDL0219051	MAB5696	Purified mouse monoclonal IgG
Human/Mouse/Rat STAT3 MAb (Clone 232209), 25 µg	R&D Systems	JXW041912A	MAB1799	Purified mouse monoclonal IgG
Human PI 3-Kinase p110 beta MAb (Clone 269020), 25 µg	R&D Systems	VCK042001A	MAB2686	Purified mouse monoclonal IgG
Anti-G3PDH/GAPDH (T0893), 20 µL	R&D Systems	20481	2275-PC-020	Polyclonal rabbit antibody
Human EGF R/ErbB1 Polyclonal Ab, 25 µg	R&D Systems	AUC1118111	AF231	Affinity purified goat IgG

Reagent/kit	Manufacturer	LOT	Catalogue No.	Description
Novex Sharp pre-stained protein standard	Life Technologies	2115579	LC5800	consists of 12 pre-stained protein bands in molecular weight range 3.5–260 kDa
Clarity Western ECL Substrate	Bio-Rad	102031366 102031363	1705060	Supplied in two parts: peroxide solution and luminol/enhancer solution
Ponceau S solution	Sigma-Aldrich	SLCB3855	P7170-1L	Bioreagent 0.1% (w/v) supplied in 5% acetic acid: $C_{22}H_{12}N_4Na_4O_{13}S_4$
Anti-goat IgG HRP conjugate	R&D Systems	XGD10161011	HAF009	Secondary antibody specific to primary antibody source
Anti-rabbit IgG HRP conjugate	R&D Systems	FIN1819021	HAF008	Secondary antibody specific to primary antibody source
Anti-mouse IgG HRP conjugate	R&D Systems	WVA00919011	HAF018	Secondary antibody specific to primary antibody source
NuPAGE LDS sample buffer (4X)	Invitrogen	1981103	NP0007	Used to prepare protein samples for denaturing gel electrophoresis with Bis-Tris or Tris-Acetate gels. It contains lithium dodecyl sulfate, pH 8.4; contains Coomassie G250 and Phenol Red
NuPAGE 10% bis-tris gel	Invitrogen	19050170	NP0302BOX	1 mm × 12 well
NuPAGE 10% bis-tris gel	Invitrogen	19071070	NP0301BOX	1 mm × 10 well

Reagent/kit	Manufacturer	LOT	Catalogue No.	Description
20X NuPAGE MOPS SDS Running Buffer	Invitrogen	-	NP0001	500 ml contains 50 mM MOPS, 50 mM Tris Base, 0.1% SDS, 1 mM EDTA, pH 7.7
Apoptotic assay				
CellEvent Caspase-3/7 Green Detection Reagent 25 µl	Invitrogen	2119122	C10723	2.0 mM solution in DMSO
TNF α enzyme-linked immunosorbent assay (ELISA)				
Human TNF α ELISA kit	Invitrogen	225688-001	KHC3011	Supplied with all the reagents

TABLE A2: Human oral cancer and normal oral cell line.

TABLE A2: Human oral cancer and normal oral cell line.

	Cell line				
	OKF6	**SCC4**	**SCC9**	**SCC25**	**CAL 27**
Source	Cellosaurus	ATCC	ATCC	ATCC	ATCC
Specimen site	Floor of mouth; normal oral keratinocytes	Tongue SCC	Tongue SCC	Tongue SCC	Tongue SCC
Type	Immortalised normal oral cells	Primary	Primary	Primary	Primary
Treatment	No	Radiation & methotrexate	No	No	No
Sex	Male	Male	Male	Male	Male
Age (years)	57	55	25	70	56
TNM staging	-	T3N0M0	T2N1	T1N1M0	-
Culture media	K-SFM media + growth factors	DMEM + 10% FBS + P/S	DMEM + 10% FBS + P/S	K-SFM media + growth factors + P/S	DMEM + 10% FBS + P/S
Freezing media	50% FBS + 10% DMSO + DMEM	50% FBS + 10% DMSO + DMEM	50% FBS + 10% DMSO + DMEM	20% FCS + 20% DMSO + DMEM/F12	50% FBS + 10% DMSO + DMEM

Note: ATTC: American Type Culture Collection; SCC: squamous cell carcinoma; K-SFM: keratinocyte serum free medium; DMEM: Dulbecco's Modified Eagle Medium; FBS: foetal bovine serum; P/S: penicillin + streptomycin; DMSO: dimethyl sulfoxide. TNM: T: number of tumours, N: lymph node, M: number of sites of metastasis.

TABLE A3: Human positive control cell line.

	Cell line			
	MCF-7	**HT-29**	**PBMC**	**SH-SY5Y**
Source	ATCC/Dr Benjamin Heng	ATCC/Dr Charlie Ahn	Precision Cancer Therapy Group (Macquarie University)	ATCC
Culture media	DMEM + 10% FBS + P/S	DMEM + 10% FBS + P/S	RPMI	DMEM + 10% FBS + P/S
Type	Adherent	Adherent	Non-adherent	Adherent
Treatment	No	No	No	No
Sex	Female	Female	Unknown	Female
Age (years)	69	44	Unknown	4

Specimen site	Mammary gland, breast; derived from metastatic site: pleural effusion	Colon: colorectal adenocarcinoma	Primary peripheral blood mononuclear cells (PBMC), normal	Bone marrow, neuroblastoma
Freezing media	DMEM + 20% FBS + 5% DMSO	DMEM + 20% FBS + 5% DMSO	No	DMEM + 20% FBS + 5% DMSO

A.3 Mean Ct values of each receptors

TABLE A4: Mean C_t values of each receptors.

Receptors	Cell lines				
	SCC4	SCC9	SCC25	CAL27	OKF6
Cav 3.1	36.072	35.836	33.591	35.197	34.418
Cav 3.2	-	-	33.416	-	-
Cav 3.3	36.464	38.170	36.948	35.109	36.432
TRPV1	29.107	30.014	29.949	30.9	30.533
TRPA1	-	-	-	-	35.563
GPR55	36.382	21.684	20.001	37.633	-
CB1	-	-	-	-	-
CB2	-	-	-	-	-

A.4 DMSO assay

CAL27, SCC25, SCC4, SCC9 and OKF6 cells were harvested from stock cultures and plated at densities of 5000 cells per well in 400 µl of growth medium in 24-well plated in their respective growth medium, in triplicate. They were incubated in 5% CO_2 at 37°C for 24 hours. Before treating the cells, their attachment was confirmed under the microscope. The medium was then replaced with medium that contained varying concentrations of DMSO (1%, 0.3%, 0.1%, 0.03%, 0.01%), or medium without DMSO (the control group). The cells were grown for 10–14 days. The culture medium was changed twice per week. The plates were kept in an incubator in 5% CO_2 at 37°C until cells on the control plates had formed sufficiently large clones or the confluence of the wells had reached approximately 90%. After analysis of the results, 0.1% DMSO (that did not affect the proliferation of the oral cancer cells) was used as vehicle for all the calcium channel drugs (Figure A1).
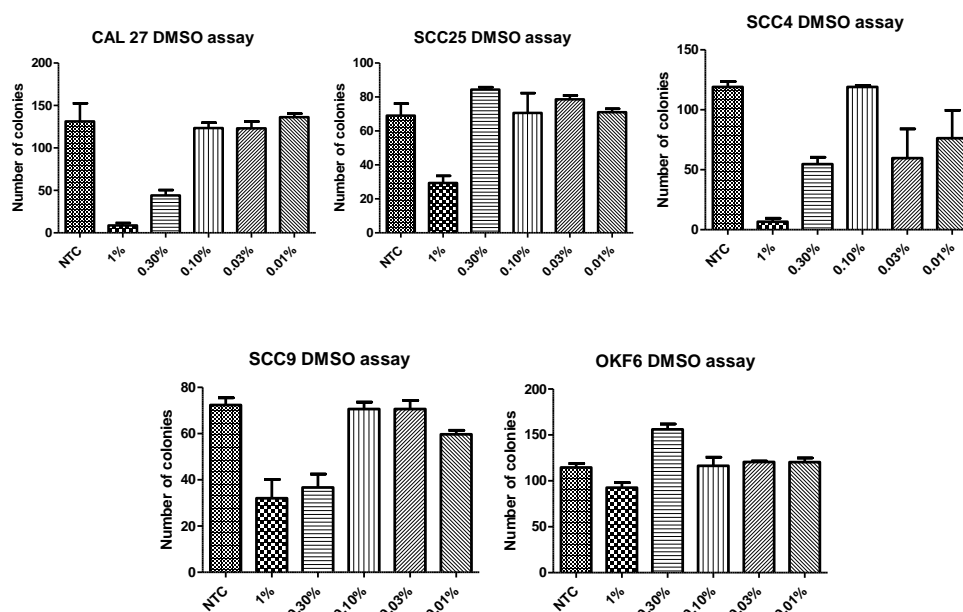
FIGURE A.1: DMSO assay. Comparison of number of colonies under different DMSO concentrations at $n = 3$; Error bars represent standard error of the mean. Here 'n' represents biological replicates. Biological replicates were obtained from one cell passage and totalled three.

A.5 Calcium channel drug optimization

A drug optimisation experiment with varying concentrations of capsaicin, ML218 HCl, capsazepine, and CID 16020046 was performed on CAL27 and SCC25, which helped to identify the concentration of drug that result in the lowest metabolic activity or viability of oral cancer cells. It was found that capsaicin at 150 µM and ML218 HCl at 100 µM resulted in the lowest metabolic activity of CAL27. Capsazepine at 25 µM and 30 µM led to a similar reduction in the metabolic activity of CAL27. However, capsaicin, ML218 HCl and capsazepine had different effects on SCC25: SCC25 showed higher metabolic activity than was seen in CAL27 after treatment with 150 µM capsaicin, 100 µM ML218 HCl and 30 µM capsazepine. This indicates that SCC25, which is a less active cancer cell line than CAL27, responds differently to calcium channel drugs (Figure A2).

Capsaicin at 150 µM resulted in the maximum reduction in the metabolic activity of CAL27. An (kinetic) MT Glo assay was thus performed to determine the time point at which capsaicin at 150 µM maximally lowered CAL27 metabolism. It was found that the metabolic activity of CAL27 was quite stable up to 24 hours with 150 µM capsaicin.
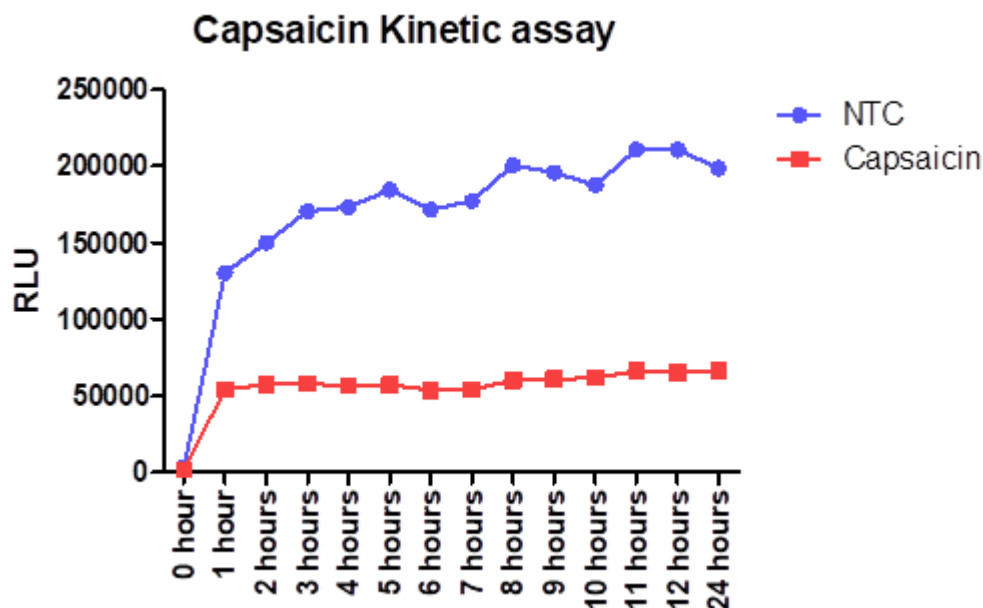
FIGURE A.2: Capsaicin MT Glo kinetic assay. Comparison of metabolic activity of untreated and capsaicin treated CAL27 for 24-hours at $n = 3$; Here 'n' represents biological replicates. RLU represents relative luminescence unit. NTC: no treatment control. Biological replicates were obtained from one cell passage and totalled three.

CID 16020046 (a GPR 55 antagonist) was selected for the project because the relative gene expression of GPR 55 was upregulated in all cancer cells compared with their normal counterpart (OKF6). However, increasing concentrations of CID 16020046 resulted in increases in metabolic activity of both SCC25 and CAL27 (Figure A3). This again may suggest that a) GPR 55 has cross-talk with other receptors related to cancer-proliferating mechanisms or proteins that counterbalance its action in its absence, b) CID 16020046 itself triggers other proliferating mechanisms, or c) GPR55 is non-functional. Overall, CID 16020046 may not be the ideal choice of drug for inhibiting the growth of oral cancer cells. Therefore, functionality assays for GPR55 ought to be done in the future; if it is found to be functional, alternative drugs should be tested to suppress its activity.
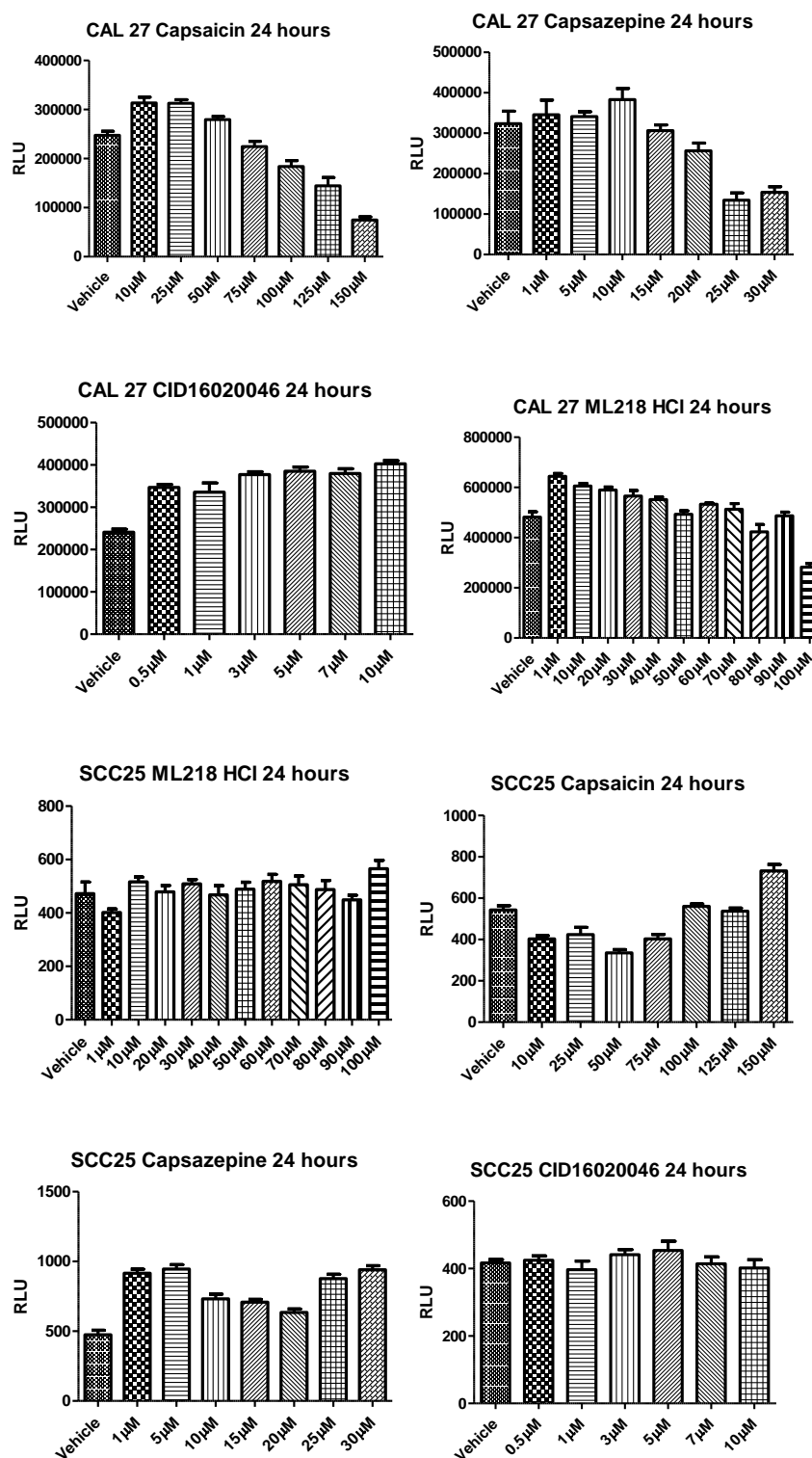
FIGURE A.3: Calcium channel drug optimization assay. Comparison of metabolic activity of SCC25 and CAL 27 under different concentrations of calcium channel drugs at $n = 3$; Error bars represent standard error of the mean. Here 'n' represents biological replicates. RLU represents relative luminescence unit. Biological replicates were obtained from one cell passage and totalled three.

A.6 Methods of Clonogenic and Caspase analysis

Using Colony Area Plugin: For colony area intensity the image straightening and region of interest (ROI) options were first selected. For image straightening '.tiff' image opened → transform → rotate → set angle to 0 → gridline 20 → based on visual inspection angle was selected until the image was nearly horizontal → rectangular selection tool for ROI → plugin → colony area plugin → colony area → desired postfix chosen for all the names of the processed images and results files → ROI converted to grey scale (8-bit) → plate size chosen → image stack file created → image stack of the cropped and selected wells was thresholded to detect the pixels containing the cells and the background removed → colonies identified with their respective intensities using fire lookup table (LUT) → thresholded values achieved → plugins → colony area → colony measurer → colony area intensity of the thresholded wells measured.

To analyse the total number of colonies the image was first opened → image → type → 8 bit → invert → edit → clear outside → image → adjust → threshold → process → binary → watershed → analyse → size (pixel^2): 10 -infinity, circularity: 0.00-1.00 →analyse particles → total number of colonies achieved.

To analyse the total number of cells and the number of apoptotic cells, first the image was opened → image → type → 8 bit → invert → edit → clear outside → image → adjust → threshold → process → binary → watershed → analyse → size (pixel^2): 10 -infinity, circularity: 0.00-1.00 →analyse particles → total number of cells/caspase3/7 positive cells achieved.
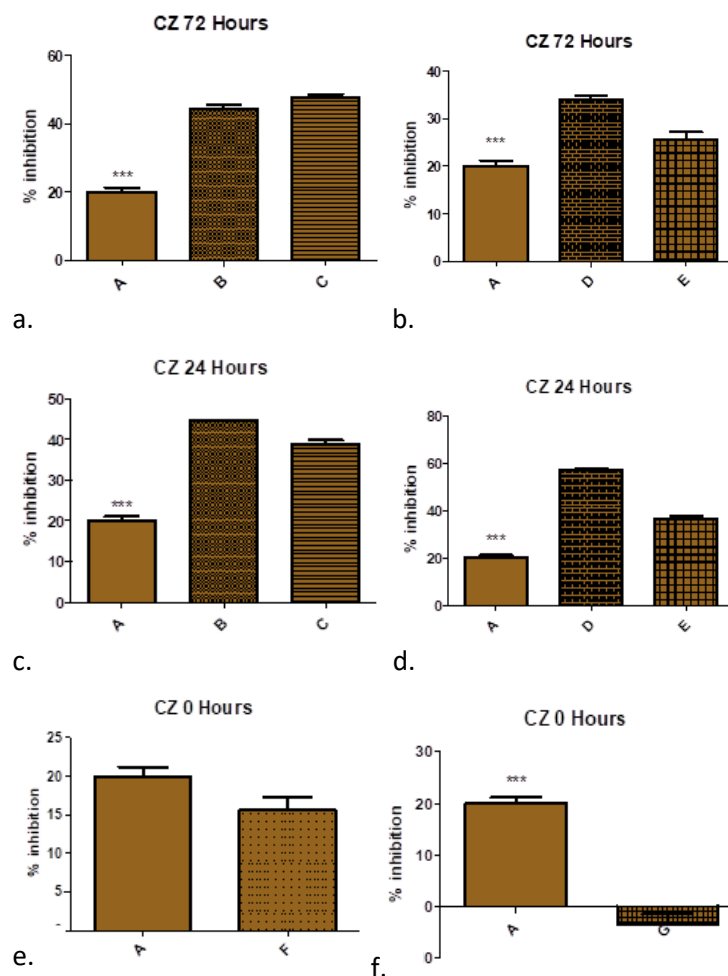
A.7 Capsazepine Drug combination assay

FIGURE A.4: MT Glo capsazepine drug combination assay. a. and b. 72-hour stimulation luminescence assay; c. and d. 24-hour stimulation luminescence assay; e. and f. 0-hour stimulation luminescence assay; *** $p \leq 0.001$ are statistically significant at $n = 6$. Error bars represent standard error of the mean. Here 'n' represents biological replicates. A: Capsazepine only (brown); B: after LPS stimulation addition of Capsazepine (brown dotted); C: after LPS stimulation addition of (Capsazepine+LPS) (brown stippled); D: after LPS+LTA stimulation addition of Capsazepine (brown bricked); E: after LPS+LTA stimulation addition of (Capsazepine+LPS+LTA) (brown webbed); F: after 0 hour LPS stimulation addition of (Capsazepine+LPS) (brown fine dotted); G: after 0 hour LPS+LTA stimulation addition of (Capsazepine+LPS+LTA) (brown fine netted). Biological replicates were obtained from two cell passage and totalled six.
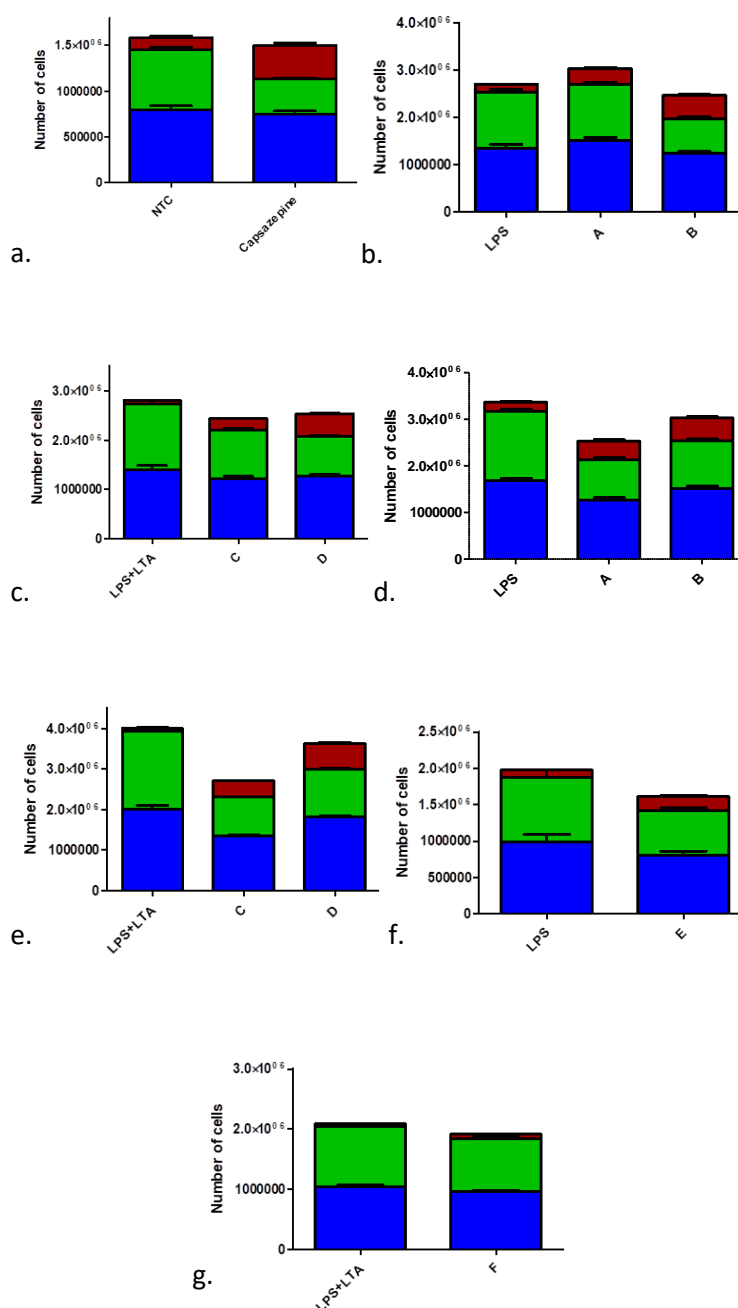
FIGURE A.5: Trypan blue capsazepine drug combination assay. a. only drug cell viability assay; b. and c. 24-hour stimulation cell viability assay; d. and e. 72-hour stimulation cell viability assay; f. and g. 0-hour stimulation cell viability assay; at $n = 6$. Error bars represent standard error of the mean. Here 'n' represents biological replicates. NTC: no treatment control; A: Capsazepine after LPS stimulation; B: after LPS stimulation, addition of (Capsazepine+LPS); C: Capsazepine after LPS+LTA stimulation; D: after LPS+LTA stimulation, addition of (Capsazepine+LPS+LTA); E: after 0 hour LPS stimulation, addition of (Capsazepine+LPS); F: after 0 hour LPS+LTA stimulation, addition of (Capsazepine+LPS+LTA); red represents dead cells; green represents live cells; blue represents total cells; statistical significance not shown in the figure. Biological replicates were obtained from one cell passage and totalled three.

A.8 Additional Results

Capsazepine did not produce an appreciable reduction in metabolism or viability of cells in the presence of bacterial antigen, unlike ML218 HCl and capsaicin. Thus, capsazepine was not used further in the project. Additional PHA, LTA, 10 µM capsaicin and 1 µM ML218 HCl drug combination assay results are archived on the Surgical Infection group V drive. The characterisation of forward and reverse primers used in the RT-qPCR has been submitted as supplementary information to the thesis.

A.9 BCA analysis for estimation of protein

The unknown sample protein concentration estimation was done following BCA analysis protocol. Here an example of the protein estimation is shown in Figure A6, Table A5 and Table A6.

BCA Protein estimation
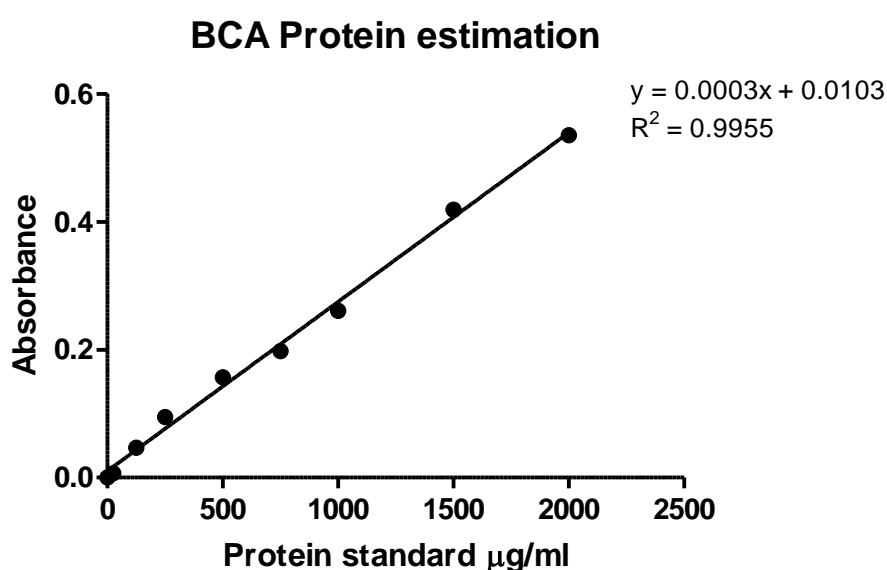
$y = 0.0003x + 0.0103$
$R^2 = 0.9955$

FIGURE A.6: BCA protein estimation. Absorbance plotted against the protein standard (Bovine serum albumin) varying concentrations (Table A5). Coefficient of linear regression (R^2) and the formula of the slope was used for the estimation of the unknown sample protein concentration. Here y represents absorbance and x represents the unknown protein concentration in µg/ml. The same formula (shown in the figure) was used to estimate the unknown protein concentration of different samples that is shown in Table A6.

TABLE A5: Example of protein standard absorbance.

Protein standard µg/ml	Absorbance at 562nm	Absorbance
0	0.087	0
25	0.094	0.007
125	0.134	0.047
250	0.182	0.095
500	0.244	0.157
750	0.285	0.198
1000	0.348	0.261
1500	0.506	0.419
2000	0.622	0.535

TABLE A6: Example of estimated protein concentration.

Samples	Samples µg/ml	Absorbance at 562nm	Absorbance
Cal-27	837	0.348333333	0.261333333
LPS	410	0.220333333	0.133333333
LTA	428	0.225666667	0.138666667
LPS + LTA	932	0.377	0.29

A.10 RNA quantification

The concentration and purity of RNA samples was checked based on the A260/280 ratio and A260/230 ratio (Table A7).

TABLE A7: RNA concentrations of different samples.

Name of the sample	Concentration of RNA ng/µl	260/280	260/230
Cal-27 P10	36	1.63	0.29
Cal-27 P11	36.1	1.69	0.42
Cal-27 P12	31.5	1.71	1.31
LPS P10	35.5	1.86	0.96
LPS P11	35.3	1.74	1.07
LPS P12	42.5	1.74	0.37
LPS+LTA P10	27.4	1.71	0.07
LPS+LTA P11	26.1	1.76	0.36
LPS+LTA P12	32.9	1.71	0.57
A P10	36.1	1.69	0.27
A P11	36.1	1.71	0.56
A P12	43	1.64	1.15
B P10	49.7	1.75	1.07
B P11	36.3	1.91	0.22
B P12	44.8	1.74	1.21
C P10	36.1	1.75	0.41
C P11	35.5	1.89	0.94
C P12	42.5	1.76	1.21
D P10	38.7	1.73	0.88
D P11	35.1	1.81	1.31
D P12	34.4	1.81	1.17
E P10	47.8	1.72	0.52
E P11	51.6	1.65	0.4
E P12	46.6	1.78	0.39